universität wien

DISSERTATION

Titel der Dissertation

VAF347, a novel low molecular weight immunomodulator, inhibits Interleukin-6 production in the human monocytic cell line Monomac1 via activation of the aryl hydrocarbon receptor

angestrebter akademischer Grad

Doktor der Naturwissenschaften (Dr. rer. nat.)

Verfasser:	Mag. Hermann Novak
Matrikel-Nummer:	9920080
Dissertationsgebiet (lt. Studienblatt):	Genetik - Mikrobiologie
Betreuerin:	Ao. Univ.-Prof. Dipl.-Biol. Dr. Angela Witte

Wien, am 20. September 2008

Für ihre Hilfe und persönliche Unterstützung möchte ich mich besonders
bei folgenden Personen bedanken:

Den Supervisoren:

Univ.-Doz. Dr. Maximilian Woisetschläger
Ao. Univ.-Prof. Dipl. –Biol. Dr. Angela Witte

Der Labormannschaft:

Ing. Nathalie Harrer
Mag. Petra Gruber
Wolfgang Neruda

Mitarbeitern anderer Labors:

Dr. Nicole Urtz
Edith Pursch
Robert Csonga
Monique Bongers

und nicht zuletzt:

meiner Familie, vor allem Nora
Franziska Wohlkönig
Bernhard Mayer

Table of Contents

Abstract

Interleukin (IL) -6 is a pleiotropic cytokine that is involved in the regulation of immune reactions, hematopoiesis, bone metabolism and inflammation. Deregulation of IL-6 has been shown to be involved in several inflammatory and autoimmune disorders, including rheumatoid arthritis, Castleman's disease and Crohn's disease. Therefore, interception of the IL-6 signaling pathway represents an interesting therapeutic target for the treatment of these diseases.

VAF347 is a novel low molecular weight immunomodulator which has been shown to selectively block IgE synthesis in human B cells and to inhibit IL-6 production in human monocyte-derived dendritic cells. This study was designed to identify the molecular target(s) of VAF347 that lead to inhibition of IL-6 synthesis. Similar to primary cells, VAF347 inhibits IL-4 and GM-CSF as well as PMA induced IL-6 production in the human monocytic cell line Monomac1. We demonstrate, that the aryl hydrocarbon receptor (AhR) is the functionally relevant target for inhibition of IL-6 response by VAF347. The AhR is responsible for mediating the biological activity of VAF347 in Monomac1, since 1) other AhR ligands display an identical activity profile, 2) ectopic over-expression of a trans-dominant negative AhR protein abolishes VAF347 activity, and 3) silencing of AhR gene expression renders Monomac1 resistant to VAF347.

Furthermore, VAF347 inhibits the activation of an IL-6 promoter reporter gene construct and blocks the binding of the transcription factor NF-IL6, which is thought to be one of the main factors involved in IL-6 regulation, to the IL-6 promoter. Over-expression of wild type NF-IL6 partially abolishes VAF347 activity. These findings showed that VAF347 mediates its inhibitory effect at the transcriptional level by inhibiting the interaction of NF-IL6 with its binding site on the IL-6 promoter.

Collectively, these data identify the AhR as the functional target of VAF347. Given the fact that IL-6 deregulation is involved in the pathology of several inflammatory and autoimmune diseases, targeting the AhR may provide a new tool for the treatment of these diseases.

Kurzfassung

Interleukin (IL) -6 ist ein pleiotropes Zytokin das sowohl an der Regulation von Immunreaktionen, der Hämatopoese, dem Metabolismus des Knochens als auch an Entzündungsreaktionen beteiligt ist. Eine deregulierte Produktion von IL-6 ist bei mehreren Entzündungs- und Autoimmunerkrankungen gefunden worden, wie etwa bei Gelenkrheumatismus, Morbus Castleman oder Morbus Crohn. Deshalb stellt die Unterbrechung des IL-6 Signalweges ein interessantes therapeutisches Angriffsziel für die Behandlung dieser Krankheiten dar.

Es wurde bereits gezeigt, dass VAF347 als ein neuer niedermolekularer Immunmodulator sowohl spezifisch die Immunglobulin-E Synthese von humanen B-Zellen, als auch die IL-6 Produktion von humanen Dendritischen Zellen monozytären Ursprungs inhibiert.

Diese Studie wurde gestaltet, um das (die) molekulare(n) Ziel(e) von VAF347, das zur Inhibierung der IL-6 Produktion führt, zu identifizieren. Ähnlich wie bei primären Zellen inhibiert VAF347 die von IL-4 und GM-CSF als auch die von PMA induzierte IL-6 Produktion in der humanen monozytären Zelllinie Monomac1. Es wird gezeigt, dass der Aryl Hydrocarbon Rezeptor (AhR) das funktionell bedeutende Target für die Inhibition der IL-6 Produktion durch VAF347 ist. Der AhR ist für die biologische Aktivität von VAF347 in Monomac1 Zellen verantwortlich, da 1) andere AhR Liganden ein ähnliches Aktivitätsprofil zeigen, 2) ektopische Überexpression eines transdominant negativen AhR Proteins die biologische Aktivität von VAF347 aufhebt und 3) die Stilllegung des AhR Gens Monomac1 Zellen resistent gegen VAF347 macht.

Darüber hinaus inhibiert VAF347 die Expression eines IL-6 Promoter Reporter-Gen Konstrukts und blockiert die Bindung des Transkriptionsfaktors NF-IL6, welcher als einer der Hauptfaktoren für die Regulation der IL-6 Expression angesehen wird, an den IL-6 Promoter. Die Überexpression des Wildtyp NF-IL6 Proteins hebt teilweise die Aktivität von VAF347 auf. Diese Ergebnisse demonstrieren, dass VAF347 seinen inhibitorischen Effekt auf transkriptioneller Ebene ausübt, da die Interaktion von NF-IL6 mit dessen Bindungsstelle im IL-6 Promoter verhindert wurde.

Zusammenfassend identifizieren diese Daten AhR als das funktionell entscheidende Target von VAF347. Da die Deregulation von IL-6 am Krankheitsbild mehrerer inflammatorischer- und Autoimmunerkrankungen beteiligt ist, könnte das Targeting von AhR eine neue Möglichkeit zur Behandlung dieser Krankheiten darstellen.

Abbreviations

aa	amino acid(s)
AhR	aryl hydrocarbon receptor
AhRR	aryl hydrocarbon receptor repressor
ARNT	aryl hydrocarbon receptor nuclear translocator
Amp	ampicillin
bp	base pair(s)
ChIP	chromatin immunoprecipitation
CYP1A1	cytochrome P450 1A1
DC(s)	dendritic cell(s)
DNA	deoxyribonucleic acid
ds	double stranded
EtOH	96% Ethanol
GFP	green fluorescent protein
GM-CSF	granulocyte macrophage colony-stimulating factor
HRP	horse radish peroxidase
IgE	Immunoglobulin-E
IL-6	Interleukin-6
JAK(s)	Janus Kinase(s)
kDa	kilo Dalton
MAPK	mitogen-activated protein kinase
MM1	Monomac1
PBS	phosphate buffered saline
PKC	protein kinase C
PMA	phorbol 12-myristate 13-acetate
RNA	ribonucleic acid
RT	room temperature
ss	single stranded
STAT	signal transducer and activator of transcription
TCDD	2,3,7,8-tetrachlorodibenzo-p-dioxin
T_H17	Interleukin-17 producing T cell
T_{reg}	regulatory T cell

1. Introduction

1.1 The immune system: cytokines and their function

The development of an effective immune response involves the interaction of multiple cell types including myeloid cells and lymphocytes. The complex interactions among these cells are in part mediated by cytokines. Cytokines are relatively small regulatory proteins that are secreted from cells of innate and adaptive immunity as well as various other cell types in response to a number of stimuli. On one hand, a subgroup of these proteins stimulate the growth and differentiation of various cells during immune homeostasis, while on the other hand, cytokines facilitate the activation and differentiation of effector cells both during the innate and adaptive phases of immune responses against foreign antigens such as bacteria, viruses or self-antigens.

Binding of cytokines to specific receptors on the membrane of target cells leads to the activation of diverse signal-transduction pathways which ultimately lead to altered gene expression.

In recent years cytokines and their receptors have become important targets for specific antagonists in various immune and inflammatory diseases. One of these cytokines that is considered as such a target, due to its pro-inflammatory functions is the cytokine Interleukin-6 (IL-6). IL-6 is a pleiotropic cytokine that is involved in the regulation of immune reactions, hematopoiesis, bone metabolism and inflammatory state. The overproduction of IL-6 has been implicated in the pathology of several inflammatory and autoimmune disorders, including rheumatoid arthritis, Crohn's disease, Castleman's disease and systemic-onset juvenile idiopathic arthritis. Therefore interception of the IL-6 signaling pathway has become an interesting target for the treatment of these diseases.

1.1.1 The discovery of Interleukin-6

The history of nomenclature reflects the diverse biological functions of this cytokine: IL-6 was initially identified as a T cell-derived B-cell differentiation factor that induces B-cells to differentiate into antibody-producing cells (1), and was therefore first termed B-cell stimulatory factor-2 (BSF-2). The complementary DNA of BSF-2 was cloned in 1986 (2). Following its discovery, BSF-2 was found to be identical to the 26 kDa protein (3), an interferon-β2 protein (4), a hybridoma/plasmacytoma growth factor (5,6) and a hepatocyte-stimulating factor (7). Later these names were unified as IL-6.

1.1.2 Structure and expression of Interleukin-6

The human IL-6 gene contains four introns and four exons and maps to chromosome 7p21 (8). With a length of 212 amino acids (aa), human IL-6 has a molecular mass of 21 to 28 kilo Dalton (kDa)

and contains two N-glycosylation sites (2). Four cysteine residues are conserved in the central portions of human and murine IL-6, which are not necessary for IL-6 activity (9). Human IL-6 shows a sequence homology of 65% at the DNA level and 42% at the protein level compared with murine IL-6 (10).

IL-6 is not constitutively expressed in the human body, but is induced by a large number of multiple stimuli including bacterial and viral infections, microbial components such as lipopolysaccharide (LPS) and different cytokines (11). IL-1β, TNF-α and IFN-γ have been shown to induce IL-6 expression in many cell types including T-cells, B-cells, monocytes, endothelial cells, fibroblasts and several kinds of tumor cells.

1.1.3 The Interleukin-6 promoter

A series of transcription factors have been described to contribute to the complex regulation of the IL-6 gene. Their interactions may vary depending on the extracellular stimuli as well as the cell type. So far, several functional cis-regulatory elements in the human IL-6 promoter have been identified, including nuclear factor-kappa B (NF-κB) (position -62 to –49 relative to the translational start codon), nuclear factor-IL6 (NF-IL6) (-144 to -132), cAMP response element-binding protein (CREB) (-152 to -145) and activator protein 1 (AP-1) (-271 to –263) binding sites (**Figure 1.1.3.1**).

NF-κB is a member of the Rel family of transcription factors that form homo- or heterodimers through the Rel homology domain (12). In resting cells, NF-κB is located in the cytoplasm bound to a member of the family of inhibitors of κB (IκBs). Upon activation of cells by diverse stimuli, IκBs become phosphorylated and are rapidly degraded. The degraded IκBs can no longer bind to NF-κB which is therefore released and translocated to the nucleus where it binds to its specific DNA recognition site and contributes to the transcriptional activation of multiple genes.

NF-IL6, also known as CCAAT/enhancer binding protein beta (C/EBP β), belongs to the family of C/EBP transcription factors which are characterized by a basic leucine-zipper structure which is responsible for homo- or heterodimerization (13). In primary cells, NF-IL6 is usually expressed at low levels and is strongly induced upon stimulation of cells by TNF-α, IL-1β or LPS. In contrast, NF-IL6 is constitutively expressed in many cell lines. Phosphorylation of NF-IL6 has been shown to increase its transcriptional activity (14).

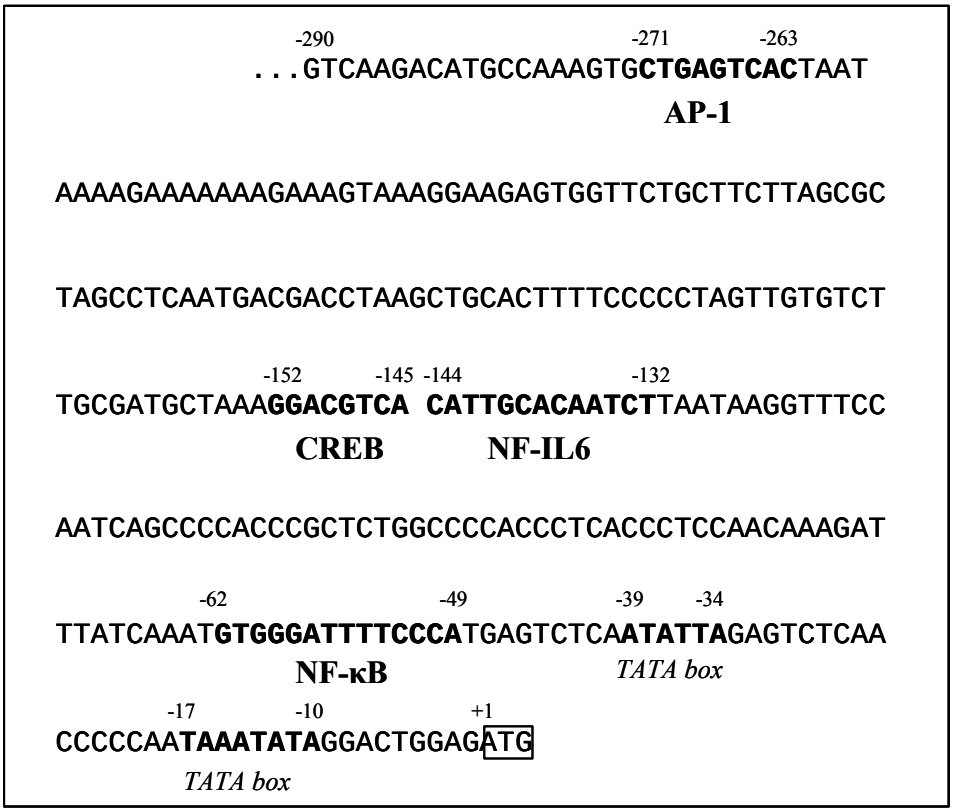

Figure 1.1.3.1: ***The human IL-6 promoter****. A part of the IL-6 promoter is shown in which core sequences for each transcription factor binding site are indicated in bold. The start codon ATG for the IL-6 gene is boxed, the TATA box is bolded. The numbers on top of corresponding nucleotides give the position relative to the start codon ATG.*

The AP-1 transcription factors are homo- or heterodimers of basic region-leucine zipper proteins belonging to the Jun and Fos subfamilies (15). Since Fos proteins do not form stable dimers, they need to form dimers with Jun proteins to bind DNA. The members of the Jun protein family vary considerably in their DNA binding affinities and transactivation capacities, with c-Jun showing the highest activation potential (16).

Studies in various cell types have shown that induction of IL-6 gene transcription is complex and involves the coordinated regulation of factors that associate with the evolutionary conserved NF-κB, NF-IL6 and AP-1 sites in the mouse and human IL-6 promoter (17-21).

1.1.4 Cellular signaling and regulation of Interleukin-6

IL-6 has a unique receptor system (22). The IL-6 receptor consists of two functional membrane proteins: an 80 kDa IL-6 binding chain (IL-6R, IL-6R α-chain, CD126) (23) and a 130 kDa signal transducer (gp130, IL-6R β-chain CD130) involved in IL-6 signal transduction (24,25). The 80 kDa IL-6 receptor can exist in transmembrane form or in soluble form. The transmembrane form has a short intracytoplasmatic region consisting of 82 aa, that lacks tyrosine-kinase domains and does not have an enzymatic role in IL-6 signaling.

Binding of IL-6 to the membranous IL-6 receptor brings the intracellular segments of two IL-6R chains in close proximity, thus permitting the association of the intracellular IL-6R segments with the 130 kDa glycoprotein (**Figure 1.1.4.1**). This is thought to induce the formation of a multimeric complex consisting of two IL-6 molecules bound to two IL-6R proteins and two gp130 molecules bound to the intracytoplasmatic segments of the two IL-6R proteins.

On the other hand, the soluble form of IL-6R, which is produced by cleavage of the membranous IL-6R or by alternative splicing, can bind IL-6. A complex of two IL-6 molecules bound to two soluble IL-6R proteins forms a complex with two gp130 proteins. This complex is able to transmit signals in a process called *trans*-signaling (26).

Dimerization of gp130 proteins transduces a signal to activate members of the JAK tyrosine kinases (Janus family tyrosine kinases). JAKs represent a family of four non-receptor tyrosine kinases, comprising the members JAK1, JAK2, JAK3 and Tyk2, which selectively phosphorylate the signal transducer and activator of transcription (STAT) proteins thus leading to their activation. In the case of IL-6R signaling, JAKs recruit and induce tyrosine phosphorylation of STAT3, which is translocated to the nucleus in its phosphorylated form and induces gene expression.

Overproduction of IL-6 leads to inflammation and disease, therefore this cytokine must be regulated to control the duration and magnitude of IL-6 response. A negative feed-back loop regulates the IL-6 signaling system via activation of the suppressors of cytokine signaling (SOCS) and the protein inhibitors of activated STATs (PIAS). Phosphorylated and thus activated STAT3 translocates to the nucleus and induces the expression of SOCS3, which in turn binds to JAKs and thus suppresses gp130 signal transduction (27). PIAS are constitutively expressed negative regulators of STAT proteins. In the case of IL-6 signaling, PIAS3 associates specifically with activated STAT3 and blocks further STAT3 mediated gene transcription (28).

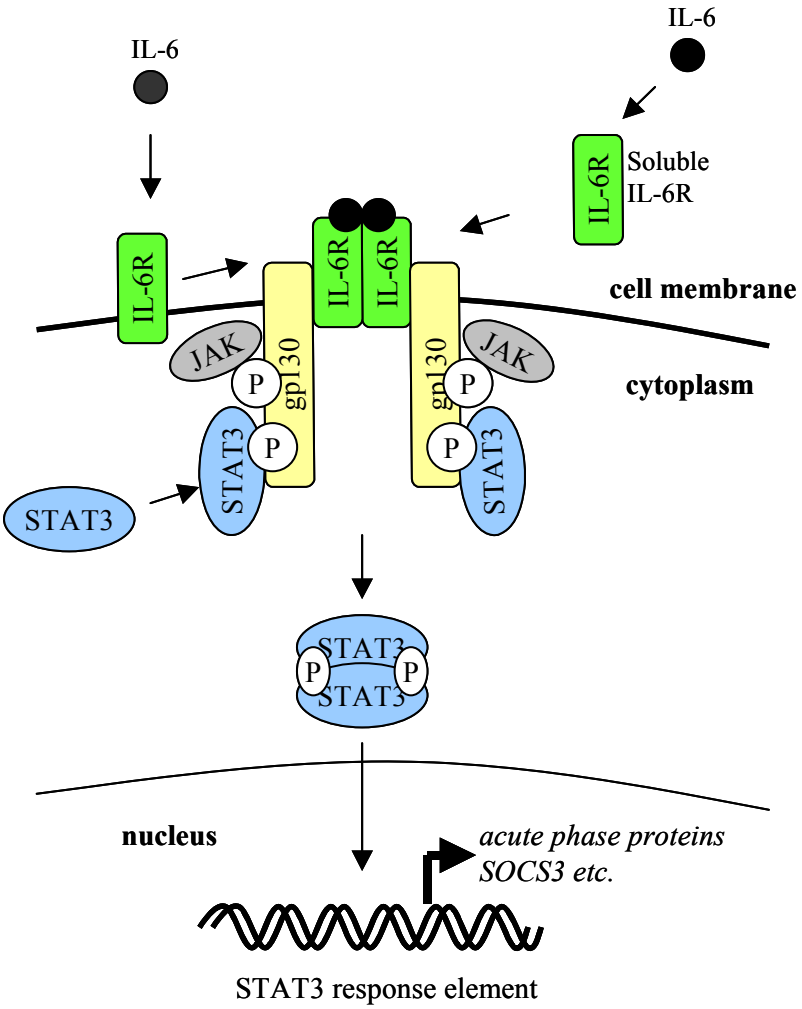

Figure 1.1.4.1: ***An overview of the IL-6 signaling pathway****. A unique receptor system consisting of two functional membrane proteins mediates IL-6 signaling: an 80 kDa ligand binding IL-6 receptor (IL-6R) together with a 130 kDa signal-transducing chain (gp130). The IL-6R can exist in either membrane-bound or soluble form. The soluble IL-6R, lacking the cytoplasmatic domain is observed in normal serum. Soluble IL-6R is capable of transmitting signals in a process called trans-signaling. The binding of IL-6 to IL-6R triggers receptor activation by the formation of a multimeric complex, consisting of two IL-6R proteins and two gp130 molecules. Receptor activation facilitates recruitment of JAKs, which when transphosphorylated, subsequently phosphorylate the gp130 tails. Phosphorylated gp130 residues recruit STAT3 proteins, which are also phosphorylated by JAKs. Phosphorylated and thus activated STAT3 dimerizes, translocates to the nucleus and induces the transcription of target genes, including acute phase proteins and its own negative regulator SOCS3.*

1.1.5 Biological effects of Interleukin-6

Originally IL-6 was described as a T-cell-derived B-cell differentiation factor. Further B-cell studies showed that IL-6 enhances the production of IgM, IgG and IgA in activated human B-cells (29). Addition of anti-IL-6 antibody to stimulated B-cells abrogates the production of these immunoglobulins, however anti-IL-6 antibody does not affect the proliferation of activated B-cells. Thus, IL-6 is thought to be essential for antibody production by activated B-cells but not for their proliferation.

The effects of IL-6 are not limited to B-cells, in fact IL-6 exerts diverse functions on multiple cell types. In contrast to B-cells, IL-6 induces the proliferation of mitogen-activated T-cells by inducing both IL-2 production (30) and IL-2 receptor expression (31). In addition to the stimulation of IL-2 synthesis and secretion, IL-6 acts synergistically with IL-2 in driving the differentiation of human T-cells into cytotoxic T-cells (32). Furthermore, IL-6 acts as a terminal differentiation factor for macrophages (33).

IL-6 is also involved in the acute phase response to inflammation or tissue injury which is characterized by increased serum levels of acute phase proteins such as fibrinogen and haptoglobin, and decreased serum levels of albumin. The acute phase response is a consequence of liver cells responses to inflammatory signals. Studies in human hepatocytes show that IL-6 induces the expression of a variety of acute phase proteins (34), including C-reactive protein, fibrinogen, α1-antitrypsin and serum amyloid A, while it suppresses the synthesis of albumin (35,36). Thus, IL-6 is considered as a major mediator of the acute phase response.

IL-6 acts on hematopoietic stem cells synergistically with IL-3 to induce the formation of multilineage blast cell colonies (37). Soluble IL-6 receptor is involved in bone metabolism by triggering osteoclast differentiation (38). Furthermore, IL-6 acts on the differentiation of megakaryocytes to produce platelets (39) and has been shown to support the survival of cultured cholinergic neurons (40,41).

1.1.6 Interleukin-6 in rheumatoid arthritis

Overproduction of IL-6 is involved in the pathology of a series of inflammatory and autoimmune diseases including rheumatoid arthritis (RA), Crohn's disease, Castleman's disease and systemic lupus erythematosus.

RA is a chronic inflammatory disease that is characterized by inflammation and cellular proliferation in the synovial lining of joints, that can ultimately lead to irreversible destruction of cartilage and periarticular bone. Abnormal laboratory findings in RA patients show elevated levels of acute-phase reaction related proteins and the emergence of autoantibodies. Although the etiology

and pathogenesis of this disease still remain incompletely understood, it is clear that cytokines play a key role in the activation of synovial cells. The most important cytokines in RA are the pro-inflammatory cytokines TNF-α and IL-1β. Both cytokines stimulate the production of IL-6 from synovial cells in RA patients *in vitro* (42). Elevated levels of IL-6 are constantly observed in RA patients (43,44) and moreover, correlations between elevated IL-6 levels in sera or synovial fluid and the grade of disease activity have been established (45,46). A polymorphism in the IL-6 promoter which seems to be associated with an increase in disease susceptibility and activity has been noted in some RA patients (47). It is believed that the biological activity of IL-6 contributes to some symptoms of RA such us the induction of acute phase proteins (35), autoantibody production, induction of osteoclasts (38) and increased platelet numbers (39).

Therefore, inhibition of IL-6 signaling constitutes a new therapeutic tool for the treatment of this disease. So far, the only anti-IL-6 strategy in humans has been the use of tocilizumab, a humanized murine anti-human IL-6R antibody (48). In vitro, tocilizumab has been confirmed to bind both the soluble and membrane-bound forms of IL-6R and to inhibit the pro-inflammatory activity of IL-6 by inhibiting the binding of IL-6 to its receptor (49).

A series of clinical studies using tocilizumab in RA patients showed that administration of anti-IL6R antibody significantly improved all measures of disease activity based on the American College of Rheumatology criteria (50,51).

In other clinical trials tocilizumab has been shown to be therapeutically effective for other inflammatory diseases such as Castleman's disease (52,53), juvenile idiopathic arthritis (54) and Crohn's disease (55). Since IL-6 is a physiologically essential cytokine, adverse effects following anti-IL-6 therapy may occur. The long term safety of humanized anti-IL-6R therapy remains to be carefully examined.

1.2 Dendritic cells and their functions

Dendritic cells (DCs) are antigen-presenting cells that are specialized in the activation of naive T-cells and the initiation of an immune response. They originate from hematopoietic stem cells and can be characterized as immature or mature DCs as defined by the expression of phenotypic cell surface markers (56). Immature DCs are typically characterized by the lack of co-stimulatory molecules CD80 and CD86. They are located in the peripheral tissues, where they are adapted to capture antigen and alert for multiple danger signals such as inflammatory cytokines, microbial products and cytoplasmatic/nuclear molecules released as a consequence of cellular necrosis. Exposure to these factors triggers DC maturation, a process that leads to expression of high levels of the co-stimulatory molecules CD80, CD86 and CD40, the acquisition of high surface levels of major histocompatibility complex (MHC) II as well as the production of a broad panel of cytokines

including TNF-α, IL-6, IL-10 and IL-12. Subsequently, mature DCs leave the peripheral tissues and migrate to the T-cell rich areas of draining lymphoid organs where they activate antigen-specific T-cells.

During the process of antigen-presentation, DCs are also activated via the interaction of CD40 with CD40 ligand expressed on T-cells and thereby produce IL-12 and IL-6. Multiple studies have shown that DC-derived IL-12 drives polarization of naïve $CD4^+$ T-cells towards a T-helper 1 (T_H1) type, while IL-6 is involved in T_H2 polarization (57) and has been shown to impede T_H1 responses (58). Recently, it has been shown that IL-6 produced by DCs from Lupus-prone mice inhibits the suppressive function of $CD4^+$ $CD25^+$ regulatory T-cells (59). T-regulatory ($T_{reg)}$ cells control the autoreactive components of the immune system (60) and suppress pathogenic autoimmunity in healthy individuals. Therefore impaired T_{reg} cells development and functions have been shown to be the cause of several autoimmune diseases (61).

1.3 VAF347, a novel low molecular weight immunomodulator

VAF347 was originally identified in a screening campaign designed for the identification of compounds that inhibit IgE production in human B-lymphocytes in an isotype-specific fashion. The initiation of IgE synthesis in B-lymphocytes requires the T_H2-cell derived cytokine IL-4 and direct T-cell/B-cell contact which involves interaction of CD40 ligand on T-cells and CD40 on B-cells. Together these two signals induce B-cell activation and trigger the differentiation into plasma cells which undergo immunoglobulin class switching (62) to secrete IgE. VAF347 inhibits IL-4 + anti-CD40 as well as IL-13 + anti-CD40 induced IgE production in purified human B-cells in a dose-dependent fashion with an inhibitory concentration (IC_{50}) of approximately 1 nM (63). In contrast, VAF347 does not inhibit the production of IgG isotypes or IgA in B-cells, demonstrating that VAF347 inhibits IgE production in an isotype-specific fashion.

Further biological profiling of VAF347 in other cell types known to be relevant in atopic disease showed that VAF347 had no effect on T-cells, mast cells, endothelial cells, keratinocytes and fibroblasts. In contrast to these cells, VAF347 inhibits human monocyte-derived DCs in their function to induce T-cell proliferation and cytokine production (63). VAF347 does not directly act on T-cells since activation of T cell proliferation and IL-2 production by antibodies to CD3 and CD28, in the absence of DCs are not affected. Furthermore, VAF347 was shown to downregulate the induced expression of CD86 and human leukocyte antigen (HLA)-DR on the cell surface of human monocyte-derived DCs. Thus, VAF347 has inhibitory effects on DC differentiation and maturation as well as the antigen presenting and T-cell stimulatory capacity of these cells. In addition, VAF347 was shown to inhibit the production of IL-6 in mature DCs in a dose-dependent fashion with an IC_{50} of 1nM. The synthesis of other soluble products like the chemokines MDC or

TARC, known to be induced in mature DCs, was not affected. Due to the specific inhibition of IL-6, VAF347 does not act as a general inhibitor of DC maturation suggesting that the compound targets a specific signaling pathway(s) induced by the maturation stimuli.

In vivo profiling of the biological effects of VAF347 showed that in an antigen-induced mouse model of eosinophilic lung inflammation, VAF347 blocked lung eosinophilia, mucus hyperplasia and serum IgE levels (63). In these experiments VAF347 was superior to suplatast tosilate, a marketed compound (Taiho) which has been used since 1995 for the treatment of patients with asthma. Suplatast tosilate was considered a relevant mechanistic comparator based on the proposed mode of action as an inhibitor of T-cell derived IL-4 and IL-6 production (64), thus resulting in suppression of IgE synthesis and block of pulmonary inflammation *in vivo* (65). The anti-inflammatory effects of VAF347 *in vivo* are most likely mediated by the immunoregulatory role of VAF347 on DCs since allergic lung inflammation was also inhibited in B-cell-deficient mice (63).

A novel study with VAG539, a water-soluble derivative of VAF347, demonstrated that oral administration of VAG539 promotes long-term graft acceptance and active tolerance in Balb/c mice transplanted with MHC-mismatched pancreatic islet allografts (66). Tolerance induction was due to immuno-modulation of DCs since transfer of tolerant DCs into naive mice followed by allogeneic islet transplantation prevented graft rejection. Furthermore, cell therapy with *in vitro* VAF347 treated bone marrow derived DCs also led to strongly decreased numbers of rejected islets. DCs probably were not the only cell type responsible for tolerance induction since treatment with VAG539 resulted in increased frequency of splenic $CD4^+$ T-cells expressing CD25 and Foxp3, markers associated with T_{reg} cells. The transfer of $CD4^+$ $CD25^+$ T_{reg} cells from these mice into newly transplanted mice promoted graft acceptance.

1.3.1 Identifying the molecular target(s) of VAF347

The molecular target(s) of VA347 have not been identified so far. As an approach to better understand which pathways may be regulated by VAF347, immature monocyte derived DCs were activated by engagement of CD40 in the presence or absence of VAF347 for 8 hours before the genome wide expression pattern profile was determined by RNA chip analysis (67). Among the top 15 down–regulated genes in VAF347 treated DCs was the IL-6 gene, thus validating the RNA chip analysis.

To identify genes that are known to be regulated by a common signaling pathway the top 15 induced genes were examined. Interestingly, 3 out of the 15 top induced genes namely the aryl hydrocarbon receptor repressor (AHRR), cytochrome P450 1B1 (CYP1B1) and TCDD inducible poly(ADP-ribose) polymerase (TiPARP), are known to be regulated by aryl hydrocarbon receptor

(AhR) signaling. These results indicated that VAF347 may function as an activator of AhR signal transduction.

1.4 The aryl hydrocarbon receptor (AhR)

1.4.1 Function and structure of the AhR

The aryl hydrocarbon receptor is a ligand-activated transcription factor that plays a central role in the induction of a broad range of biotransformation enzymes. AhR is found to be ubiquitously expressed in most cells and organs of the body (68) and is considered as the crucial factor in regulation of xenobiotic metabolism. Xenobiotics are innumerable chemical compounds of natural or synthetic origin, which are foreign to the human body, such as environmental pollutants, drugs or food additives. Biotransformation of xenobiotics is formally divided into three phases: in Phase I usually a polar moiety is introduced into the molecule. In Phase II the oxygenated products of Phase I are conjugated to small endogenous molecules such as glutathione, glucuronic acid, cysteine or acetate. Phase III describes the transmembrane export of these metabolized xenobiotics (69).

The aryl hydrocarbon receptor belongs to the small family of basic helix-loop-helix (bHLH) transcription factors which also includes the transcriptional regulators Per (Period), AhR nuclear translocator protein (ARNT) and Sim (Single minded). All members of this protein family share a bHLH motif in the NH_2 terminal region (**Figure 1.4.1.1**), which is involved in DNA binding and homo- or heterodimerization.

Adjacent to the COOH-terminus of the bHLH region follows the PAS domain, which has been named after the first three proteins identified with this motif: the Drosophila Per protein, human ARNT and Drosophila Sim (70). Proteins of the bHLP/PAS family can mediate a broad range of diverse biochemical functions including the involvement in circadian rhythms, organ development, neurogenesis and metabolism. Members of the bHLH protein family have been found in mammals, flatworms, insects, fungi, plants and cyanobacteria (71,72). Usually the PAS domain consists of 260-310 amino acids and contains two conserved hydrophobic repeats of 50 aa, named PAS-A and PAS-B, which are both involved in homo- or heteroformation. In the case of AhR the PAS domain facilitates heterodimerization of the AhR with its partner molecule aryl hydrocarbon receptor nuclear translocator (ARNT) (73).

The ligand binding domain is located between amino acids 230 – 431 of AhR (**Figure 1.4.1.1**), and thus partially overlaps with the PAS-B region as well as the region necessary for binding of heat shock protein 90 (Hsp90) (74). Hsp90 interacts with parts of the PAS-B region and also with the bHLH-region to mask the nuclear localization signal of AhR, thus keeping the receptor in the cytoplasm.

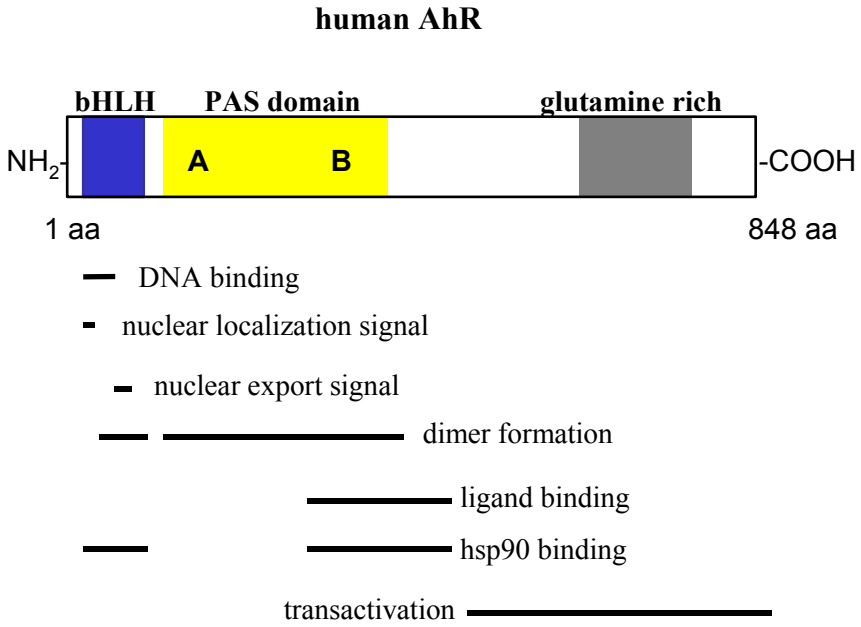

Figure 1.4.1.1: ***Schematic representation of functional domains of AhR****. In the NH_2-terminal region AhR contains a bHLH (basic helix-loop-helix) motif (blue box), involved in DNA binding and homo- or heterodimerization. Adjacent to the COOH-terminus of the bHLH region follows a PAS (Per-ARNT-Sim) domain (yellow box) which is considered as an interactive platform for homo- or heterodimer formation. A glutamine rich region at the COOH-terminus is shown in grey. The location of functional domains is indicated by bars.*

In addition, AhR contains a nuclear export signal in the second helix of the bHLH domain which is necessary for the nuclear export of AhR (75). The transactivation domain is broadly distributed in the COOH-terminal half of the AhR (**Figure 1.4.1.1**). Upon dimerization with ARNT, the AhR/ARNT heterodimer transmits its transactivation activities to general transcription factors through interaction with Sp1, CBP/p300, RIP140, and SRC-1 (76-79).

1.4.2 Ligands of AhR

The AhR can be activated by a broad range of diverse classes of compounds, including exogenous ligands such as polycyclic aromatic hydrocarbons (PAHs) and halogenated aromatic hydrocarbons (HAHs) as well as endogenous ligands. The prototypical ligand of AhR is 2,3,7,8-tetrachlorodibenzo-p-dioxin (TCDD), which belongs to the family of HAHs. HAHs are usually generated in industrial production or as a product of waste incineration. TCDD has been shown to induce a broad spectrum of biochemical and toxic effects, including the induction of drug-

metabolizing enzymes, teratogenesis, immunosuppression, tumor promotion and the induction of chloracne. Part of TCDD's toxicity is its half-life of 11 years in humans.

PAHs compromise a large class of AhR ligands that usually contain four or more conjugated benzene rings. PAHs are produced as a product of combustion processes and are therefore commonly found in charbroiled foods, smoke exhaust and chimney soot.

Studies which examined the binding activity of AhR ligands, using large numbers of PAHs and HAHs suggest that the AhR ligand binding pocket accepts planar ligands with maximal van der Waal's dimensions of 14 x 12 x 5 Å (80,81). For a high binding affinity the electronic and thermodynamic properties of the ligand seem to be important, though the formulation of an exact structure has yet to be determined (81).

Some of the ligands that bind AhR include therapeutic drugs, such as the benzimidazole omeprazole. Omeprazole is a proton pump inhibitor which is used for the treatment of heartburn and peptic ulcers. At high concentrations omeprazole induces the expression of CYP1A1, CYP1A2 and related monooxygenases via activation of AhR (82,83).

Since PAHs and HAHs are not commonly synthesized by living organisms but are mainly products of industrialization, exposure of AhR to these "novel" pollutants represents a new event from the standpoint of evolutionary pressure. Although PAHs may have been generated by naturally occurring combustion processes such as forest fires, it is believed that the emergence of the AhR signaling system throughout evolution was also dependent on endogenous AhR ligands.

So far, only a few naturally occurring endogenous AhR ligands have been proposed, including the indigoids indirubin and indigo (84,85), the heme metabolites bilirubin and biliverdin (86), arachidonic acid metabolites (87,88) as well as tryptophan metabolites (89). These supposed endogenous ligands all have in common that they induce AhR activation *in vitro* only at very high doses, at concentrations which are normally not present in a physiologic environment (90). Therefore, the ability of these endogenous ligands to activate AhR and induce specific target gene transcription under physiological conditions remains to be determined.

1.4.3 The AhR signaling pathway

In the absence of a ligand, AhR is located in the cytoplasm associated in a complex with two molecules of the heat shock protein 90 (hsp90), a molecular chaperone that maintains the cytosolic complex (91-93), a 38kDa immunophilin-related protein named hepatitis B virus X-associated protein 2 (XAP2) (94-96) and the co-chaperone p23 (97) (**Figure 1.4.3.1**).

Interestingly, the AhR has been shown to rapidly shuttle between the cytoplasm and the nucleus in a ligand independent fashion (98-100). However, the physiological significance of these observations remains to be elucidated.

Upon binding of ligand to AhR, the receptor undergoes conformational changes which ultimately lead to the exposure of the AhR nuclear localization signal (**Figure 1.4.3.1**). The whole complex is translocated to the nucleus where AhR dissociates from its chaperone proteins and associates with its partner molecule ARNT. The association of AhR and ARNT reconstitutes an active transcription factor that can bind to defined DNA sequences with high affinity. Binding of this heterodimeric transcription factor to xenobiotic-responsive elements (XRE) (101), located in the promoter region of AhR regulated genes finally leads to their transcription. The typical XRE core consensus sequence was determined to be 5'-TNGCGTG-3'.

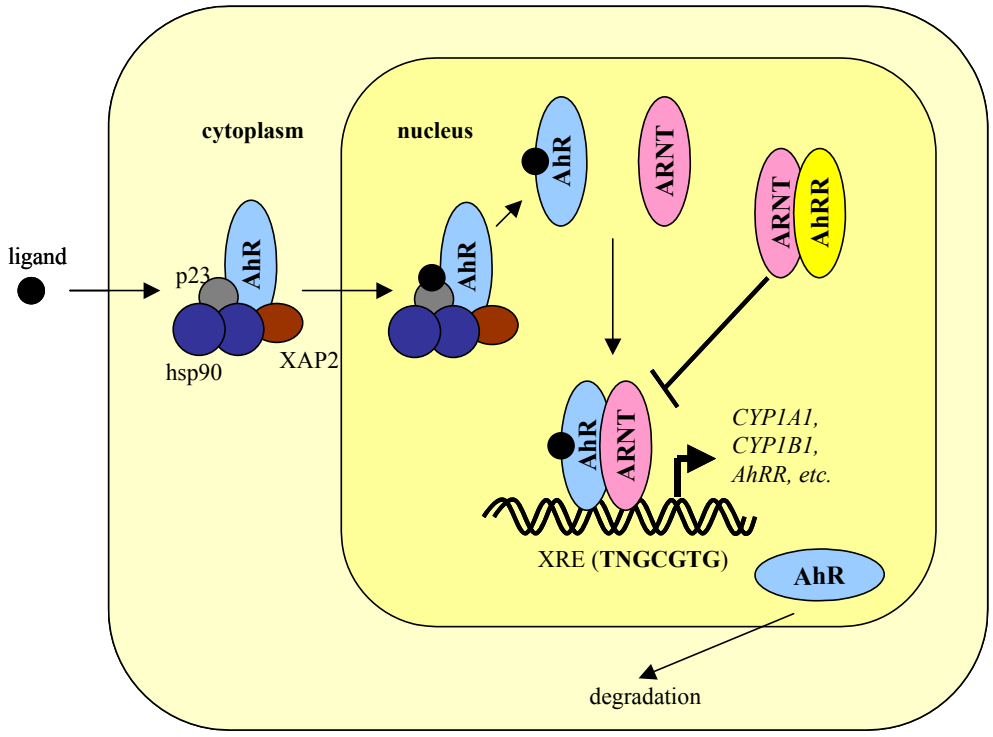

Figure 1.4.3.1: ***An overview of the AhR signaling pathway****. In the absence of ligand AhR exists in an inactive complex with the cochaperones p23 and XAP2 as well as two molecules of the chaperone hsp90. Ligand diffuses into the cell and is bound by cytosolic AhR, leading to a conformational change that exposes the nuclear localization signal of AhR. Ligand-bound receptor complex translocates to the nucleus, AhR is released and dimerizes with its partner molecule ARNT. Together the AhR/ARNT dimer binds to XREs (xenobiotic-responsive elements) and leads to the transcriptional activation of target genes, such as CYP1A1, CYP1B1 and AhRR. The dimer of ARNT and AhRR downregulates the transcriptional activity of AhR. AhR is exported to the cytoplasm and degraded.*

Up to now a wide number of target genes for the AhR are known including Phase I drug metabolizing enzymes such as members of the cytochrome P450 family including CYP1A1, CYP1A2 and CYP1B1, and Phase II drug metabolizing enzymes including uridine diphosphate glycosyltransferase 1 family polypeptide A1 (UGT1A1), NADPH-quinone-oxidoreductase and glutathione S-transferase (GST)-YA subunit (69).

AhR is also subject to negative regulation: the activation of AhR leads to the upregulation of the aryl hydrocarbon receptor repressor (AhRR), a basic HLH-PAS protein with high sequence similarity to the AhR. AhRR represses the transcriptional activity of AhR by binding to ARNT and by having repressive activity derived from the interaction of the AhRR/ARNT complex with XREs (102), thus negatively regulating AhR signaling. Following ligand-activation and nuclear export (75), the AhR is degraded via a 26S proteasome pathway (103-105).

1.4.4 Molecular mechanisms of AhR functions in the regulation of cytochrome P450 genes

Much of our knowledge about the multiple functions of AhR derives from studies of the mechanisms by which the prototypical ligand TCDD activates AhR and induces target gene transcription. One of the genes that was found to be activated upon TCDD exposure was CYP1A1 (106), a member of the cytochrome P450 family which consists of 57 members in humans. CYP1A1 is a microsomal enzyme, predominantly found in the endoplasmatic reticulum and is primarily expressed in hepatic tissues in human. It catalyzes the monooxygenation of a broad range of xenobiotics as a part of their detoxification process, thus bioactivating many of these xenobiotics to carcinogens (107). For example, CYP1A1 first metabolizes benzo[a]pyrene (B[a]P) to B[a]P-4,5-epoxide, which is then hydrolysed by the Phase II enzyme epoxide hydrolase to B[a]P-7,8 diol-9,10 epoxide, a molecule which is highly active with DNA. Other compounds which are bioactivated in a similar way like B[a]P are benzo[a]anthracene and benzo[a]fluoranthene (108).

Binding of ligand to AhR triggers its translocation to the nucleus where it partners with ARNT to form a heterodimeric transcription factor that binds to XRE elements in the 5' upstream region of the CYP1A1 gene. For instance, in the mouse CYP1A1 promoter at least six copies of XREs were identified. Successful binding of AhR/ARNT heterodimer induces chromatin remodeling and facilitates the association of the transcription factor Sp1 to its consensus recognition site in the CYP1A1 promoter (109). The AhR/ARNT complex has been described to interact with Sp1, thus enhancing CYP1A1 transcription synergistically with Sp1 (76). Together AhR/ARNT transmit their transactivation activities to general transcription factors. In the case of ARNT through interaction with CBP/p300 and for AhR by acting as a coactivator on RIP140 and SRC-1 (77,78).

1.4.5 AhR-null mice

Studies in mice lacking AhR gene expression have provided first-hand information about the involvement of AhR in diverse physiological processes. These animal models demonstrated that the AhR is essential for mediating dioxin-induced toxicity (110) and carcinogenesis (111). AhR null mice exhibit skin alterations (112), cardiac hypertrophy (113) and decreased accumulation of lymphocytes in the spleen and lymph nodes (114). The livers of mice lacking AhR gene expression are smaller in size and show lipid accumulation and portal fibrosis (114,115). Furthermore, AhR has been shown to be involved in ovary development which affects reproduction. Female AhR-null mice have difficulties in maintaining pregnancy and their pubs show poor numbers of survival during lactation and weaning (116).

1.4.6 Roles of AhR in cell physiology

The constitutive expression pattern of AhR during development and in adult tissues (117), the large degree of conservation among different species (118) and the phenotypic alterations in AhR-null mice (114,119,120), have provided strong support that AhR is involved in multiple cell physiologic processes independently of xenobiotic metabolism.

One intriguing aspect of AhR biology is the ability of AhR to either promote or inhibit cell proliferation depending on the cell type. For example, the AhR has been shown to physically interact with NF-κB p65 in human breast cancer MCF-7 cells, leading to transactivation of the c-Myc proto-oncogene and thereby increased cell proliferation (121). Constitutive over-expression of active AhR in mice resulted in increased frequency of N-nitrosodiethyl-amine induced hepatocarcinomas (122) and tumors in the glandular stomach (123), demonstrating oncogenic activity of this receptor.

On the other hand, multiple reports demonstrated that the AhR has anti-proliferative activity. Physical interaction of AhR with the retinoblastoma (pRb) tumor suppressor protein has been shown, a process leading to pRB-mediated inhibition of E2F-dependent transcription and thus resulting in cell cycle arrest (124).

Activation of the AhR in mice by a single exposure to TCDD leads to profound immune suppression of both antibody- and cell-mediated immune responses which alters host resistance to many diseases (125). Also in humans exposure to TCDD has been linked to altered immune functions, especially when exposure occurred during fetal/neonatal development (126,127). The mechanisms that drive AhR dependent immune suppression became elucidated only recently by the observation that activation of AhR by TCDD in $CD4^+$ T-cells leads to the generation of $CD4^+$ T-cells that express high levels of CD25, glucocorticoid-induced TNFR (GITR) and CTLA-4 and only low levels of CD62L, a phenotype associated with regulatory T cells (T_{reg}) (128). T_{reg} cell

function and differentiation are driven by the transcription factor Foxp3 (129,130). The development of T_{reg} cells is closely related to the generation of IL-17 producing T cells (T_H17), which express the transcription factor ROR-γt (131). T_H17 cells are involved in the control of extracellular pathogens and were shown to have important roles in experimental and human autoimmunity (132). T_{reg} cells are usually induced by transforming-growth factor (TGF)-β1, while TGF-β1 in combination with IL-6 or IL-21 has been shown to induce the differentiation of T_H17 cells (133,134).

Recently, activation of AhR by TCDD has been shown to induce the generation of T_{reg} cells in mice that were able to suppress experimental autoimmune encephalomyelitis (EAE, a mouse model for multiple sclerosis) by a TGF-β1-dependent mechanism (135). In contrast, activation of AhR by 6-formylindolo[3,2-b]carbazole (FICZ) interfered with T_{reg} cell differentiation and instead boosted T_H17 cell differentiation (136) and worsened EAE (135). Finally, activation of AhR signaling by TCDD in human synovial tissue obtained from rheumatoid arthritis (RA) patients was shown to induce the expression of inflammatory cytokines, an effect that was transmitted via the NF-κB and ERK signaling cascades (137). Therefore, exposure of RA patients to AhR activators, which are commonly found in normal dietary food in industrialized countries, is thought to exacerbate RA pathophysiology. These data demonstrate that AhR regulates both T_{reg} and T_H17 cell differentiation in a ligand specific fashion which could make AhR a novel target for the therapeutic manipulation of the immune response.

1.5 Aim

The aim of this study was to identify the molecular target(s) of VAF347 that leads to inhibition of IL-6 expression in Monomac1 (MM1) cells. Similar to human monocyte-derived DCs, VAF347 inhibits expression of IL-6 in MM1, however the molecular mechanism is unknown.

Overproduction of IL-6 is critically involved in several inflammatory and autoimmune diseases including rheumatoid arthritis, Crohn's disease, Castleman's disease and juvenile idiopathic arthritis. Therefore, understanding the molecular mechanism(s) by which VAF347 interferes with IL-6 expression might provide new insights for the treatment of these diseases.

2. MATERIALS AND METHODS

All work was done in the Novartis Institutes for Biomedical Research (NIBR), Vienna, Austria in the laboratory of Univ.-Doz. Dr. Maximilian Woisetschläger. If not mentioned otherwise all reagents/solutions were supplied by the Nährbodenküche of the NIBR.

2.1 Standard Methods

2.1.1 Qiagen Plasmid Miniprep

A single TG1 E. coli colony from a freshly streaked LB-Ampicillin selective plate was used to inoculate 2ml of Luria-Bertani (LB)-Broth medium, containing the antibiotic ampicillin at a concentration of 100µg/ml and was shaken for 16h at 37°C. 1.5ml of this dense bacteria suspension were transferred into an eppendorf tube and harvested by centrifugation for 5min at 5.000rpm in an Eppendorf Centrifuge. After removal of the supernatant the pellet was resuspended in 250µl of resuspension buffer P1, supplemented with 250µl of Lysis buffer P2 and turned over a few times to mix. After the addition of 350µl of neutralisation buffer P3 the tube was inverted immediately 4-6 times and then centrifuged for 10min at 13.000rpm. The complete supernatant was transferred onto a QIAprep 2ml collection tube and centrifuged for 1min at 13.000rpm. The eluate was discarded, 0.5ml of washing buffer PB were added onto the column and the tube was again centrifuged for 1min at 13.000rpm. The eluate was discarded, 0.75ml of buffer PE were added and the tube was centrifuged for 1min at 13.000rpm. After the eluate was discarded completely, the tube was centrifuged for 1 min at 13.000rpm to remove residual wash buffer. The dry spin column was put into a fresh eppendorf tube, 50µl of nuclease free H_2O was added to the center of the column and incubated for 1min at RT. The DNA was eluted by centrifugation for 1min at 13.000rpm. The eluate in the tube contained the plasmid-DNA which was stored at –20°C until use.

2.1.2 Qiagen Plasmid Maxiprep

A single TG1 E. coli colony from a freshly streaked LB-Ampicillin selective plate was picked to inoculate a starter culture of 2ml Luria-Bertani (LB)-Broth medium containing the antibiotic ampicillin at a concentration of 100µg/ml. This starter culture was incubated for about 8h at 37°C with vigorous shaking. 500µl of this culture were used to inoculate 250ml LB-medium, with 100µg/ml ampicillin added and the culture was shaken for 16h at 37°C. The dense bacterial culture was transferred into a GS3 plastic container and was harvested by centrifugation for 10 minutes at 6000rpm in a Sorvall Centrifuge (RC-5C, Sorvall Instruments) at 4°C. The supernatant was removed and the pellet was resuspended in 10ml of Buffer P1 (Resuspension Buffer containing RNase A). After the pellet was completely resuspended, 10ml of Buffer P2 (Lysis Buffer) were added, mixed gently by swirling and incubated for 5min at RT. After the addition of 10ml of chilled

Buffer P3 (Neutralisation Buffer) and immediate mixing, the complete lysate was poured into the barrel of the QIAfilter Cartridge, which has been closed with a cap on its outlet noozle before, and left for 20min at RT. In the meantime a QIAGEN-tip 500 was equilibrated by applying 10ml Buffer QBT and allowing the column to empty by gravity flow. After the incubation of the lysate, the cap from the QIAfilter Cartridge outlet noozle was removed. The supplied plunger was gently inserted into the QIAfilter Cartridge and the lysate was directly filtered onto the previously equilibrated QIAGEN-tip 500. The cleared lysate was allowed to enter the resin by gravity flow. The QIAGEN-tip 500 was washed twice with 30ml buffer QC. Afterwards the DNA was eluated with 15ml Buffer QF (Elution Buffer) into a SS34 tube and precipitated by adding 10.5ml RT-Isopropanol (Merck). After mixing the precipitated DNA was centrifuged immediately at 15.000rpm for 30min at 4°C in the SS34 rotor. After the supernatant was carefully removed, 5ml of room temperature (RT) 70% ethanol were added onto the pellet to remove precipitated salt. Then the tube was centrifuged at 15.000rpm for 10 minutes at 4°C. The supernatant was removed completely and the pellet was air-dried for 5 min and redissolved in 400µl nuclease free H_2O. The DNA concentration was first measured at 260/280nm in a Biophotometer (Eppendorf) and afterwards diluted to a final concentration of 1µg/µl and stored at –20°C until use (see 2.1.3).

2.1.3 DNA-Concentration Measurement

2µl of DNA solution (in nuclease free H_2O) were diluted 1:50 with nuclease free H_2O in an Eppendorf UVette and measured in a photometer (Eppendorf) at 260nm and 280nm after calibration with nuclease free H_2O alone as blank. And optical density OD_{260}=1 equals 50µg/ml dsDNA, meaning that a measured OD of 0.2 (of a 1:100 dilution) gives a concentration of 1µg/µl.

2.1.4 Agarose gel electrophoresis

All DNA gel seperations were done on a 1% agarose gel, run in 1xTBE. Ethidium bromide (Sigma-Aldrich) was added to make DNA visible under UV-light. Usually 1g of agarose (GIBCO) was heated to 100°C in 1xTBE, cooled down to 60°C and then 6µl ethidium bromide were added. DNA samples were mixed with 10xBlue Juice Gel loading buffer (Invitrogen) before loading onto the gel. The 100 base pairs (bp) ladder (Invitrogen) was used as size marker. All gels were run using the BioRad Electrophoresis Power Supply Unit, for 45min at 80V.

2.1.5 QIAquick Gel Extraction Kit

DNA was visualized with ethidium bromide on a 1% agarose gel, run in 1xTBE. The DNA fragment was cut out from the agarose gel with a clean, sharp scalpel and transferred into a 1.5ml Eppendorf tube. After the gel slice was weight, 3 volumes of Buffer QG were added to 1 volume of

gel (for example 0.3ml of Buffer QG were added to 0.1g gel slice) and incubated for 10 min on a heating block at 50°C. To ensure that the agarose was dissolved completely the tube was shaken every 3 minutes during heat incubation. After the gel slice had dissolved completely, 1 gel volume of isopropanol (Merck) was added to the sample and mixed. To bind DNA, the complete solution was transferred on a QIAquick column and centrifuged for 1 min at 13.000rpm. After the flow-through was discarded, 0.5ml of Buffer QG were added to the QIAquick colum and centrifuged again for 1 min at maximum speed. Flow-through was discarded and 0.75ml of wash Buffer PE were added to the QIAquick column and centrifuged for 1 min at 13.000rpm. After complete removal of flow-through the QIAquick column was again centrifuged for 1 min at maximum speed to remove residual wash buffer. The QIAquick column was placed in a clean 1.5ml Eppendorf tube and 10µl of nuclease free H_2O were added to the centre of the QIAquick membrane. To elute DNA, the Eppendorf tube was centrifuged for 1 min at 13.000 rpm. Eluted DNA was ready for further use e.g. enzyme restriction, ligation or transformation.

2.2 Generation of templates usable for RT-PCR

2.2.1 Absolutely RNA RT-PCR Miniprep Kit (Stratagene)

Suspension cells were harvested by centrifugation at 1300rpm for 7 min, medium was removed completely and the cell pellet was lysed in an appropriate amount of Lysis Buffer, usually 400µl Lysis Buffer for $1x10^6$ cells. Before use 0.7µl β-Mercaptoethanol/100µl Lysis Buffer were added, then the cells were lysed. The cell pellet was completely homogenized by vortexing and repeated pipetting. Up to 700µl of this homogenate were transferred to a Prefilter Spin Cup that was seated in a 2-ml receptacle tube and the cap was snapped onto the spin cup. The tube was centrifuged for 5 min at 13.000 rpm in an Eppendorf Centrifuge. The spin cup was removed and discarded, only the filtrate was retained. An equal volume of 70% ethanol was added to the filtrate, and the tube was vortexed thoroughly for at least 5 seconds. Up to 700µl of this mixture were transferred to an RNA Binding Spin Cup that was seated in a fresh 2-ml receptacle tube. The tube was centrifuged for 1min at maximum speed. The flow-through was discarded and this step was repeated for the remaining lysate-ethanol mixture.

After the lysate had been loaded onto the RNA Binding Spin Cup, 600µl of 1xLow-Salt Wash Buffer were added onto the column, the cap of the tube was snapped and the tube was centrifuged for 1 min at maximum speed. The flow-through was discarded and the tube was centrifuged for two further minutes to allow the spin cup to dry. In the mean time the DNase solution was prepared by gently mixing of 50µl DNAse digestion buffer with 5µl of reconstituted RNase-free DNAseI. The DNase solution was added directly onto the fibre matrix inside the spin cup, and the tube was capped. Each sample was incubated for 15 min at 37°C in an air incubator to allow complete DNase

digestion. After this incubation step 600µl of 1x High-Salt Wash Buffer were added to the spin cup and the tube was centrifuged for 1 min at maximum speed. Again the flow-through was discarded, and 600µl of 1x Low-Salt Wash Buffer were added onto the spin cup. The tube was centrifuged for 1 min at maximum speed, flow-through was discarded and 300µl of 1x Low-Salt Wash Buffer were added onto the spin cup. The tube was centrifuged for 2 min at maximum speed to allow the RNA binding membrane to dry. The spin cup was then transferred to a clean and RNase free 1.5ml Eppendorf tube. Finally 100µl of Elution Buffer (supplied in the Kit) were added directly onto the centre of the fiber matrix inside the spin cup. The tube was capped and incubated for 2 min at room temperature. Then the tube was centrifuged for 1 min at maximum speed to elute RNA. The purified RNA was quantified by measuring the optical density (2.2.2) and stored immediately at -80°C until further use.

2.2.2 RNA-Concentration Measurement

2µl of RNA solution (in nuclease free H_2O) were diluted 1:50 with nuclease free H_2O in an Eppendorf UVette and measured in a photometer (Eppendorf) at 260nm after calibration with nuclease free H_2O alone as blank. And optical density OD_{260}=1 equals 40µg/ml ssRNA, meaning that a measured OD_{260} of 0.1 (of a 1:100 dilution) gives a concentration of 4µg/ml RNA.

2.2.3 iScript cDNA Synthesis

The cDNA synthesis was performed with the iScript cDNA Synthesis Kit (Bio Rad) as suggested by the manufacturer. 0.7µg of RNA were diluted to a volume of 15µl with nuclease free H_2O and mixed with 4µl of 5x iScript Reaction Mix. Then 1µl of the enzyme *Reverse Transcriptase* was added to each sample. The samples were put in a Mastercycler gradient (Eppendorf) using the conditions 5 min at 25°C, 30 min at 42°C and 5 min at 85°C. The cDNA was used for RT-PCR as described in 2.3. After use the cDNA was stored at -20°C.

2.3 Quantitative Reverse Transcription Polymerase Chain reaction (RT-PCR)

Quantitative RT-PCR reactions were performed in an ABI Prism 7700 Sequence Detector machine (Perkin Elmer) using 96well Optical Reaction Plates with Barcode, code 128 (Applied Biosystems). The Sybr-Green 2x Mix (Applied Biosystems) was used as a fluorescent dye which already contained all components necessary, excluding the primer and the cDNA template. Every cDNA template was analyzed in duplicates with the same primer pair. Therefore, maximally 4 different primers were distributed horizontally, each single primer covering two rows of the 96well plate when using 12 samples. Primers for the elongation Factor-1α (eF-1α) were always included in every experiment for the normalization of the template.

A single 25µl PCR reaction, consisted of 12.5µl of the 2x Sybr-Green mix, 9.84µl of nuclease free H_2O and 0.83µl of forward and reverse primer (100ng/µl). Routinely, this was pipetted as a mastermix for each template needed and then 24µl were aliquoted into the corresponding wells of the 96 well plate. Then 1µl of cDNA was added into the upper part of each well. After a short quickspin of the 96well plate, the PCR plate was fully sealed with Optical Adhesive Covers (Applied Bioscience). Finally a compression pad was put onto top of the sealed 96well plate with the grey side down. Now the 96well plate was ready for insertion into the ABI7700 machine. The following PCR-parameters were used: one cycle of 2min at 50°C and 10min at 95°C followed by 40 cycles of 15sec at 95°C and 1min at 60°C with continuous data measurement. No 72°C incubation step normally found in a PCR was used for the quantitative PCR. For every primer pair used a dissociation curve PCR was performed once. This was necessary because if a primer pair would amplify more than one template this could not be distinguished with the fluorescence detection system. Therefore, afterwards the amplified products were analyzed for different dissociation temperatures which would indicate different reaction products. The following incubation parameters were used to test this: 2min at 95°C, 15sec at 60°C with a continuous temperature increase to 95°C over a period of 19min and 59sec and a final incubation at 95°C for 15sec.

For calculation of the expression values, the average of the Ct values of the gene of interest were normalized to the average of the Ct values of the elongation Factor-1α (eF-1α) with the following equation:

$2^{(Ct\ \text{“eF-1}\alpha\text{”}-Ct\ \text{“gene of interest)}}$x1000. One example is shown in more detail: the average of the eF-1α Ct values was 20.68 and the average of the Ct values of the gene of interest IL-6 was 25.48. This resulted in the equation $2^{(20.68-25.48)}$, therefore $2^{-4.8}$ x1000 or in the end 35.89. The raw data was analyzed and graphs were made using the Excel program.

Following oligonucleotides were used:

MW1235: upstream 5´- CAGCTGACTTCATCCCTATTC-3´ and MW1236: downstream 5´-AGCTGGACATTGGCGTTCTCA-3´ for CYP1A1.

MW1237: upstream 5´- GTACATCCTCGACGGCATCTC-3´ and MW1238: downstream 5´-GGCAAGTCTCCTCATTGAATC-3´ for IL-6.

MW1556: upstream 5´- AGCGCAACAACATCGCCGTG-3´ and MW1492: downstream 5´-CTGACTCGAGCTAGCAGTGGCCGGAGGAGGCG-3´ for NF-IL6.

MW1557: upstream 5´- CCATCAAGATCAATGGCTAC-3´ and MW1558: downstream 5´-ACTGGATTCCCAGGTTCTGG-3´ for NF-κB p65.

MW1493: upstream 5´- GACTGGATCCCTGGGCACCATGATGTTCTCGGGCTTCAA-3´
and MW1560: downstream 5´- TCGAGATGGCAGTGACCGTG-3´ for c-Fos.

MW1495: upstream 5´- GACTGGATCCCTGGGCACCATGACTGCAAAGATGGAAAC-3´

and MW1559: downstream 5´- AGGTGAGGAGGTCCGAGTTC-3´ for c-Jun.
MW1554: upstream 5´- CCAGCTCAGATGAGGAGGAG -3´
and MW1555: downstream 5´- CAGGTCCAACAGGAACTGGT-3´ for PU.1.
MW1247: upstream, 5'- TTTGAGACCAGCAAGTACTATGTGACT-3' and MW1248: downstream 5'- TCAGCCTGAGATGTCCCTGTAA-3' for eF-1α. Specificity of this amplicon was verified by using the VIC^{TM} labelled probe 5'- TCATTGATGCCCCAGGACACAGAGAC -3'.

2.4 Cloning strategy of promoter reporter constructs, expression and silencing vectors

2.4.1 Cloning of an Interleukin-6 promoter reporter construct

The wild type Interleukin-6 promoter with a length of about ~800bp was cloned into the vector pGL3-basic (Invitrogen), resulting in a plasmid that contained the wild type Interleukin-6 promoter before the gene for luciferase. This plasmid was named pGL3b- IL-6 promoter.

2.4.2.A. Amplification of the wild type Interleukin-6 Promoter

The wild type IL-6 promoter was cloned as a 5' - HindIII (Klenow filled up) and 3' - BamHI cut ~820bp fragment into the vector pGL3-basic (Invitrogen). The promoter was amplified from 10ng human genomic DNA (Roche) using the PCR Primers MW1473 5'-CAGTCCATGGAAGCTTAGAGCAAAGTCCTCACTGGG-3' containing an artificial HindIIII adapter (underlined) and MW1474 5'- GACTGGATCCAGATAGAGCTTCTCTTTCGTTC-3' containing an artificial BamHI adapter (underlined). The Herculase Hotstart polymerase (Stratagene) and its corresponding 10x buffer were used in all following PCR reactions because of the high fidelity of this polymerase. The following parameters were used for amplification: 1min incubation at 95°C followed by 35 cycles of incubation for 30sec at 95°C, 30sec at 62°C and 2.30min at 72°C. The resulting PCR products were loaded onto a 1% agarose gel, containing ethidium bromide and was run for 45 min at 80V (2.1.4). Under UV-light the desired bands were cut out with a clean scalpel and the DNA was further isolated using the QIAquick gel extraction Kit protocol (2.1.5).

2.4.2.B. Restriction digestion of PCR products

The isolated PCR fragment, which was eluted in 10µl nuclease free H_2O (2.1.5) was first cut with HindIII at the 5' site in 1xNEB2 buffer, supplemented with 1xBSA for 1h at 37°C. 1µl of dNTP's (10mMol) and 1µl of Klenow Enzyme (Roche) were added to fill up the HindIII site for 20 min at RT. This reaction was stopped on a heating block at 75°C for 20 min. Then the appropriate volume of 10xBamHI buffer was added to reach a final concentration of 1xBamHI buffer in the reaction

volume, followed by the addition of 1µl of BamHI and incubation for 1h at 37°C. This resulted in a 5'- filled up HindIII site and 3'- BamHI site Interleukin-6 promoter fragment.

At the same time 0.5µg vector pGL3-basic was first cut with SmaI in 1xNEB4 buffer, supplemented with 1xBSA for 1h at 25°C. Then the appropriate volume of 10x NEB3 buffer was added to reach a final concentration of 1x NEB3 in the reaction volume, followed by the addition of 1µl of BglII and incubation for 1h at 37°C.

The digested PCR fragment and the restricted vector were both loaded onto a 1% agarose gel, after gel run the digested fragments were isolated as described above (2.1.5).

This pGL3-basic vector fragment and the Interleukin-6 promoter Insert (5'- HindIII, Klenow filled up / 3'- BamHI) were ligated as described in 2.4.2.C. Then 2µl of ligation were transformed as described in 2.4.2.D. Positive clones were selected after a XhoI, SacI control cut (in 1x NEB1 buffer, supplemented with 1xBSA, 1h at 37°C) which should result in a ~800bp fragment. One positive clone was amplified with Qiagen Maxiprep (2.1.2).

All enzymes, buffers and additional reagents (1xBSA) were purchased from New England Biolabs.

2.4.2.C. Ligation of PCR products and vector

1µl digested and gel-isolated vector DNA, 5-10µl of digested and gel-isolated insert-DNA, 2µl of 10x Ligase Buffer (Roche), 1µl of T4-DNA-ligase (Roche) and nuclease free H_2O up to a volume of 10µl were mixed together. The ligation reaction took place in a water bath at 12°C over night. As a negative control for ligation, one sample with vector only (without any insert) was always included.

2.4.2.D. Transformation

50µl of competent E. coli TG1 cells and 1-2µl of a ligation reaction (or 10ng of Qiagen Maxiprep purified DNA) were mixed gently and incubated on ice for 30min. After a heatshock for 90sec at 42°C on a heat block, the cells were left on ice for further 10min. Then 900µl of LB-Broth medium, without antibiotics were added to the cells. After an incubation for 45min at 37°C, 100µl of the bacteria solution was plated out onto a LB-Amp agar plate using a trigalski spatula. The plates were incubated at 37°C for 16h and then stored at 4°C. DNA-Minipreps from single bacterial colonies were prepared (2.1.1) and analyzed by digestion with the same enzymes used for cloning (if not mentioned otherwise). Positive clones, containing the expected fragment, were sent to Sequiserve (Germany). One correct plasmid which had one mismatch with the wild type sequence of the Interleukin-6 promoter was afterwards amplified by maxiprep (2.1.2) to generate sufficient DNA for transient transfections.

2.4.3 Cloning of a retroviral trans-dominant negative AhR expression construct

A trans-dominant negative version of AhR, corresponding to amino acids 1-515, was cloned into the retroviral vector pMX-pie, which contained an internal ribosome entry site (IRES)-GFP element. The pMX-pie vector was kindly provided by T. Kitamura, University of Tokyo, Tokyo, Japan. This plasmid was named pMX- AhR 515.

2.4.3.A. Amplification of trans-dominant negative AhR

A shorter fragment of the gene for AhR, corresponding to amino acids 1-515, was cloned as a 5' - NotI (Klenow filled up) and 3' - XhoI cut ~1550bp fragment into the vector pMX-pie and named pMX-pie-AhR 515. The shorter DNA fragment for AhR 515 was amplified from 1µl cDNA (2.2.3) of the cell line Monomac 1 (2.7.3) using the PCR Primers MW1310 5'-GTCAGCGGCCGCCTGGGCACCATGAACAGCAGC-3' containing an artificial NotI adapter (underlined) and MW1312 5'- CTGACTCGAGGTCAATTTGCTCATGTTTCAGGATT-3' containing an artificial XhoI adapter (underlined). The Herculase Hotstart polymerase (Stratagene) and its corresponding 10x buffer were used in all following PCR reactions because of the high fidelity of this polymerase. The following parameters were used for amplification: 1min incubation at 95°C followed by 35 cycles of incubation for 40sec at 95°C, 40sec at 62°C and 3.30min at 72°C. The resulting PCR products were loaded onto a 1% agarose gel, containing ethidium bromide and the gel was run for 45 min at 80V (2.1.4). Under UV-light the desired bands were cut out with a clean scalpel and the DNA was further isolated using the QIAquick gel extraction Kit protocol (2.1.5).

2.4.3.B. Restriction digestion of AhR515 PCR product and vector

The isolated PCR fragment, which was eluted in 10µl nuclease free H_2O (2.1.5) was first cut with NotI at the 5' site in 1xNEB2 buffer, supplemented with 1xBSA for 1h at 37°C. Then 1µl of 10mM dNTP's and 1µl of Klenow Enzyme (Roche) were added to fill up the NotI site for 20 min at RT. This reaction was stopped on a heating block at 75°C for 20 min. Then 1µl of XhoI was added and the reaction was further incubated for 1h at 37°C. This resulted in a 5'- filled up NotI site and 3'-XhoI site AhR 515 fragment.

At the same time 0.5µg vector pMX-pie was first cut with BamHI in 1xBamHI buffer, supplemented with 1xBSA for 1h at 37°C. Then 1µl of 10mM dNTP's and 1µl of Klenow Enzyme (Roche) were added to fill up the BamHI site for 20 min at RT. This reaction was stopped on a heating block at 75°C for 20 min. Then 1µl of XhoI was added and the reaction was further incubated for 1h at 37°C.

The digested PCR fragment and the restricted vector were both loaded onto a 1% agarose gel, after gel run the digested fragments were isolated as described above (2.1.5).

This pMX-pie vector fragment and the AhR 515 insert (5'- NotI cut, Klenow filled up / 3'- XhoI cut) were ligated as described in 2.4.2.C. Then 2µl of ligation were transformed as described in 2.4.2.D. A positive clone was selected after a EcoRI, XhoI control cut (in 1x EcoRI buffer, supplemented with 1xBSA, 1h at 37°C) which should result in a ~1250bp fragment. One positive clone which had been sequenced by Sequiserve and showed no mismatch with genomic sequence of AhR was amplified with Qiagen Maxiprep (2.1.2).

2.4.4. Cloning of a retroviral AhR gene silencing construct LMP-shAhR

The retroviral vector constructs LMP-shAhR and LMP-shControl were kindly provided by Prof. Dr. H. Strobl (University of Medicine, Vienna). First, a lentiviral vector backbone encoding shRNA mir for the AhR gene or a non silencing shRNA mir Control were purchased from Open Biosystems. The coding seqeunces for either shAhR or shControl were then subcloned into the retroviral vector MSCV-LMP (Open Biosystems) using the EcoRI and XhoI restriction sites.

2.4.5. Cloning of a retroviral NF-IL6 expression construct

The sequence of the full length NF-IL6 protein was cloned as a 5' - BamHI and 3' - XhoI cut ~1050bp fragment into the expression vector pMX-pie, resulting in the plasmid pMX-pie-NF-IL6. The DNA fragment for NF-IL6 protein was amplified from 1µl cDNA (2.2.3) of the cell line Monomac 1 (2.7.3).

The PCR Primers MW1491 5'- GACTGGATCCCTGGGCACCATGCAACGCCTGGTGGCCTG -3' containing an artificial BamHI adapter (underlined) and MW1492 5'- CTGACTCGAGCTAGCAGTGGCCGGAGGAGGCG-3' containing an artificial XhoI adapter (underlined) were used for PCR. The Herculase Hotstart polymerase (Stratagene) and its corresponding 10x buffer were used for PCR. The following parameters were used for amplification: 1min incubation at 95°C followed by 35 cycles of incubation for 40sec at 95°C, 40sec at 62°C and 3.30min at 72°C. The resulting PCR products was loaded onto a 1% agarose gel, containing ethidium bromide and the gel was run for 45 min at 80V (2.1.4). Under UV-light the desired band was cut out with a clean scalpel and the DNA was further isolated using the QIAquick gel extraction Kit protocol (2.1.5)**.** The isolated PCR fragment, which was eluted in 10µl nuclease free H_2O (2.1.5) and the vector pMX-pie were cut with BamHI and XhoI in 1xBamHI buffer, supplemented with 1xBSA and incubated for 1h at 37°C.

The digested PCR fragment and the restricted vector were both loaded onto a 1% agarose gel. After gel run the digested products were isolated as described above (2.1.5).

The pMX-pie vector fragment and the NF-IL6 insert were ligated as described in 2.4.2.C. Then 2µl of ligation were transformed as described in 2.4.2.D. Positive clones were selected after a BamHI, XhoI control cut which should result in a ~1050bp fragment and then sequenced by Sequiserve. A clone that showed no mismatch with the genomic sequence of NF-IL6 was amplified with Qiagen Maxiprep (2.1.2).

2.4.6. Cloning of a retroviral NF-κB p65 expression construct

The sequence of the full length NF-κB p65 protein was cloned as a 5' - BamHI and 3' - XhoI cut ~1650bp fragment into the vector pMX-pie, resulting in the plasmid pMX-pie- NF-κB p65. The DNA fragment for NF-κB p65 was amplified from 1ng of the plasmid RcCMV-p65 which already contained the sequence of wild-type NF-κB p65. This plasmid was kindly provided by R. deMartin (University of Medicine, Vienna).

The PCR Primers MW1467 5'- GACTGGATCCCTGGGCACCATGGACGAACTGTTCCCCCTC -3' containing an artificial BamHI adapter (underlined) and MW1468 5'- CTGACTCGAGTTAGGAGCTGATCTGACTCAGC-3' containing an artificial XhoI adapter (underlined) were used for PCR. The Herculase Hotstart polymerase (Stratagene) and its corresponding 10x buffer were used for PCR. The following parameters were used for amplification: 1min incubation at 95°C followed by 35 cycles of incubation for 40sec at 95°C, 40sec at 62°C and 3.30min at 72°C. The resulting PCR products was loaded onto a 1% agarose gel, containing ethidium bromide and the gel was run for 45 min at 80V (2.1.4). Under UV-light the desired band was cut out with a clean scalpel and the DNA was further isolated using the QIAquick gel extraction Kit protocol (2.1.5)**.** The isolated PCR fragment, which was eluted in 10µl nuclease free H_2O (2.1.5) and the vector pMX-pie were cut with BamHI and XhoI in 1xBamHI buffer, supplemented with 1xBSA and incubated for 1h at 37°C.

The digested PCR fragment and the restricted vector were both loaded onto a 1% agarose gel, after gel run the digested fragments were isolated as described above (2.1.5).

The pMX-pie vector fragment and the NF-κB p65 insert were ligated as described in 2.4.2.C. Then 2µl of ligation were transformed as described in 2.4.2.D. Positive clones were selected after a BamHI, XhoI control cut which should result in a ~1650bp fragment and then sequenced by Sequiserve. A clone that showed no mismatch with the genomic sequence of NF-κB p65 was amplified with Qiagen Maxiprep (2.1.2).

2.4.7. Cloning of the lentiviral PU.1 gene silencing construct GIPZ-sh-PU.1

The lentiviral vector constructs GIPZ-sh-PU.1 and GIPZ-sh-Control were kindly provided by Prof. Dr. H. Strobl (University of Medicine, Vienna). The lentiviral vectors encoding shRNA mir for the

PU.1 gene or a non silencing shRNA mir Control were purchased from Open Biosystems. The two lentiviral packaging vectors pPAX2 and pMD2G were also kindly provided by Prof. Dr. H. Strobl.

2.5 ELISA for human Interleukin-6

First all used wells of a Maxisorp Immuno plate (Nalgene Nunc International) were coated with 50µl 1x PBS containing anti-human Interleukin-6 antibody (R+D MAB206; 500µg/ml in PBS + 0,1% FCS) at a final concentration of 2µg/ml at 4°C over night. Then the plate was washed four times with wash buffer (PBS def. pH 7,5 + 0,05% Tween 20). Recombinant human Interleukin-6 (R+D, 20ng/µl, in PBS + 0,1% FCS) was used as standard with 2ng/ml start concentration and then diluted 1:2 in dilution buffer (PBS + 0,05% Tween 20). All samples were also diluted in dilution buffer in a final volume of 50µl/well and incubated for 2h at RT. Then the plate was washed again four times with wash buffer. Detection anti body a-human Interleukin-6-biotin conjugate (R+D BAF206, 50µg/ml in PBS + 0,1% FCS) was added at a final concentration of 40ng/ml in 50µl dilution buffer per well and incubated for 2h at RT. The plate was washed again four times with wash buffer before the enzyme-conjugate strepdavidin peroxidase (R+D), diluted 1:200 in 50µl dilution buffer, was added to each well and incubated for 30 min at RT. Meanwhile fresh substrate was prepared by mixing one volume of Solution A with one volume of Solution B supplied in the Substrate Reagent Pack Kit (R+D). The plate was washed four times in wash buffer. 50µl of fresh substrate solution were added to each well and incubated for 30 min at RT. The reaction was stopped by adding 25µl 15% H_2SO_4 to each well. Then the plate was measured in a Spectramax 190 luminometer (Molecular Devices) at 450nm (reference 570nm). Then raw data was analyzed and graphs were made using the Excel program.

2.6 Western blot analysis

2.6.1 Preparation of whole cell lysates

For the generation of whole cell lysates 2 x 10^5 Monomac1 cells were harvested by centrifugation for 7 min at 1300rpm, medium was removed and cells were resuspended in 80 µl 1 x PBS containing 1x protease inhibitor cocktail solution (Roche) and 1x phosphatase inhibitor cocktail solution (Roche). Then 80 µl of sample reducing buffer (Santa Cruz Biotechnology), which had been prewarmed to RT first, were added to the cells and mixed by pipetting up and down several times. Lysate samples were then heated on a heating block for 5 min at 95°C and cooled down to RT before they were loaded onto a Tris-Glycine gel (2.6.2).

2.6.2 Tris-Glycine gel electrophoresis, blotting to nitrocellulose membrane and blocking

Before usage of ready-made 4-20% SDS Tris-Glycine gels (Invitrogen) each slot was washed with 1 x Tris-Glycine SDS running buffer (Invitrogen) before inserting the gel into the Xcell Sure Look device (Invitrogen), which was then filled with 1 x Tris-Glycine SDS running buffer. About 50 µg of protein per sample were loaded into each slot, and 8 µl of SeeBlue®Plus2 prestained standard (Invitrogen) was used as a size marker. All gels were run using the PowerEase500 Electrophoresis Supply Unit (Invitrogen) for 1.5 h at 125V.

After the gel electrophoresis run had completed, the Tris-Glycine gel was opened by careful breakage and transferred to a Xcell II™ Blot Module (Invitrogen). Starting from the cathode core side, sandwich blotting was used: two blotting pads were inserted first, followed by a filter paper onto which the Tris-Glycine gel was carefully placed. A nitrocellulose membrane (Invitrogen) with a pore size of 0.2µm was laid slowly onto the gel, avoiding the forming of air bubbles between nitrocellulose membrane and gel. The nitrocellulose membrane was then covered with one filter paper and two blotting pads and the sandwich was closed with the anode side. All blots were run using the PowerEase500 Electrophoresis Supply Unit (Invitrogen) for 1.5 h at 25V.

After the blotting process, the nitrocellulose membrane was carefully transferred to a plastic container, with the protein side on top. Then the nitrocellulose membrane was blocked in blocking buffer (1 x TBS containing 0.1% Tween 20 and 2.5% non-fat milk (Fluka Biochemica)) and incubated at RT for at least one hour or over night at 4°C.

2.6.3 Western Blot of the aryl hydrocarbon receptor

After blocking, the nitrocellulose membrane was washed two times with wash buffer (1 x TBS containing 0.1% Tween 20) for 10 minutes each washing step, at RT. The membrane was then incubated with a 1:500 dilution of the first antibody polyclonal goat anti-human Ah Receptor IgG (Santa Cruz Biotechnology, N-19) in blocking buffer for 2 hours at RT. Then the membrane was washed with wash buffer four times, 10 min each wash step, at RT. Next the membrane was incubated with a 1:5000 dilution of the second antibody donkey anti-goat IgG (Santa Cruz Biotechnology) coupled to horse radish peroxidase (HRP) for 2 h at RT. The membrane was washed again four times with wash buffer at RT before subtrate for HRP was added (2.6.9).

2.6.4 Western Blot of STAT5 and STAT6

The nitrocellulose membrane was blocked in blocking buffer (2.6.2) over night at 4°C. On the next day the membrane was washed two times with wash buffer (2.6.3) for 10 minutes each washing step, at RT. Then the membrane was incubated with a 1:1.000 dilution of the first antibody mouse anti-human STAT5 or mouse anti-human phospho STAT5 in blocking buffer for 2 hours at RT.

The same dilution was used for mouse anti-human STAT6 or mouse anti-human phospho-STAT5 antibodies. All STAT antibodies were provided in the STAT activation sampler kit (BD Biosciences, #612477). Then the membrane was washed with wash buffer four times, 10 min each wash step, at RT. Next the membrane was incubated with a 1:10.000 dilution of the second antibody donkey anti-mouse IgG (Santa Cruz Biotechnology) coupled to horse radish peroxidase (HRP) for 2 h at RT. The membrane was washed again four times with wash buffer at RT before subtrate for HRP was added (2.6.9).

2.6.5 Western Blot of the p44/p42 MAP kinases

After blocking the nitrocellulose membrane for one hour at RT, the membrane was incubated with a 1:1000 dilution of the first antibody polyclonal rabbit anti-human p44/p42 MAP kinase (Cell Signaling Technology, #9102) or polyclonal rabbit anti-human phospho p44/p42 MAP kinase (Cell Signaling Technology, #9101) in blocking buffer over night at 4°C. On the next day the membrane was washed with wash buffer (2.6.3) four times, 10 min each wash step, at RT. Next the membrane was incubated with a 1:15.000 dilution of the second antibody goat anti-rabbit IgG (BioRad) coupled to horse radish peroxidase (HRP) for 2 h at RT. The membrane was washed again four times with wash buffer at RT, followed by incubation of the membrane with substrate for HRP (2.6.9).

2.6.6 Western Blot of NF-IL6

The nitrocellulose membrane was blocked in blocking buffer (2.6.2) over night at 4°C. On the next day the membrane was washed two times with wash buffer (2.6.3) for 10 minutes each washing step, at RT. Then the membrane was incubated with a 1:1.000 dilution of the first antibody mouse anti-human C/EBP β (Santa Cruz Biotechnology, SC-7962) in blocking buffer for 2 hours at RT. Then the membrane was washed with wash buffer four times, 10 min each wash step, at RT. Next the membrane was incubated with a 1:10.000 dilution of the second antibody sheep anti-mouse IgG (Amersham) coupled to horse radish peroxidase (HRP) for 2 h at RT. The membrane was washed again four times with wash buffer at RT before substrate for HRP was added (2.6.9).

2.6.7 Western Blot of NF-κB p65

After blocking the nitrocellulose membrane for one hour at RT, the membrane was incubated with a 1:1000 dilution of the first antibody polyclonal rabbit anti-human NF-κB p65 (Upstate Cell Signaling, #06-418) in blocking buffer over night at 4°C. On the next day the membrane was washed with wash buffer (2.6.3) four times, 10 min each wash step, at RT. Next the membrane was incubated with a 1:15.000 dilution of the second antibody goat anti-rabbit IgG (BioRad) coupled to

horse radish peroxidase (HRP) for 2 h at RT. The membrane was washed again four times with wash buffer at RT, followed by incubation of the membrane with substrate for HRP (2.6.9).

2.6.8 Western Blot of PU.1

After blocking the nitrocellulose membrane for one hour at RT, the membrane was incubated with a 1:1000 dilution of the first antibody polyclonal rabbit anti-human PU.1 (Santa Cruz Biotechnology, SC-352) in blocking buffer over night at 4°C. On the next day the membrane was washed with wash buffer (2.6.3) four times, 10 min each wash step, at RT. Next the membrane was incubated with a 1:15.000 dilution of the second antibody goat anti-rabbit IgG (BioRad) coupled to horse radish peroxidase (HRP) for 2 h at RT. The membrane was washed again four times with wash buffer at RT, followed by incubation of the membrane with substrate for HRP (2.6.9).

2.6.9 Substrate for HRP and western blot developing

The substrate for HRP was prepared by mixing one volume of SuperSignal® West Pico Stable Peroxide solution with one volume of SuperSignal® West Pico Luminol/Enhancer Solution supplied in the SuperSignal™ kit (Pierce).

After washing the membrane was incubated with fresh-prepared substrate mix for 5 min at RT. Then substrate was removed and the membrane was sealed into a transparent plastic bag and transferred to a BioMax cassette (Kodak) where it was exposed to a high performance chemiluminescence film (GE Healthcare), followed by the development of the film in a Curix60 film developer (Agfa).

2.7 Cells, cell culture conditions and inducers

2.7.1 Thawing and growing of cells from liquid nitrogen

The vials containing the frozen cells were thawed by RT and were immediately poured into prewarmed full medium. The cells were washed once, by centrifugation for 7 min at 1300rpm, removing the supernatant and resuspending them in prewarmed full medium. Cells were transferred in a cell culture flask and grown at 37°C with 5% CO_2. Cells were split every 3 to 4 days at a ratio between 1:5 and 1:10 (depending on growth speed of each cell line) with fresh medium to a final volume of 20ml.

2.7.2 Freezing of cells for liquid nitrogen storage

Cells were counted using a Neubauer type hematocytometer and were harvested by centrifugation for 7 min at 1300rpm. The cell pellet was resuspended with the needed amount of ice-cold freezing medium (90% Fetal Bovine Serum (GIBCO) and 10% DMSO) to get $1x10^7$ cells/ml. The cells were aliquoted

into 1ml Nunc Cryo tubes (Nalgene Nunc International), capped and left in a *Nalgene™ Cryo 1°C Freezing Container* (Nalgene) on -80°C for about one week. Then the cells were inserted into the liquid nitrogen tank for long term storage.

2.7.3 Monomac1 cells

The human monocytic cell line Monomac1 growed in suspension, with a round shape similar to that of fresh human monocytes. Cells were split every 3 to 4 days with fresh medium at a ratio of about 1:10. MM1 were kept in RPMI1640 supplemented with 10% heat-inactivated fetal bovine serum (GIBCO), 2mM glutamine, 100 U/ml penicillin, 100 µg/ml streptomycin, 1.5g/l sodium bicarbonate, 4.5g/l glucose, 10mM HEPES, 1mM sodium pyruvate and 1% non essential amino acids (GIBCO) at 37°C supplemented with 5% CO_2.

2.7.4 PhoenixA cells

The PhoenixA cell line is derived from primary human embryonal kidney and grows adherent on the cell culture flask. PhoenixA cells were cultured in DMEM medium supplemented with 10% heat-inactivated Fetal Bovine Serum (GIBCO), 2mM glutamine, 100 U/ml penicillin, 100 µg/ml streptomycin and kept in culture at 37°C supplemented with 5% CO_2. When split, the complete medium was carefully decanted from the cell culture flask and the adherent cells were shortly incubated with 4ml Trypsin/EDTA solution (Invitrogen). The Trypsin/EDTA solution was poured of completely and the cells were incubated for 5 min at 37°C. Upon gently shaking of the cell culture flask, the cells would get off the surface and were resuspended in 10ml of fresh medium. Then the cells were split at a ratio of 1:10 with fresh medium.

2.7.5 PhoenixGP cells

The PhoenixGP cell line, also known as HEK 293T cell line is derived from primary human embryonal kidney and grows adherent on the cell culture flask. PhoenixGP cells were cultured in DMEM medium supplemented with 10% heat-inactivated Fetal Bovine Serum (GIBCO), 2mM glutamine, 100 U/ml penicillin, 100 µg/ml streptomycin and kept at 37°C supplemented with 5% CO_2. When split, the complete medium was carefully decanted from the cell culture flask and the adherent cells were detached by trypsination (2.7.4) and split at a ratio of 1:10 with fresh medium.

2.7.6 Cell inducers, compounds and inhibitors

If not available as stock in house, recombinant human cytokines were purchased from RnD Systems. Human recombinant GM-GSF stock was available in house and used at a final concentration of 50ng/ml. Human recombinant IL-4 was used at a final concentration of 40ng/ml.

Human recombinant TNF-α and IFN-γ were used at a final concentration of 100U/ml. Human recombinant IL-1β and IL-3 were used at a final concentration of 10ng/ml. Lipopolysaccharide (LPS) was purchased from Calbiochem and used at a final concentration of 100ng/ml. *Saccharomyces cerevisiae* zymosan A was purchased from Sigma-Aldrich and was used at a final concentration of 5µg/ml. Phorbol 12-myristate 13-acetate (PMA) was also purchased from Sigma-Aldrich and used at a final concentration of 20 nM. A mouse anti-human CD40 (α-CD40)-IgG antibody was available in house and was used together with a cross linking goat anti-mouse IgG antibody at a final concentration of 1µg/ml each.

VAF347 ([4-(3-chloro-phenyl)-pyrimidin-2-yl]-(4-trifluoromethyl-phenyl)-amine) and VAG005 (4-(2-chloro-pyridin-4-yl)-2-(4-chloro-3-trifluoromethyl-phenoxy)-pyrimidine) were synthesized at Novartis. TCDD, with a purity of >99%, was purchased from Crescent Chemical Company. Omeprazole was available in house.

The JAK-3 inhibitor CP-690,550 was available in house. The NF-κB inhibitor pyrrolidinedithiocarbamate was purchased from Sigma-Aldrich. An "NF-κB activation inhibitor" (6-Amino-4-(4-phenoxyphenylethylamino)quinazoline), the MAP kinase inhibitor PD98059 as well as the PKC inhibitors Calphostin C, BisindolylmalmeideI, Ro-32-0432 and Goe6976 were obtained from Calbiochem.

2.8 Induction of Monomac1 cells

2.8.1 Induction of Monomac1 cells for RT-PCR and IL-6 ELISA

$1x10^6$ cells/sample (counted with a Neubauer hematocytometer) of Monomac1 cells (2.7.3) were harvested, resuspended in 3ml full medium (2.7.3) and seeded in a 6 well plate (Costar). VAF347 was always added to cells first, then cytokines were added (2.7.6). Samples containing inhibitors (2.7.6) were pre-incubated with the respective inhibitor for 1h at 37°C supplemented with 5% CO_2, before VAF347 and/or cytokines (2.7.6) were added. Following induction cells were incubated for 24h at 37°C with 5% CO_2, if not stated otherwise.

After 24h incubation cells were transferred into 15ml Tubes (Falcon) and harvested by centrifugation at 1300rpm for 7 min. Medium was completely removed, with aliquots of each supernatant being stored at –80°C for the detection of human IL-6 by ELISA (2.5). Each sample was lysed in 400µl of Lysis Buffer, containing 3.5µl β-Mercaptoethanol. All reagents for RNA isolation were provided in the Absolutely RNA RT-PCR Miniprep Kit (Stratagene). All further steps regarding the total RNA isolation were done as described in 2.2.1. Following RNA isolation, cDNA generation was done according to the description in 2.2.2 . Gene expression was analyzed by input of cDNA into quantitative RT-PCR (2.3).

2.8.2 Induction of Monomac1 cells for analysis of intracellular signaling events

Monomac1 cells were counted with a Neubauer hematocytometer and harvested by centrifugation at 1.300rpm for 7min. $3x10^5$ cells/sample were resuspended in 1ml full medium (2.7.3) and seeded into a 24 well plate (Costar). Samples containing inhibitors (2.7.6) were pre-incubated with the respective inhibitor for 1h at 37°C supplemented with 5% CO_2 before VAF347 or cytokines (2.7.6) were added. Various time points after stimulation, cells were harvested by centrifugation at 1.300rpm for 2min and whole cell lysates were prepared immediately (2.6.1). Whole cell lysates were then used for the detection of multiple phosphorylated or unphosphorylated proteins by western blotting (2.6.2).

2.9 Transient transfection of MM1 using the Amaxa electroporation device

$2x10^6$ of Monomac1 cells (2.7.3) per sample were harvested by centrifugation for 7min at 1.300 rpm. Pelleted cells were washed once with 20 ml of cold 1xPBS and centrifuged for 7min at 1.300rpm. PBS was decanted completely and cells were carefully resuspended in 100µl transfection solution V. 2µg plasmid DNA (eGFP expression vector or pGL3-Interleukin-6 promoter) were added to 100µl of cell suspension. Then the cell solution was pipetted into a 1ml Amaxa certified transfection cuvette, and the cuvette was shaken by hand shortly.

The cuvette was then inserted into the cuvette holder of the Amaxa Nucleofetor device™ and the electroporation program V-01 was selected and started. To avoid damage to the cells, samples were removed immediately after the program had finished and 900µl of prewarmed full medium (2.7.3) were added directly to the cells in the cuvette. Then the cell suspension was transferred into 3ml of prewarmed medium in six well plates (Costar) and incubated for 24h with or without PMA (20nM), human IL-4 (40ng/ml) + GM-CSF (50ng/ml) in the presence or absence of VAF347 (50nM) or VAG005 (50nM) respectively, at 37°C supplemented with 5%CO_2 before luciferase activity was measured (2.9.2). GFP expression was checked in a confocal fluorescence microscope (Leica).

2.9.1 Luciferase activity measurement

24h after cytokine stimulation, each sample was transferred to a 15ml centrifugation tube (Costar) and cells were harvested by centrifugation at 1.300 rpm for 7min.

The supernatants were removed by pipetting and the cells were lysed in 90µl of 2x Passive Lysis buffer (Promega). 2x 40µl of each lysate were pipetted into a 96 well plate (Dynex Technologies) resulting in duplicates for each well. The samples were measured in a luminometer (Luminoskan, Labsystems) with the following parameters: 50µl of luciferase assay substrate were injected into each well and after a lag-time of 1sec the light quantity was measured for 4sec. The raw data was analyzed and graphs were made using the Excel program.

2.10 Viral infection of Monomac1 cells

2.10.1 Transfection of packaging cell lines with retroviral constructs

On the day before transfection $1.7x10^6$ PhoenixA (2.7.4) or Phoenix GP (2.7.5) cells were seeded in 4ml of fresh medium (2.7.4) without antibiotics, per 25 cm² cell culture flask (Costar). The packacking cell line was transfected with plasmid DNA using Lipofectamine 2000 (Invitrogen). First 15µl of Lipofectamine2000 reagent were diluted gently in 500µl Opti-MEM® I medium (Invitrogen) and incubated for 5 min at RT. Meanwhile 9µg of plasmid DNA (pMX-pie vector, pMX-pie-AhR515, LMP-shAhR, LMP-shControl, pMX-pie-NF-IL6, pMX-pie-NF-κB p65) were diluted in 500µl Opti-MEM® I reduced serum medium and mixed gently. In the case of PhoenixGP transfection, 5µg of the packaging vector GalV were added to each transfection sample.

After 5 min incubation, DNA and Lipofectamine2000 (Invitrogen) solutions were combined, mixed gently and incubated for 20 min at RT. The complete mixture was then added drop-wise onto the cells which were then further incubated for 24h at 37°C supplemented with 5%CO_2. On the next day the medium was removed completely by pipetting and replaced with 4 ml of fresh prewarmed medium (2.7.4), containing 100 U/ml penicillin, 100 µg/ml streptomycin. Then the cells were further incubated for 24 h at 37°C supplemented with 5%CO_2.

2.10.2 Transfection of a packaging cell line with lentiviral constructs

On the day before transfection $1.7x10^6$ Phoenix GP cells were seeded in 4ml of fresh medium (2.7.5) without antibiotics, per 25 cm² cell culture flask (Costar). The packacking cell line was transfected with plasmid DNA using Lipofectamine 2000 (Invitrogen). First 32µl of Lipofectamine2000 reagent were diluted gently in 500µl Opti-MEM® I medium (Invitrogen) and incubated for 5 min at RT. Meanwhile 10µg of sh-RNA construct (GIPZ-sh-Control or GIPZ-sh-PU.1), 7µg of the packaging vector pPAX2 as well as 3µg of the second packaging vector pMD2G were diluted in 500µl Opti-MEM® I reduced serum medium and mixed gently.

After 5 min incubation, DNA and Lipofectamine2000 (Invitrogen) solutions were combined, mixed gently and incubated for 20 min at RT. The complete mixture was then added drop-wise onto the PhoenixGP cells which were then further incubated for 24 h at 37°C supplemented with 5%CO_2. On the next day, the medium was removed completely by pipetting and replaced with 4 ml of fresh prewarmed medium (2.7.5), containing 100 U/ml penicillin, 100 µg/ml streptomycin. Then cells were further incubated for 24 h at 37°C supplemented with 5%CO_2.

2.10.3 Retroviral infection of Momomac1 cells

For the successful retroviral infection and deliverage of virus information into the mammalian cell, cells needed to be in a dividing phase. Therefore Momomac1 cells were split at a ratio of 1:10 two

days before transduction to allow cells to grow. On the day of infection Monomac1 cells were counted, harvested by centrifugation for 7min at 1.300 rpm and resuspended at a concentration of 5 x 10^5 cells per 100µl in fresh full medium (2.7.3).

The virus containing supernatant of PhoenixA or PhoenixGP cells was collected by pipetting and filtered through a 0.45 µm filter (Millipore). After filtration polybrene (Sigma-Aldrich) was added to the supernatant to give a final concentration of 1µg/ml. To control Lipofectamine 2000 transfection efficiency, GFP expression in PhoenixA or respectively PhoenixGP cells was checked in a confocal fluorescence microscope (Leica).
Infection of Monomac1 cells was achieved by adding 2 ml of viral supernatant to 5 x 10^5 Monomac1 cells, seeded in 24-well plates (Costar), followed by centrifugation at 310 x g for 3 h at RT. Immediately after centrifugation cells were incubated again at 37°C supplemented with 5%CO_2. After a 24 h incubation step cells were harvested by centrifugation for 7min at 1.300 rpm, the medium was removed and replaced with fresh Monomac1 medium (2.7.3) and the cells were allowed to grow for 2-3 days. Then cells expressing high levels of GFP were sorted using a FACSVantage SE machine (Becton Dickinson). Sorted GFP positive cells were cultured in medium (2.7.3) supplemented with 1 µg/ml puromycin (Sigma-Aldrich) at 37°C supplemented with 5%CO_2.

2.10.4 Lentiviral infection of Momomac1 cells

Lentiviral infection of MM1 cells was achieved by using the same protocol applied for retroviral infection of MM1 cells (2.10.3).

2.11 Chromatin Immunoprecipitation

2.11.1 Induction of Monomac1 cells

If not stated otherwise, all reagents necessary for Chromatin Immunoprecipitation (ChIP) were supplied in the ChIP Kit from Millipore. First 1x10^6 cells/ ChIP sample (counted with a Neubauer hematocytometer) of Monomac1 were harvested, resuspended in 3ml full medium (2.7.3) and seeded into a 6 well plate (Costar). Monomac1 cells were left untreated or stimulated with IL-4 (with a final concentration of 40ng/ml) and GM-CSF (with a final concentration of 50ng/ml) in the absence or presence of 50 nM VAF347 and incubated for 24h at 37°C, supplemented with 5%CO_2.

2.11.2 Crosslinking and lysis

To cross link histones to DNA, formaldehyde (Sigma-Aldrich) was added directly to Monomac1 cells to a final concentration of 0.7% and incubated for 10 min at 37°C. Then Monomac1 cells were harvested by centrifugation for 6min at 1.300 rpm. Pelleted cells were washed twice with ice cold

1xPBS containing 1x protease inhibitor cocktail (Roche Diagnostics). PBS was decanted completely and $1x10^6$ cells were lysed in 200µl SDS Lysis Buffer, which had been pre-warmed to RT first and contained 1x protease inhibitor cocktail. Lysates were left on ice for 10 min before protocol was continued with DNA fragmentation (2.11.3)

2.11.3 Random DNA fragmentation

All cross linked ChIP samples (2.11.2) were sonicated with the Bioruptor™ machine (Diagenode). DNA was sheared to a length between 400-1000 bp in 10 sonication cycles using the Bioruptor™ on power setting "High" (200 W). One sonication cycle of 1 min included 30 sec sonication and 30 sec pause. Lysate samples were always kept on ice or in ice cold water during sonication.
After sonication ChIP samples were centrifuged for 10 min at 13.000 rpm at 4°C, then supernatants (containing sheared DNA) were transferred into new 2ml Eppendorf microcentrifuge tube.

2.11.4 Immunoprecipitation and washing

Before protocol was continued 50µl of sonicated DNA lysate of each sample were taken away and labelled with Input. Input samples were stored at –20°C until the elution step (2.11.5).
For each immunoprecipitation ChIP sample sonicated DNA of $1x10^6$ cells (2.11.3), contained in 200µl lysate, was usded. Each ChIP sample was diluted 10 fold in ChIP dilution buffer, containing 1x protease inhibitor cocktail, meaning that 200µl lysate were filled up with 1800µl ChIP dilution buffer in a 2 ml Eppendorf microcentrifuge tube. To reduce non-specific background, all samples were pre-cleared with 60µl of Salmon Sperm DNA/Protein A Agarose-50% Slurry for 1 h at 4°C with rotation. Agarose was pelleted by centrifugation for 1min at 1.800 rpm, at 4°C. Pre-cleared supernatants were transferred into fresh 2ml Eppendorf microcentrifuge tube, before the immunoprecipitating antibodies were added. To precipitate the transcription factor NF-IL6 10µg of the polyclonal rabbit anti-human C/EBP β antibody SC-150 X (Santa Cruz Biotechnology) were added. As negative controls samples containing 10µg of normal rabbit IgG SC-2027 (Santa Cruz Biotechnology) or samples containing no antibody were inculded. After antibodies were added, samples were incubated over night at 4°C with rotation. On the next day 60µl of Salmon Sperm DNA/Protein A Agarose-50% Slurry were added to each sample for 4 h at 4°C with rotation to collect antibody/histone complex. Agarose was pelleted by centrifugation for 1min at 1.800 rpm, at 4°C and supernatant containing unbound non-specific DNA was removed carefully by pipetting. Then samples were washed for 5 min on a rotation platform with 1 ml of each of the wash buffers listed in the order as given bellow:

a) Low Salt Immune Complex Wash Buffer, one wash at 4°C
b) High Salt Immune Complex Wash Buffer, one wash at 4°C

c) LiCl Immune Complex Wash Buffer, one wash at 4°C

d) 1 x TE, two washes at RT

Protocol was continued with elution of the histone complex from the antibody (2.11.5).

2.11.5 Elution and Proteinase K digest

Fresh elution buffer containing 1%SDS and 0.1M $NaHCO_3$ was prepared. The histone complex was then eluted from the antibody ba adding 250µl of fresh elution buffer, samples were vortexed briefly and incubated for 15 min on rotation at RT. Agarose was pelleted by centrifugation for 1min at 1.800 rpm, at RT and supernatant fraction (eluate) was transferred into a fresh 1.5 ml Eppendorf microcentrifuge tube by pipetting. The elution step was repeated one more time and both eluates were combined (~500µl eluate). At this point the protocol was also continued for the Input samples: Input samples were thawed and filled up with elution buffer to a final volume of 500µl. Then 50µl of 5M NaCl were added to the eluates and all samples were incubated at 65°C over night to reverse DNA/Histone crosslinks. On the next day 10µl of 0.5M EDTA, 20µl of 1M Tris-HCl pH 6.5 and 1µl of 600 mAu/ml Protease K (Novagen) were added to each sample and incubated for 1 h at 45°C.

2.11.6 Phenol/chloroform extraction and PCR

After Proteinase K digest (2.11.5) DNA was recovered by phenol/chloroform extraction. Therefore 500µl of phenol/chloroform/isoamylalcohol 25:24:1 (Sigma-Aldrich) were added to each sample, followed by 5 sec vortexing. Samples were centrifuged for 2 min at 13.000 rpm, before the top phase was carefully transferred into a fresh 1.5 ml Eppendorf microcentrifuge tube by pipetting. Before precipitation 20µg of glycogen (Calbiochem) were added as an inert carrier to help visualize the DNA pellet. To precipitate DNA 1ml of 96% ethanol was added and samples were left on –20°C over night. On the next day DNA was pelleted by centrifugation of the samples for 25 min at 13.000 rpm, at 4°C. The supernatant was removed carefully and DNA pellets were washed with 500µl of 70% ethanol, followed by centrifugation of the samples for 10 min at 13.000 rpm, at 4°C. the 70% ethanol was removed carefully and the DNA pellets were allowed to air dry before pellets were resuspended in 50µl of nuclease free H_2O.

For PCR the conditions already described for RT-PCR were used (2.3). For the detection of the C/EBP-β (NF-IL6) binding site in the human IL-6 promoter by RT-PCR, following oligonucleotides were used:

MW1482: upstream 5´- AATGACGACCTAAGCTGCAC-3´ and MW1483: downstream 5´-CTTTGTTGGAGGGTGAGGGT-3´.

For each ChIP sample 5µl of recovered DNA were used for RT-PCR, for Input samples only 1µl of recovered DNA were used. After RT-PCR 18µl of each PCR reaction were mixed with 2µl of

10xBlue Juice Gel loading buffer (Invitrogen) and loaded onto a 1.3% agarose gel, which was run as described above (2.1.4).

2.12 Statistical analysis

The Student's *t*-test was used to analyse data for significant differences. *P*-values less than 0.05 were regarded as significant.

3. RESULTS

3.1 IL-4 + GM-CSF induce Interleukin-6 expression in human Monomac1 cells

Fresh human Monomac1 (MM1) cells (2.7.3) were seeded into 6 well plates at a density of $1x10^6$ cells per well and incubated for 24 hours (or different time points if stated otherwise) in the presence or absence of the cytokines IL-4, GM-CSF (2.7.6) or IL-4 and GM-CSF in combination (2.8.1). After 24 hours RNA was isolated with the Absolutely RNA Kit (2.2.1) and used to generate cDNA according to the protocol of the iScript cDNA synthesis Kit (2.2.3). These cDNA templates were then further analyzed by RT-PCR (2.3) for the expression levels of Interleukin-6 and elongation Factor-1α (eF-1α) as a house keeping control gene (2.3). For the calculation of the expression values for this and all following RT-PCR experiments, the average Ct values of the gene of interest were normalized to the average of the Ct values of the eF-1α gene.

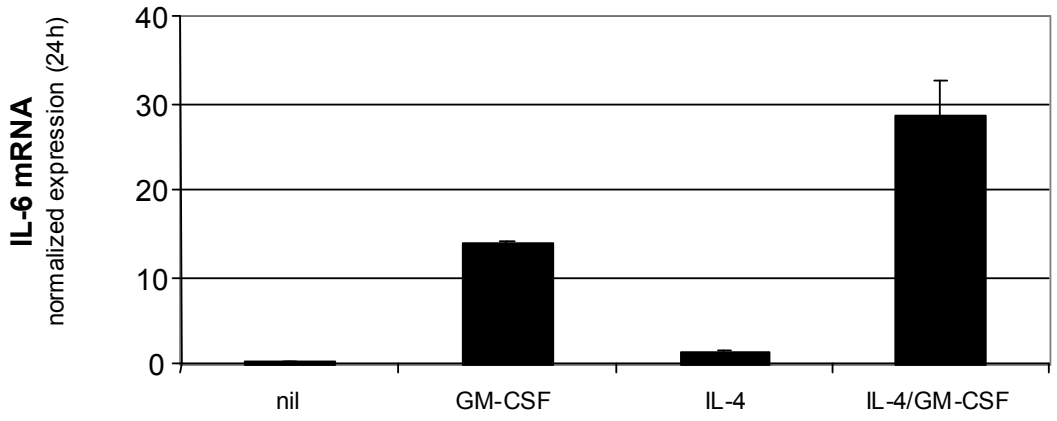

Figure 3.1.1: ***GM-CSF induces IL-6 production in Monomac1 cells****. IL-4 induces only little IL-6 synthesis but enhances IL-6 expression in combination with GM-CSF. RT-PCR for IL-6 mRNA 24h after cytokine stimulation is shown. IL-6 expression was normalized to eF-1α expression. The error bars indicate standard deviation.*

The RT-PCR data showed that IL-6 expression was induced 24 hours after stimulation with GM-CSF in Monomac1 cells (**Figure 3.1.1**). IL-4 alone had only very little effect on IL-6 expression on its own but acted in a synergistic way with GM-CSF on Monomac1 cells.

To determine the time course of interleukin-6 induction, Monomac1 cells were cultured for up to 48 hours with IL-4 + GM-CSF before IL-6 mRNA expression was determined by RT-PCR as described above. As shown in **Figure 3.1.2** IL-6 expression levels increased with time, reaching a maximum at 48 hours after cytokine induction. After three days of cytokine stimulation the

interleukin-6 response measured at the mRNA level was already down-regulated to the starting level (data not shown).

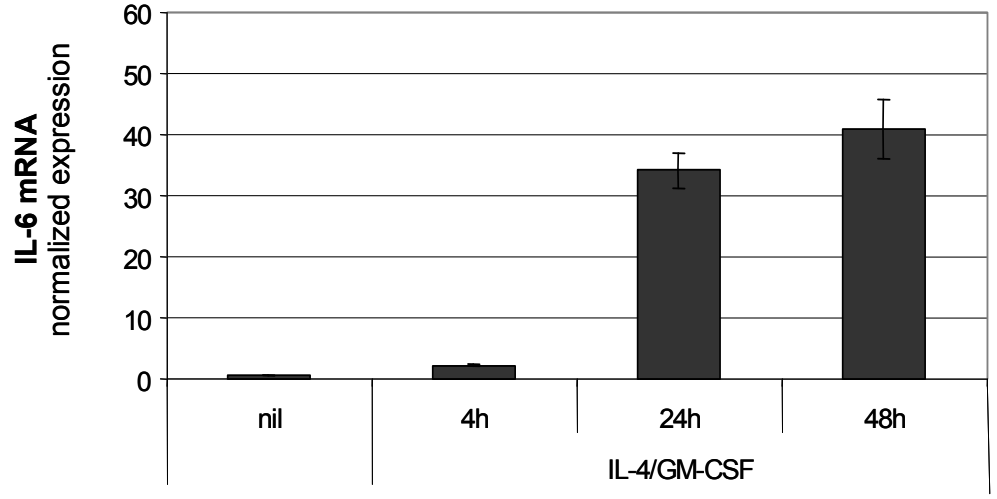

Figure 3.1.2: ***Il-4 + GM-CSF induce IL-6 production in Monomac1 cells****. IL-6 mRNA levels were measured by RT-PCR 4h, 24h and 48h after cytokine stimulation. IL-6 expression was normalized to eF-1α expression.*

3.2 VAF347 inhibits IL-4 + GM-CSF induced IL-6 production in Monomac1 cells

To answer the question whether the inhibitory effect of VAF347 on IL-6 production by human monocyte-derived DCs (63) was restricted to primary cells or could also be seen in a monocytic cell line, we examined the biological activity of VAF347 on Monomac1 cells.

MM1 cells (2.7.3) were stimulated with IL-4 + GM-CSF in the presence or absence of VAF347 (2.7.6) for 24 hours, before IL-6 mRNA expression was analyzed by RT-PCR (2.3).

As shown in **Figure 3.2.1**, stimulation of Monomac1 cells with IL-4 + GM-CSF lead to induction of IL-6 expression. In MM1 cells that had been stimulated with IL-4 + GM-CSF in the presence of VAF347, IL-6 expression was inhibited in a dose-dependent fashion. Usually, the IL-4 + GM-CSF induced IL-6 mRNA expression was inhibited by >4-fold at a concentration of 50nM VAF347.

The half-maximal inhibitory concentration (IC_{50}) of VAF347 in Monomac1 cells was approximately 5nM, a concentration which was very similar to that calculated for the blockade of interleukin-6 production in monocyte-derived DCs (63). VAF347 on its own did not induce IL-6 expression in MM1 cells (**Figure 3.2.1**).

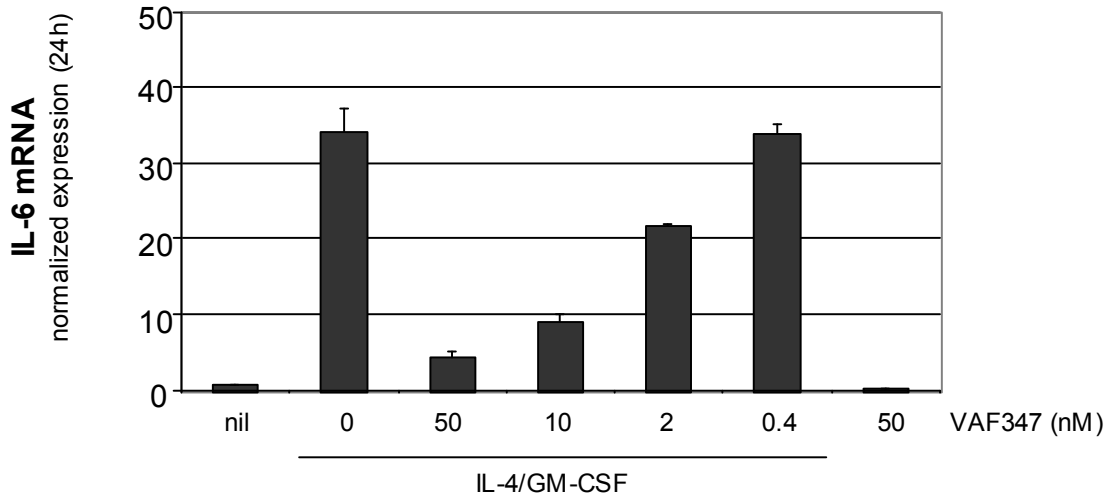

Figure 3.2.1: ***VAF347 inhibits IL-4 + GM-CSF induced IL-6 production in Monomac1 in a dose-dependent fashion.*** *IL-6 mRNA expression was analyzed by RT-PCR 24h after cytokine stimulation. IL-6 expression was normalized to eF-1α expression.*

The inhibitory effect of VAF347 still persisted in cells stimulated for 48 hours (**Figure 3.2.2**).

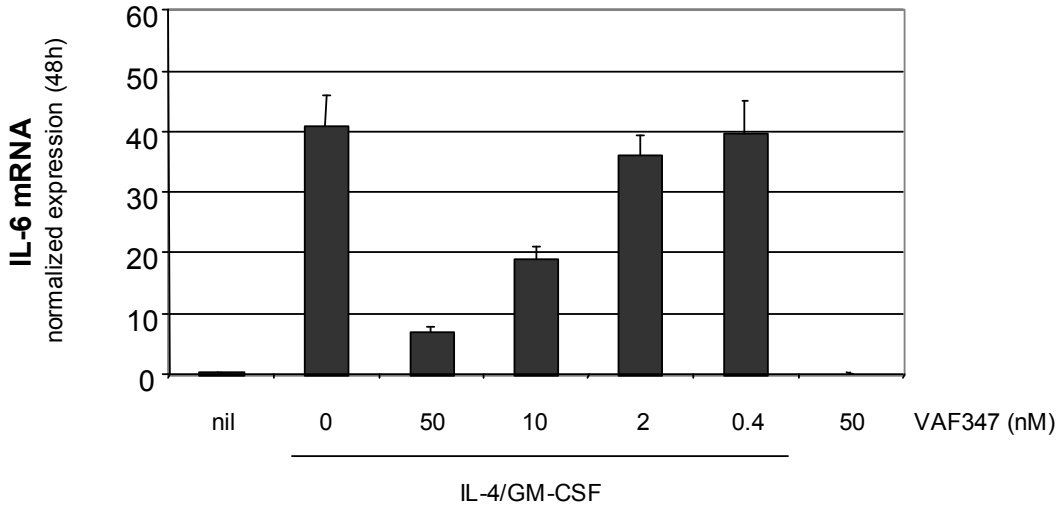

Figure 3.2.2: ***VAF347 inhibits IL-4 + GM-CSF induced IL-6 production in Monomac1****. IL-6 mRNA expression was analyzed by RT-PCR 48h after cytokine stimulation and normalized to eF-1α expression.*

To examine if the inhibitory effect of VAF347 on IL-6 mRNA expression could also be seen at the protein level, IL-6 protein was measured in cell supernatants by ELISA (2.5).

The ELISA data shown in **Figure 3.2.3** demonstrated that IL-6 protein was detectable in supernatants of MM1 cells at a concentration of 250pg/ml 24 hours after stimulation with IL-4 + GM-CSF. VAF347 inhibited the production of IL-6 protein in a concentration dependent manner. Usually, the factor of inhibition of IL-6 protein production by 50nM VAF347 (which was ten times higher then the calculated IC_{50}) was 4-fold or higher, which was in accordance to the data seen at the mRNA level.

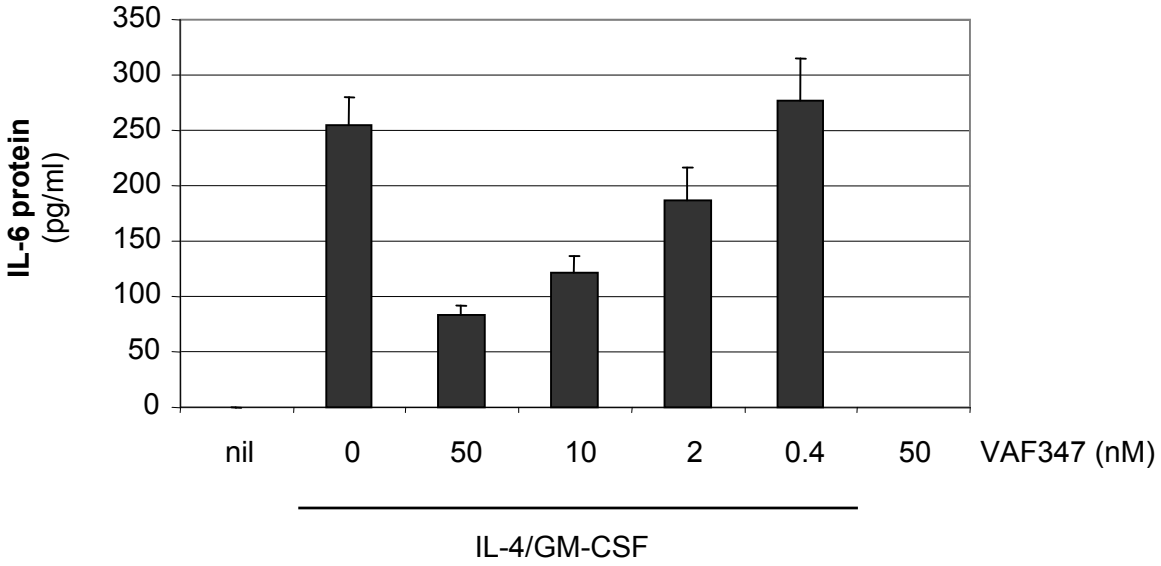

Figure 3.2.3: ***VAF347 inhibits IL-4 + GM-CSF induced IL-6 protein production in Monomac1****.*
IL-6 protein was measured in supernatants of samples 24h after cytokine induction by ELISA.

Further ELISA data for Interleukin-6 showed that IL-6 protein levels increased 48 hours after stimulation of MM1 cells with IL-4 + GM-CSF, reaching a concentration of 700pg/ml (**Figure 3.2.4**). Still, two days after cytokine stimulation VAF347 was able to maintain its inhibitory effect on IL-6 production. At a concentration of 50nM VAF347 IL-6 protein was detectable at a concentration of approximately 130pg/ml, thus showing a 5-fold decreased IL-6 response in Monomac1 cells when compound was added.

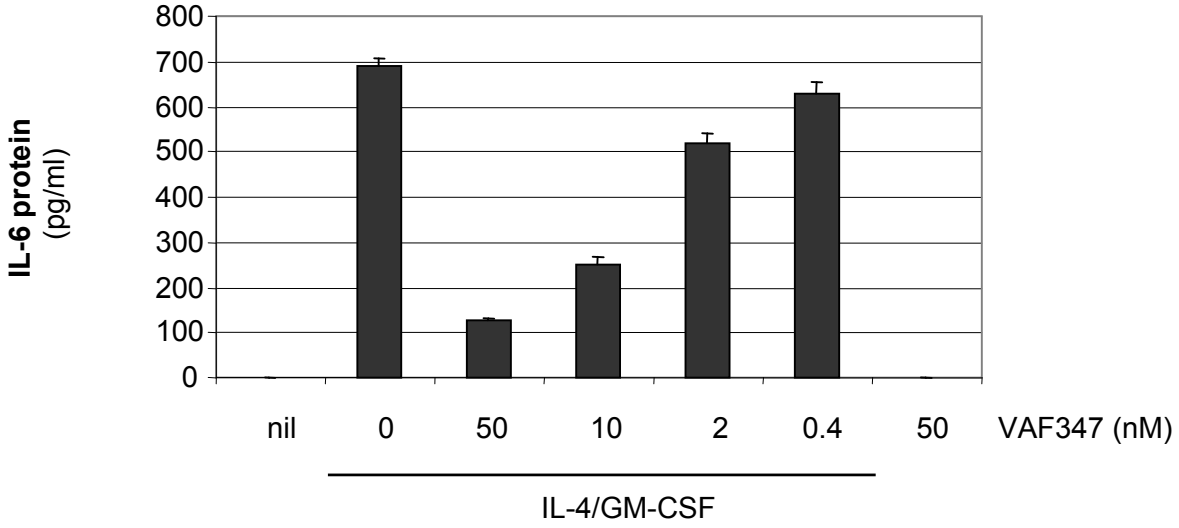

Figure 3.2.4: ***VAF347 inhibits IL-4 + GM-CSF induced IL-6 protein production in Monomac1***. *IL-6 protein was measured 48h after cytokine stimulation by ELISA.*

Collectively, these data showed that MM1 cells could be used for studying the molecular mechanisms underlying the inhibitory effects of VAF347 on IL-6 production.

3.3 VAF347 induces CYP1A1 expression in Monomac1

Genome wide gene expression profiling in CD40 antibody activated monocyte derived DCs in the presence or absence of VAF347 was performed in our laboratory. Comparing the expression pattern profiles of untreated versus VAF347 treated cells showed that VAF347 induced the expression of genes which are known to be regulated by the aryl hydrocarbon receptor (AhR), including the aryl hydrocarbon receptor repressor (AHRR) and cytochrome P450 1B1 (CYP1B1) (67). These data indicated a possible involvement of AhR in the mode of action of VAF347.

Further experiments showed that VAF347 also induced cytochrome P450 1A1 (CYP1A1) expression in human peripheral monocytes (67) another AhR dependent gene. To answer the question whether VAF347 also induced CYP1A1 expression in Monomac1 cells, MM1 cells were stimulated with VAF34 alone or in the presence of IL-4 + GM-CSF for 24 hours before CYP1A1 mRNA was measured by RT-PCR (2.3).

As shown in **Figure 3.3.1** VAF347 induced CYP1A1 gene expression in MM1 cells in a dose-dependent fashion. When the cytokines IL-4+GM-CSF were added, the increase of CYP1a1 mRNA in the presence of VAF347 was even higher, an effect which was also seen in human peripheral monocytes (67). In contrast to primary monocytes IL-4 + GM-CSF on its own had only minimal effects on CYP1A1 mRNA expression in Monomac1 (**Figure 3.3.1**).

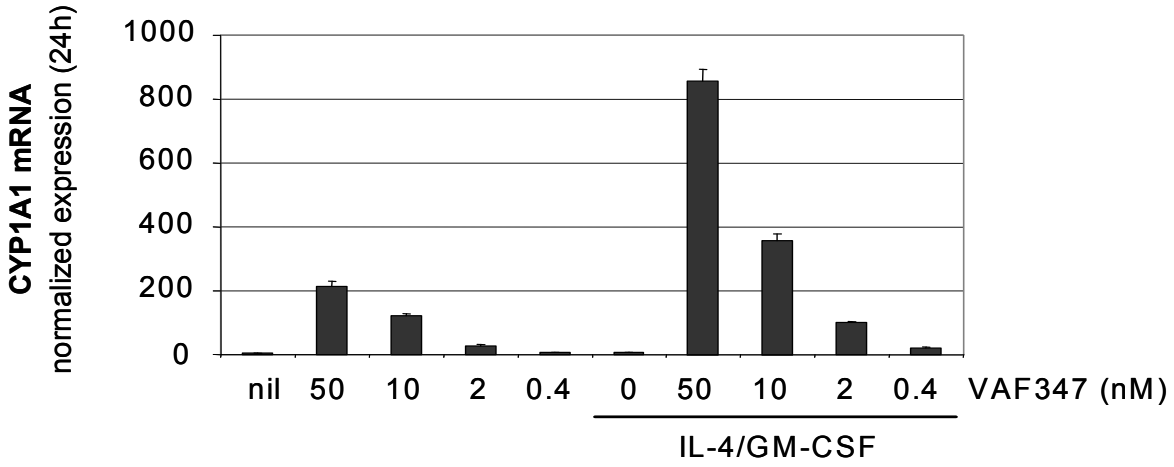

Figure 3.3.1: ***VAF347 induces CYP1A1 mRNA expression in Monomac1****. In the presence of IL-4 + GM-CSF CYP1A1 expression by VAF347 is increased. CYP1A1 expression was measured 24h after stimulation by RT-PCR and normalized to eF-1α expression.*

3.4 TCDD and omeprazole have a similar activity profile in MM1 compared to VAF347

Since VAF347 induced CYP1A1 expression, a gene which is classically induced by the activation of AhR signaling, it was interesting to investigate the biological effects of known AhR agonists in Monomac1 cells.

First, the effects of the prototypical AhR ligand TCDD on Monomac1 cells were examined. MM1 cells were stimulated with IL-4 + GM-CSF in the presence or absence of TCDD (2.7.6) for 24 hours, before CYP1A1 expression was measured by RT-PCR (2.3).

As shown in **Figure 3.4.1** TCDD induced CYP1A1 gene expression in MM1 cells. The presence of IL-4 + GM-CSF enhanced the TCDD dependent magnitude of CYP1A1 induction in a dose-dependent fashion, an effect which was already seen with VAF347 (3.3).

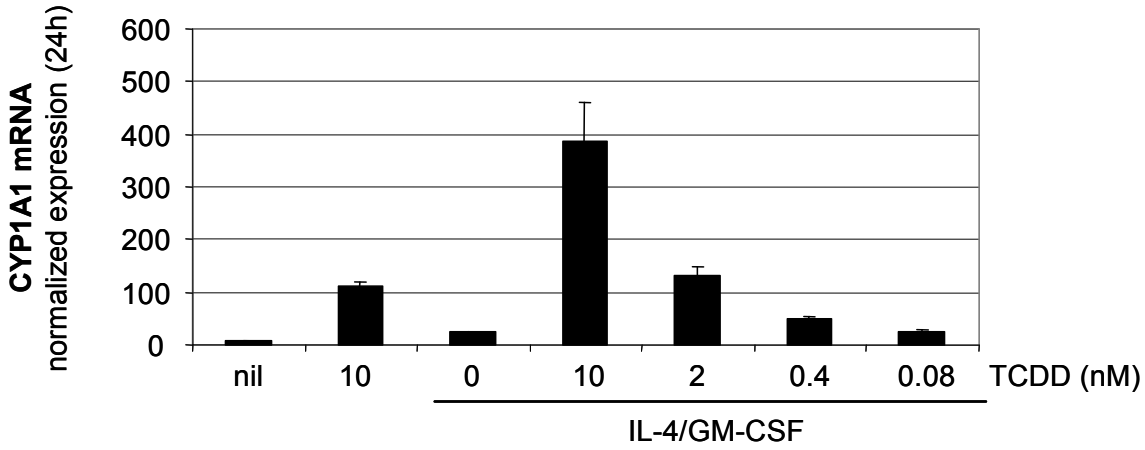

Figure 3.4.1: ***TCDD induces CYP1A1 mRNA expression in Monomac1 cells***. *The presence of IL-4 + GM-CSF enhanced the TCDD dependent magnitude of CYP1A1 induction. CYP1A1 mRNA expression was measured 24h after stimulation by RT-PCR and normalized to eF-1α expression.*

To answer the question whether TCDD could also inhibit IL-6 expression in Monomac1 cells, MM1 cells were stimulated with IL-4 + GM-CSF in the presence or absence of TCDD for 24 hours, before IL-6 mRNA was measured by RT-PCR (2.3). Interestingly, TCDD was able to inhibit the IL-4 + GM-CSF induced IL-6 response in Monomac1 cells at an even higher potency than VAF347, with an IC_{50} of approximately 80pM (**Figure 3.4.2**). TCDD on its own did not induce IL-6 mRNA expression.

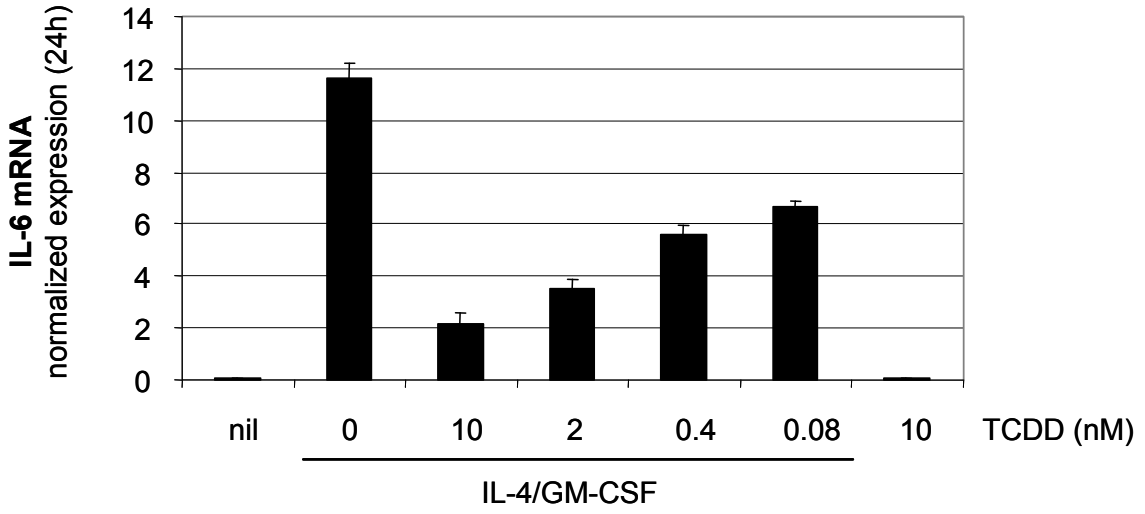

Figure 3.4.2: ***TCDD inhibits IL-4 + GM-CSF induced IL-6 mRNA synthesis in Monomac1***. *IL-6 mRNA expression was measured 24h after stimulation by RT-PCR and normalized to eF-1α expression.*

Since TCDD, the prototypical ligand of AhR showed an identical biological activity in MM1 cells compared to VAF347, these results strongly suggested that activation of AhR is involved in the mode of action of VAF347.

Another AhR agonist that has been extensively studied due to its application in the clinic is omeprazole.

Omeprazole is used for the treatment of gastric ulcers and dyspepsia due to its activity as a proton pump inhibitor. At high concentration, omeprazole has been demonstrated to bind and activate AhR, thus leading to the induction of the CYP1A1 gene (82,83). Interestingly, omeprazole stimulated AhR activity seems to be species-specific, since omeprazole activates AhR only in human and not in mouse cells (138,139).

To test the effect of omeprazole on CYP1A1 expression, Monomac1 were stimulated with IL-4 + GM-CSF in the absence or presence of omeprazole (2.7.6) for 24 hours before CYP1A1 mRNA levels were measured by RT-PCR (2.3). As shown in **Figure 3.4.3** omeprazole induced the expression of CYP1A1 mRNA in MM1 cells. The potency of the drug was approximately 1000-fold weaker than that of VAF347 in agreement with the literature as a weak AhR agonist. The presence of IL-4 + GM-CSF enhanced the omeprazole dependent magnitude of CYP1A1 levels, an effect that was already seen with VAF347 and TCDD.

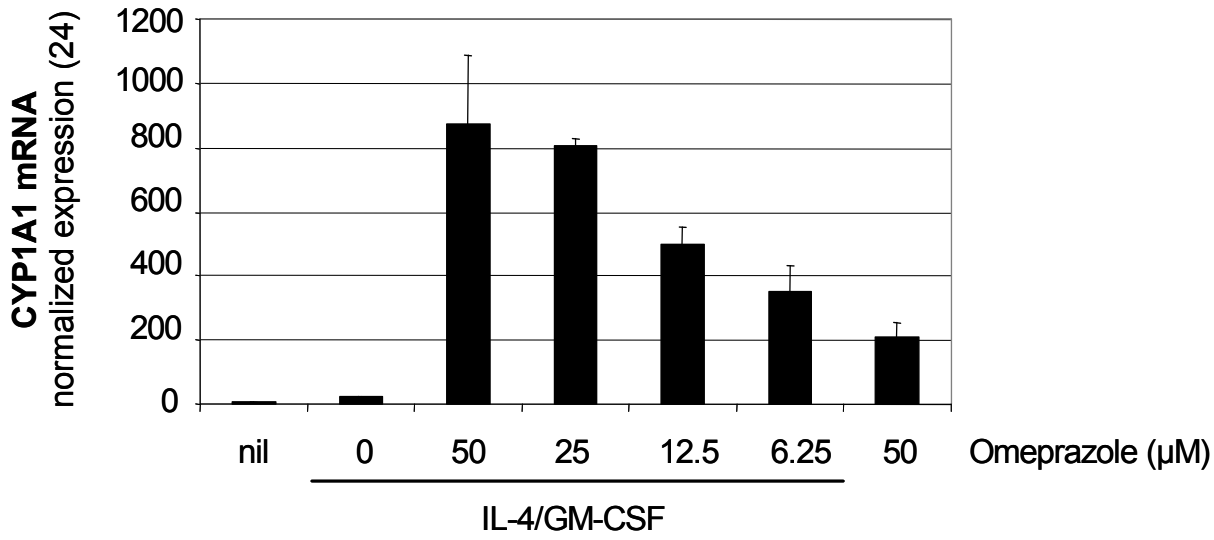

Figure 3.4.3: ***Omeprazole induces CYP1a1 expression in Monomac1***. *The presence of IL-4 + GM+CSF enhanced the magnitude of CYP1A1. RT-PCR for CYP1A1 mRNA 24 h after stimulation is shown. CYP1A1 expression was normalized to eF-1α expression.*

To examine the effect of omeprazole on IL-6 expression MM1 cells were stimulated with IL-4 + GM-CSF in the absence or presence of omeprazole for 24 hours, before IL-6 mRNA was measured

as described above. Similar to TCDD, omeprazole inhibited IL-4 + GM-CSF induced IL-6 mRNA expression in Monomac1 cells in a dose-dependent fashion in the µM range (**Figure 3.4.4**).

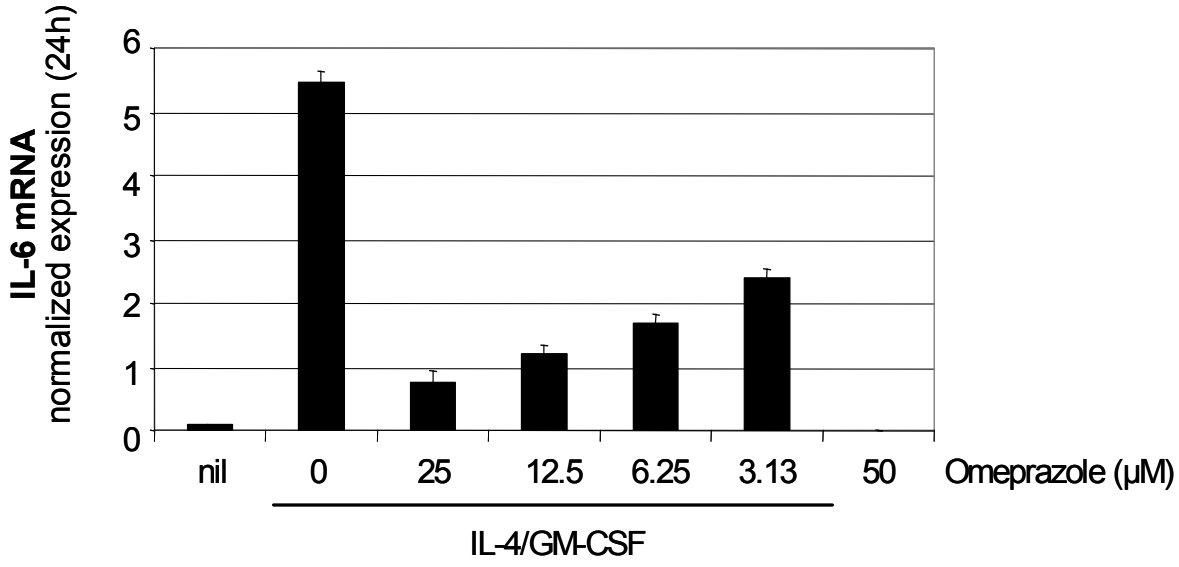

Figure 3.4.4: ***Omeprazole inhibits IL-4 + GM-CSF induced IL-6 mRNA production in Monomac1****. RT-PCR for IL-6 mRNA 24 h after stimulation is shown. IL-6 expression was normalized to eF-1α expression.*

Collectively, these data strongly indicated that activation of AhR signaling is involved in the mode of action of VAF347, since the two AhR agonists TCDD and omeprazole display an identical activity profile in MM1 cells compared to VAF347.

3.5 PMA induces IL-6 expression in Monomac1 cells

Multiple stimuli including the cytokines TNF-α, IL-1β and IFN-γ as well as bacterial components such as LPS or the yeast cell wall component zymosan have been shown to induce IL-6 expression in various cell types. Furthermore, stimulation of murine DCs by engagement of CD40 has been shown to induce IL-6 expression (140).

To answer the question whether IL-6 expression in Monomac1 cells was restricted to IL-4 + GM-CSF induction, MM1 cells (2.7.3) were stimulated with various stimuli (2.7.6) for 24 hours, before IL-6 mRNA expression was analyzed by RT-PCR (2.3). The RT-PCR results in **Figure 3.5.1** show that stimulation of Monomac1 cells with TNF-α, LPS + IFN-γ, IL-1β + IL-4, zymosan or IL-3 + IL-4 induced only very low levels of IL-6 mRNA compared to the IL-4 + GM-CSF induced IL-6 response. VAF347 did not inhibit any of these stimuli in their ability to induce IL-6 expression (data not shown) indicating considerable specificity of VAF347. Stimulation of Monomac1 with mouse anti-human CD40 (α-CD40) antibodies and IL-4 (in combination with a crosslinking

antibody) induced low levels IL-6 mRNA expression. VAF347 reduced α-CD40/IL-4 induced IL-6 mRNA expression only by two-fold or less at a concentration of 50nM (data not shown).

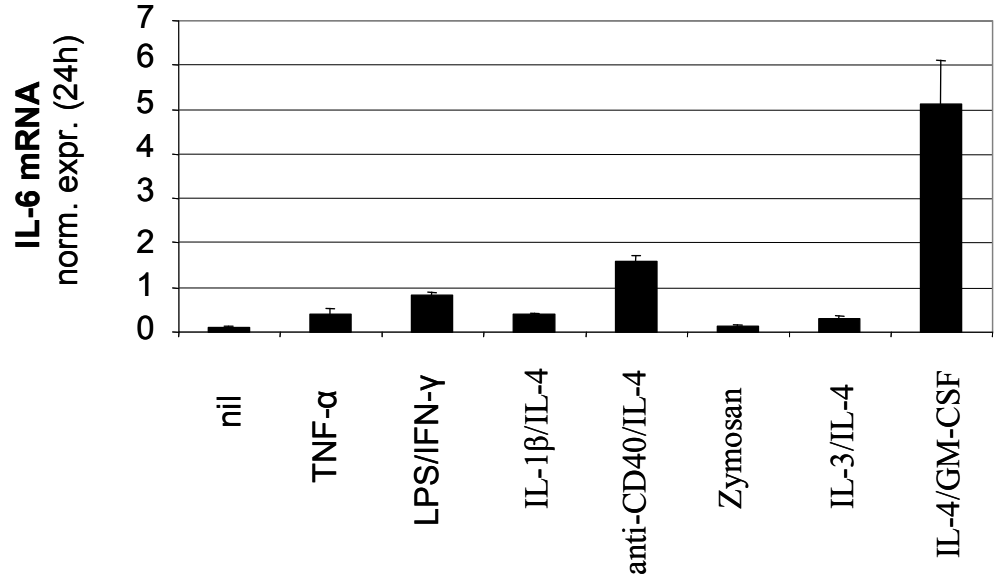

Figure 3.5.1: ***IL-6 mRNA expression in Monomac1 cells 24h after stimulation with various stimuli.*** *IL-6 mRNA expression was measured by RT-PCR and normalized to eF-1α expression.*

Phorphol esters such as phorbol 12-myristate 13-acetate (PMA) have been shown to induce IL-6 mRNA expression in human monocytes (141). To analyze the effect of PMA on IL-6 expression MM1 cells were stimulated with PMA (2.7.6) in the absence or presence of VAF347 for 24 hours, before IL-6 mRNA expression was analyzed as described above.

As demonstrated in **Figure 3.5.2** PMA induced high levels of IL-6 mRNA which were usually 2-3 fold higher compared to IL-6 levels of IL-4 + GM-CSF induced MM1 cells. VAF347 inhibited PMA induced IL-6 mRNA expression in a dose dependent fashion, with an IC_{50} of approximately 5nM. This was comparable to the calculated IC_{50} of VAF347 in IL-4 + GM-CSF induced Monomac1 cells (3.2).

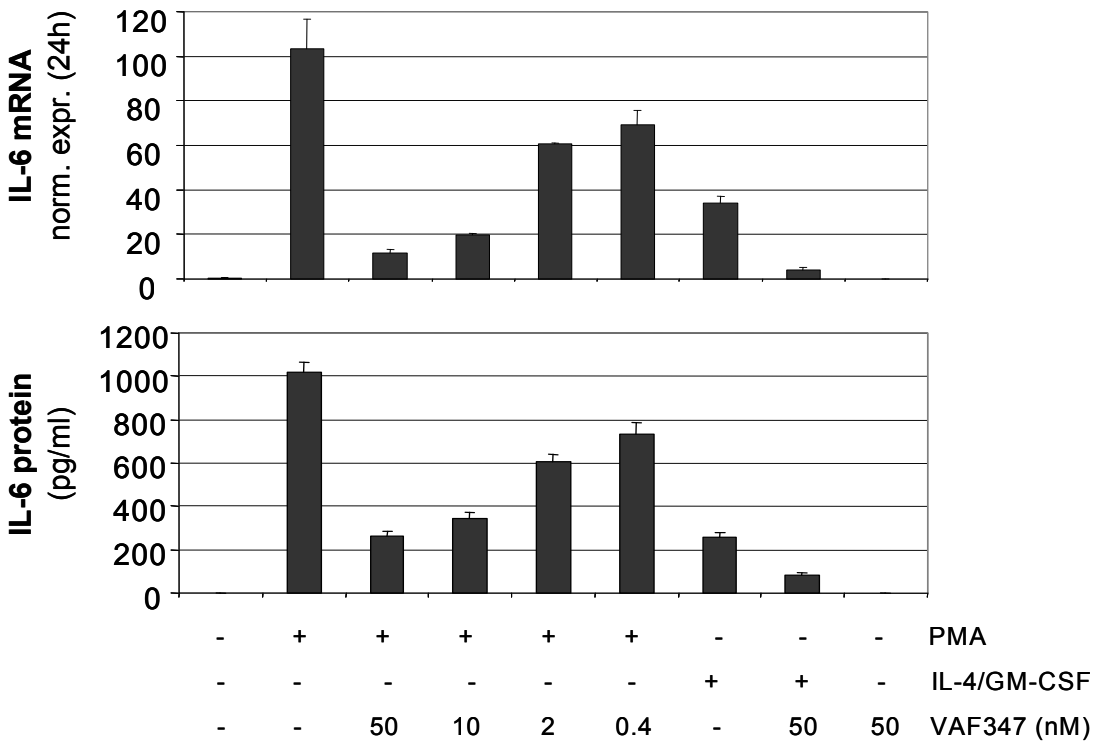

Figure 3.5.2: ***PMA induces IL-6 mRNA expression in Monomac1 cells***. *VAF347 inhibits IL-6 induction by PMA in a concentration dependent fashion. The top row shows RT-PCR for IL-6 mRNA in cells that were induced with PMA or IL-4+ GM-CSF in the presence or absence of VAF347 for 24 hours. IL-6 expression was normalized to eF-1α expression. In the lower graph IL-6 protein was measured in the supernatants from the same cells.*

ELISA (2.5) data showed that IL-6 protein was detectable in supernatants of Monomac1 cells at a concentration of 1000pg/ml, when stimulated with PMA for 24 hours (**Figure 3.5.2**). In the presence of VAF347, PMA induced IL-6 protein expression was inhibited in a dose-dependent fashion with an estimated IC_{50} of ~5nM. These results showed that also PMA induced IL-6 expression in MM1 can be inhibited by VAF347. PMA is known to activate a plethora of different signal transduction pathways. Since the potency of VAF347 to inhibit PMA induced IL-6 was practically identical with that of IL-4+GM-CSF stimulated IL-6, it is possible that PMA activated a very similar chain of signaling events in MM1 than IL-4+GM-CSF.

3.6 Functional AhR is necessary to mediate the biological phenotype of VAF347

So far, all available data strongly indicated an involvement of the AhR signaling pathway in the biological activity of VAF347. To examine the role of AhR in the mode of action of VAF347 in more detail, two different approaches were selected. First, Monomac1 cells were infected with a

trans-dominant negative version of the AhR. Secondly, AhR gene expression was silenced by using the microRNA adapted short hairpin RNA (shRNAmir) interference technique.

3.6.1 A trans-dominant negative AhR protein abolishes VAF347 activity

As a first attempt to analyze the role of AhR in the mode of action of VAF347, Monomac1 cells were infected with a recombinant retrovirus expressing a truncated form of the AhR protein lacking the transactivation domain at the carboxyl-terminus (**Figure 3.6.1.1.A**). This truncated AhR protein has already been shown to act in a trans-dominant negative fashion before (142).

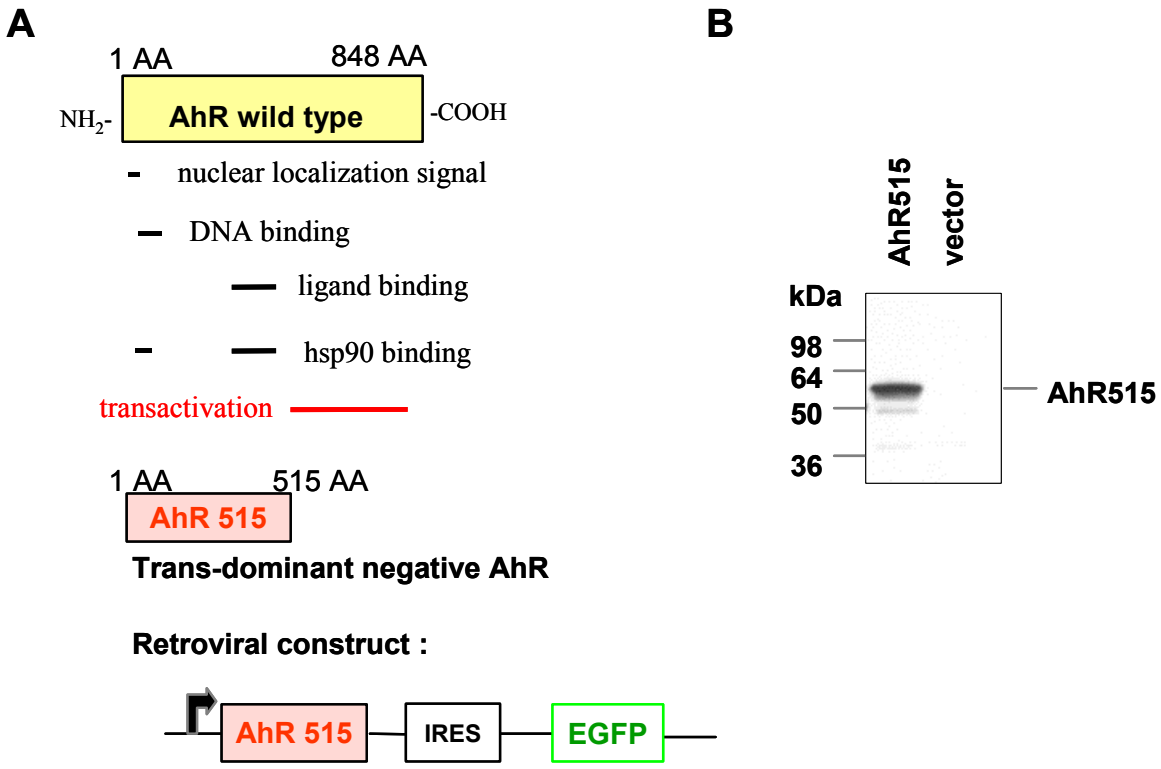

Figure 3.6.1.1: ***A trans-dominant negative AhR protein.*** *A) a truncated form of AhR containing only aa 1-515 and thus lacking the carboxyl-terminal transactivation domain was cloned into the retroviral expression vector pMX-pie. B) Ectopic over-expression of a truncated AhR (AhR515) in Monomac1 cells. A western blot analysis is shown. At the left, the positions of the molecular weight standards are indicated with the size given in kDa. At the right the position of AhR515 is indicated.*

The truncated AhR protein, containing amino acids 1-515 and therefore named AhR515, was amplified by PCR from cDNA of MM1 cells (2.4.3.A) and cloned into the recombinant retroviral expression vector pMX-pie. The resulting plasmid pMX-pie-AhR515 allows for the simultaneous

expression of the truncated AhR and the marker protein GFP due to the presence of an internal ribosome entry site (IRES) element (2.4.3.B) (**Figure 3.6.1.1.A**). This allowed for the selection of MM1 cells successfully infected with the AhR truncation mutant based on GFP positivity (2.10.3).

Ectopic over-expression of the trans-dominant negative AhR protein in Monomac1 cells was confirmed by western blot (2.6.3). In whole cell lysates of Monomac1 cells infected with pMX-pie-AhR515 the trans-dominant negative AhR protein with a size of ~59 kDa was detectable, whereas empty vector infected cells did not express this protein (**Figure 3.6.1.1.B**).

To analyze the biological activity of recombinant AhR515, Monomac1 cells over-expressing AhR515 were stimulated with IL-4 + GM-CSF in the presence or absence of VAF347 for 24 hours, before CYP1A1 mRNA expression was measured by RT-PCR (2.3).

Indeed, the AhR515 protein acted as a trans-dominant negative repressor since induction of CYP1A1 expression by VAF347 was almost completely abrogated in Monomac1 cells over-expressing the trans-dominant negative AhR (**Figure 3.6.1.2**). In cells that were infected with empty vector VAF347 was still able to induce CYP1A1 expression. These results confirmed the expression of AhR515 and its biological function in MM1 to act as a trans-dominant negative repressor.

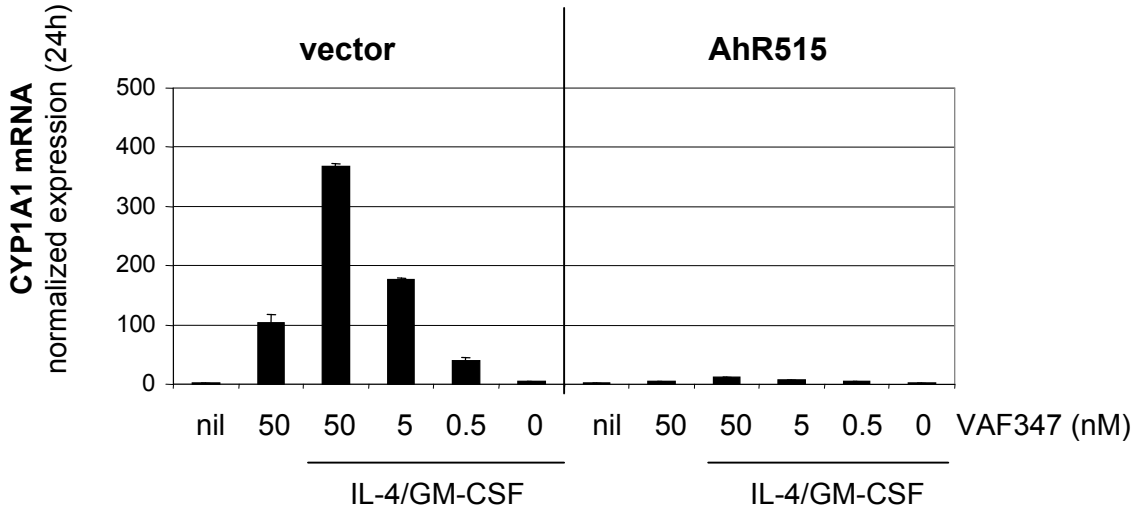

Figure 3.6.1.2: ***A trans-dominant negative AhR protein ablates CYP1a1 induction in Monomac1 cells****. AhR515 acts in a trans-dominant negative fashion by blocking the induction of CYP1A1 expression by VAF347. Vector = cells infected with parental retroviral vector. CYP1a1 expression was normalized to eF-1α expression.*

To answer the question whether the inhibitory effect of VAF347 on IL-6 expression was still observed in MM1 cells expressing the trans-dominant negative AhR, MM1 cells infected with either empty vector or AhR515 where stimulated with IL-4 + GM-CSF in the presence or absence of VAF347 for 24 hours before IL-6 mRNA production was analyzed by RT-PCR (2.3). Interestingly, VAF347 was no longer able to inhibit the IL-4 + GM-CSF induced IL-6 response in MM1 cells expressing the trans-dominant negative AhR (AhR515) (**Figure 3.6.1.3**). In contrast, VAF347 still inhibited IL-4 + GM-CSF induced IL-6 mRNA expression in vector infected cells.

To confirm these data at the protein level, IL-6 protein was measured by ELISA (2.5) in the supernatants from the same cells. Vector infected cells produced IL-6 at a concentration of approximately 160pg/ml after induction with IL-4 + GM-CSF. At a concentration of 50nM VAF347 IL-6 protein was detectable at a concentration of approximately 40pg/ml, thus inhibiting the IL-6 response by 4-fold in vector infected cells. In contrast, IL-6 protein production was no longer inhibited in MM1 cells expressing AhR515 (**Figure 3.6.1.3**).

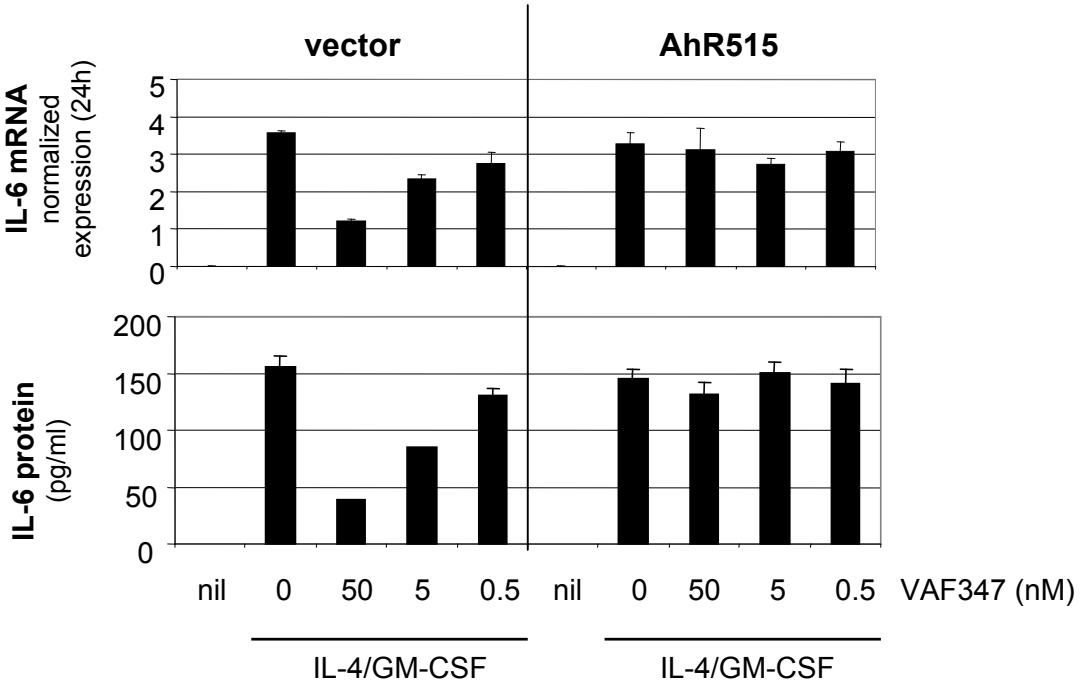

Figure 3.6.1.3: ***A trans-dominant negative AhR protein blocks the function of VAF347 to inhibit IL-6 production in Monomac1 cells****. The top row shows RT-PCR for IL-6 mRNA in control (vector) or AhR515 expressing cells that were induced with IL-4+ GM-CSF in the presence or absence of VAF347 for 24 hours. IL-6 expression was normalized to eF-1α expression. In the lower graphs IL-6 protein was measured in the supernatants from the same cells.*

Similar results were obtained when IL-6 expression was induced by PMA (data not shown). These results demonstrated that the AhR protein plays a key role in the mode of action by which VAF347 mediates inhibition of IL-6 synthesis, since over-expression of a trans-dominant negative AhR protein completely abolished VAF347 activity.

To further corroborate that AhR signaling activation can regulate IL-6 expression in MM1 cells the effects of TCDD on Monomac1 cells expressing the trans-dominant negative AhR were examined. MM1 cells infected with AhR515 protein or empty vector were stimulated with IL-4 + GM-CSF in the presence or absence of TCDD for 24 hours before IL-6 expression was analyzed by RT-PCR (2.3). As shown in **Figure 3.6.1.4** TCDD inhibited IL-6 mRNA expression in vector infected MM1 cells in a dose-dependent fashion. In contrast IL-6 expression was no longer inhibited in MM1 cells expressing a trans-dominant negative AhR (AhR515) protein.

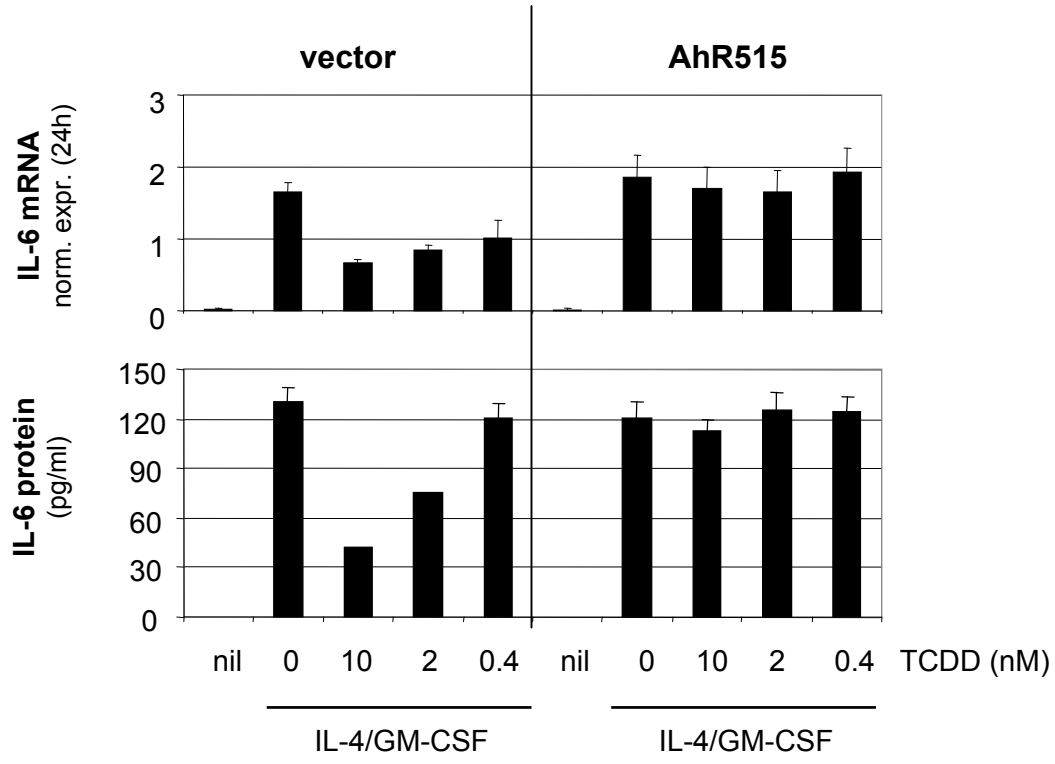

Figure 3.6.1.4: ***The trans-dominant negative AhR515 protein blocks the function of TCDD to inhibit IL-6 production in Monomac1 cells****. The top row shows RT-PCR for IL-6 mRNA in control (vector) or AhR515 expressing cells that were induced with IL-4+ GM-CSF in the presence or absence of TCDD for 24 hours. IL-6 expression was normalized to eF-1α expression. In the bottom row IL-6 protein was measured in the supernatants from the same cells.*

These data were further confirmed by measuring IL-6 protein in the supernatants of the same cells by ELISA (2.5). In vector infected cells induced with IL-4 + GM-CSF, IL-6 protein was measurable at a concentration of approximately 130pg/ml, while in the presence of 10nM TCDD the IL-6 protein was reduced to a level of around 40pg/ml (**Figure 3.6.1.4**). This effect was no longer seen in MM1 cells expressing AhR515, since TCDD did not inhibit IL-6 production in these cells.

Collectively, these data demonstrated that functional AhR protein is necessary to mediate the inhibitory effect of VAF347 on IL-6 production, since over-expression of a trans-dominant negative AhR completely abolished both VAF347 and TCDD activity in MM1 cells.

3.6.2 Silencing of AhR gene expression abolishes VAF347 activity

Another approach to analyze the functional involvement of the AhR in the mode of action of VAF347 was to silence wild type AhR gene expression. This was achieved by using the microRNA adapted short hairpin RNA (shRNAmir) interference technique. MicroRNAs are small endogenous RNAs that play important regulatory roles in animals by targeting mRNAs for cleavage or translational repression, thus reducing target gene expression (143).

The human packaging cell line PhoenixGP (2.7.5), was used to generate retroviral virus particles by transfecting PhoenixGP cells with either LMP-sh-RNA control vector (sh-control) or LMP-sh-AhR construct (2.6.4) which both contained an internal ribosome entry site (IRES)-GFP element. Retroviral infection of Monomac1 cells was achieved as described above. After infection Monomac1 cells expressing high levels of GFP were sorted (2.10.3) and kept in medium (2.7.3) supplemented with 1 µg/ml puromycin as a selection marker.

To test the functional activity of the LMP-sh-AhR construct, AhR protein expression in MM1 cells was analyzed by western blot (2.6.3). In whole cell lysates of Monomac1 cells infected with a sh-control construct wild type AhR protein with a size of approximately ~110 kDa was detectable (**Figure 3.6.2.1.A**). In contrast, AhR protein expression was strongly reduced in MM1 cells infected with the LMP-sh-AhR construct.

To analyze the biological consequences of AhR gene silencing, MM1 cells infected with either sh-control or sh-AhR were stimulated with IL-4 + GM-CSF in the presence or absence of VAF347 for 24 hours, before expression of the CYP1A1 or IL-6 gene was measured by RT-PCR (2.3).

As seen in **Figure 3.6.2.1.B** CYP1A1 mRNA response to VAF347 was nearly completely abrogated in Monomac1 cells infected with the sh-AhR construct, whereas VAF347 normally induced CYP1A1 expression in cells infected with a sh-control construct.

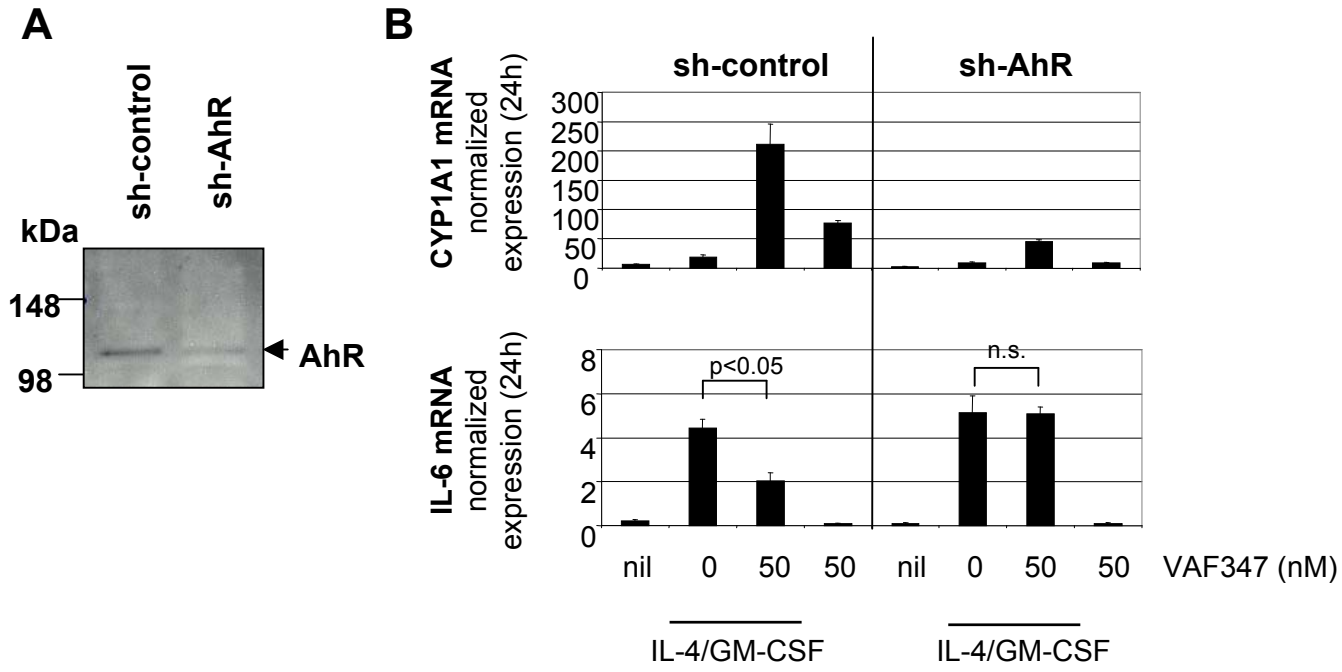

Figure 3.6.2.1: ***Silencing of the AhR gene abolishes VAF347 activity.*** *A) Reduced expression of AhR protein in Monomac1 cells infected with sh-AhR. A western blot analysis is shown. At the left, the positions of the molecular weight standards are indicated with the size given in kDa. At the right the position of AhR is indicated.*

B) The top row shows RT-PCR for CYP1A1 mRNA in sh-control (vector) or sh-AhR infected cells that were induced with IL-4+ GM-CSF in the presence or absence of VAF347 for 24 hours. In the bottom row IL-6 mRNA expression in the same samples is shown. CYP1A1 and IL-6 expression were normalized to eF-1α expression. Statistical analysis was done with two tailed Student's t-test.

More importantly, VAF347 was no longer able to inhibit IL-4 + GM-CSF induced IL-6 production in cells infected with sh-AhR (**Figure 3.6.2.1.B**).

In summary, these data identified the AhR as a functional relevant target for VAF347 since 1) other AhR agonists displayed an identical activity profile in MM1 cells compared to VAF347, 2) over-expression of a trans-dominant negative AhR completely abrogated VAF347 or TCDD activity and 3) silencing of the AhR gene was sufficient to abolish VAF347 activity.

3.7 Signaling events in Monomac1 after cytokine stimulation

Very little is known about the intracellular signaling events that lead to induction of IL-6 expression in Monomac1 cells. In order to analyze in detail how VAF347 activated AhR interferes with IL-6 expression in this cell line a thorough understanding of the signaling chains eventually leading to IL-6 expression in response to IL-4+GM-CSF was required.

3.7.1 IL-4 + GM-CSF lead to activation of members of the JAK/STAT family

Cytokines often mediate their responses through activation of the JAK/STAT pathway (144). The STAT family is known to consist of seven members STAT1-5, STAT5a, STAT5b and STAT6. JAKs represent a family of four tyrosine kinases, JAK1, JAK2, JAK3 and Tyk2, that selectively phosphorylate STATs upon binding of cytokines to their respective receptors. In unstimulated cells, STATs reside inactive in the cytoplasm. Cytokine stimulation leads to JAK mediated phosphorylation of STATs. Upon phosphorylation STATs form homo- or heterodimers and translocate to the nucleus where they regulate the expression of their target genes. IL-4 and IL-13 signaling is tightly connected to activation of STAT6 via activation of JAK1 and JAK3, and plays a key role in polarization of naïve $CD4^+$ T cells towards a T_H2 cell type (145). STAT5 is activated by multiple cytokines including IL-2, IL-3, IL-5 and GM-CSF, with GM-CSF signaling through JAK2 (146,147).

To examine which STATs were activated by IL-4+GM-CSF, Monomac1 cells were stimulated with the cytokine cocktail and the phosphorylation status of different STAT proteins was examined by western blotting: For this and all other following signaling experiments fresh Monomac1 cells (2.7.3) were seeded into 24 well plates at a density of $3x10^5$ cells per well and incubated at different time points in the presence or absence of the cytokines IL-4 and GM-CSF (2.8.2). Samples containing VAF347 were pre-incubated with 50nM VAF347 30-60 minutes prior to cytokine stimulation (2.8.2). Then whole cells lysates were prepared (2.6.1). 50µg protein of each lysate sample were used for western blot analysis, starting with Tris-glycine gel electrophoresis followed by blotting of the gel to a nitrocellulose membrane (2.6.2). Activated STATs were detected with antibodies recognizing phosphorylated STATs while the total amount of STAT protein on the gel was measured using mABs recognizing activated and quiescent protein (2.6.4).

The western blot analysis shown in **Figure 3.7.1.1** demonstrated that stimulation of Monomac1 with IL-4 + GM-CSF for 10 and 60 min lead to phosphorylation of STAT5 (Tyrosine694). Addition of VAF347 did not alter the phosphorylation status of STAT5.

Similar results were obtained when STAT6 protein expression was analyzed: IL+4 and GM-CSF in combination lead to phosphorylation of STAT6 (Tyrosine641) 10 min and 60 min after cytokine induction. VAF347 did not change the phosphorylation level of STAT6 (**Figure 3.7.1.1**).

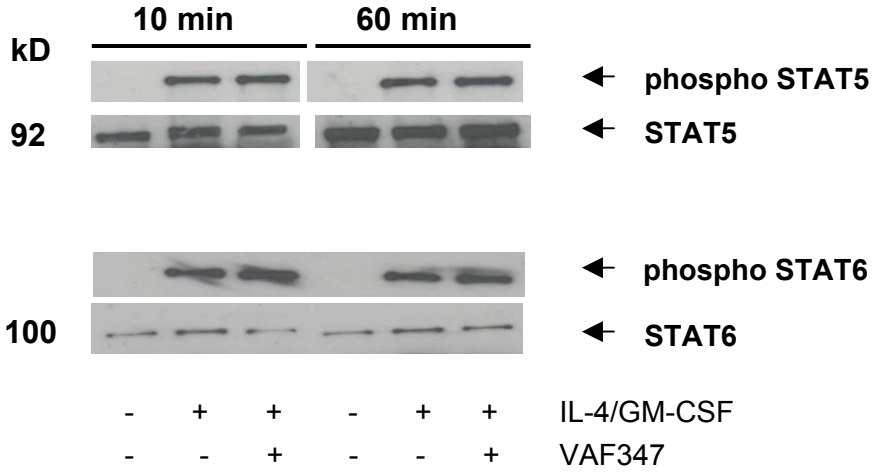

Figure 3.7.1.1: ***IL-4 + GM-CSF lead to phosphorylation of STAT5 and STAT6****. Total protein fraction of Monomac1 cells was isolated and the expression of phosphorylated and non-phosphorylated STAT proteins was determined in the same samples using western blotting.. At the left the molecular weight is indicated with the size given in kDa. At the right, positions of STAT proteins are indicated.*

The phosphorylation status of STAT1 and STAT3 proteins in MM1 cells after stimulation with IL-4 + GM-CSF was also examined by western blotting. Neither phosphorylated STAT1 nor phosphorylated STAT3 proteins could be detected (data not shown).

These results did not give any information whether activation of the JAK/STAT pathway was necessary for the induction of IL-6 expression in Monomac1 cells. An approach to examine a possible involvement of the JAK/STAT cascade in the signaling pathway(s) that leads to induction of IL-6 expression, was to inhibit members of the JAK/STAT family. The JAK inhibitor CP-690,550 has been shown to selectively inhibit JAK-3 previously and is 20- to 100-fold less potent for JAK2 (148).

Monomac1 cells (2.7.3) were stimulated with IL-4 + GM-CSF in the presence or absence of CP-690,550 for 24 hours, before IL-6 expression was analyzed by RT-PCR (2.3). Interestingly, CP-690,550 inhibited IL-6 mRNA induction by IL-4 + GM-CSF in a concentration dependent fashion with an IC_{50} of approximately 4nM (**Figure 3.7.1.2**). These results suggested that activation of JAK-3 was necessary for the induction of IL-6 expression in Monomac1.

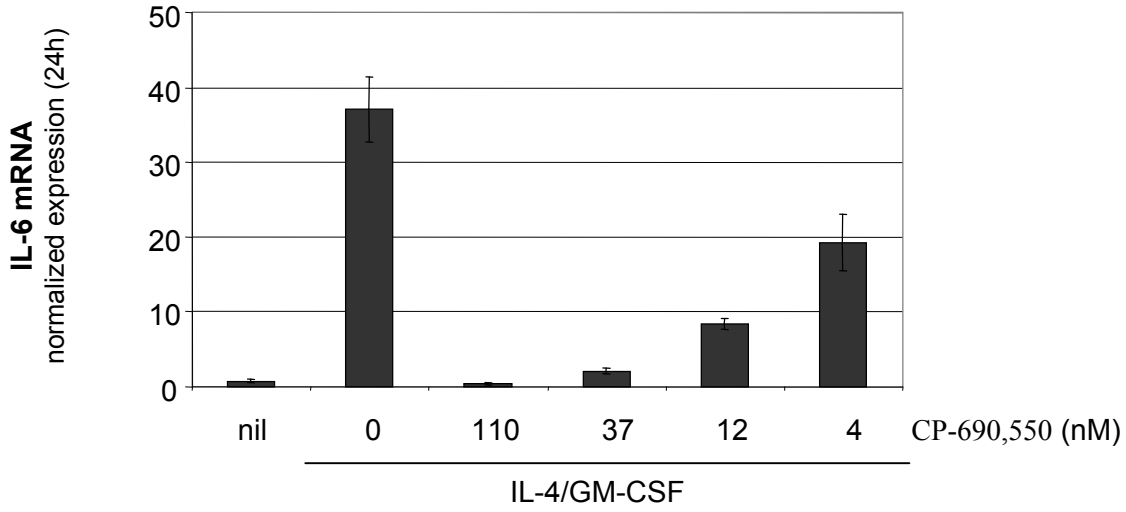

Figure 3.7.1.2: ***The JAK inhibitor CP-690,550 ablates IL-6 induction in Monomac1 cells****. RT-PCR data shown. IL-6 expression was normalized to eF-1α expression.*

3.7.2 IL-4 + GM-CSF lead to activation of proteins of the MAP Kinase cascade

GM-CSF is a hematopoietic cytokine that has important regulatory functions on cell proliferation and apoptosis in cells of myeloid, erythroid and lymphoid lineages (149,150). GM-CSF has been shown to induce multiple signaling pathways that transduce critical cell growth, differentiation or anti-apoptotic signals from the cell membrane into the nucleus. A common pathway triggered by GM-CSF is the Ras/Raf/MEK/ERK cascade. Many of the members of this pathway were initially identified as proto-oncogenes, and aberrant activation of this pathway has often been observed in malignantly transformed cells.

Activation of the Ras/Raf/MEK/ERK cascade may lead to the phosphorylation and thus activation of mitogen-activated protein kinases (MAPKs). MAPKs trigger a variety of cellular programs including cell proliferation, cell differentiation and cell death and are activated by a variety of up-stream signals including growth and neurotrophic factors, cytokines hormones and also infectious agents such as LPS. In mammals there are three main families of MAPKs: the c-Jun NH_2-terminal kinases (JNKs), p38 MAPK (p38) and extracellular-signal-regulated kinases (ERKs).

The JNK pathway contains two isoforms of the c-Jun NH_2-terminal kinase which phosphorylate multiple downstream targets such as the transcription factors c-Jun, ATF-2 and Elk-1 (151).

To test a possible involvement of the JNK pathway for IL-6 expression Monomac1 were induced with IL-4 and GM-CSF in the presence of the JNK inhibitor SP600125. Inhibition of JNK did not have any effect on the IL-6 response (data not shown), suggesting that the JNK pathway is not needed for the induction of IL-6 synthesis in MM1.

Activation of the p38 signaling cascade leads to phosphorylation of various transcription factors such as ELK-1, ATF-2, CHOP and Sap1a as well as other downstream kinases. However, inhibition of p38 signaling with a specific compound available in house did not interfere with IL-4 + GM-CSF induced IL-6 expression (data not shown).

The third MAP kinase pathway includes the two kinases p44 (ERK1) and p42 (ERK2).

Activation of the MAP kinases leads to the phosphorylation of threonine and tyrosine residues of p44 MAP kinase (ERK1) and p42 MAP kinase (ERK2) at the sequence Thr*GluTyr by the upstream mitogen-activated protein kinase/ERK kinase (MEK). Phosphorylated and thus activated p44 and p42 MAP kinases can directly phosphorylate a series of transcription factors including Ets-1, c-Jun and c-Myc.

To examine the phosphorylation status of p44/p42 MAP kinases in MM1 following cytokine stimulation, MM1 cells (2.7.3) were stimulated with IL-4, GM-CSF or a combination of both for 5 or 20 min, before whole cell lysates were prepared (2.6.1) and western blotting was performed (2.6.2). To detect p44 and p42 MAP kinases either antibodies directed against total p44/p42 MAP kinases or antibodies directed against phosphorylated p44/p42 MAP kinases (Threonin202/Tyrosine204) were used (2.6.5).

As seen in **Figure 3.7.2.1** Monomac1 cells constitutively express p44/p42 MAP kinases. Stimulation of Monomac1 with IL-4 did not activate ERK phosphorylation while GM-CSF lead to low levels of transient ERK activation after 5 minutes which decayed at 20 minutes. The combination of both cytokines resulted in robust phosphorylation of p44/p42 MAP kinases which was stronger at 5 minutes. Thus, IL-4 and GM-CSF synergistically induced ERK1/2 phosphorylation.

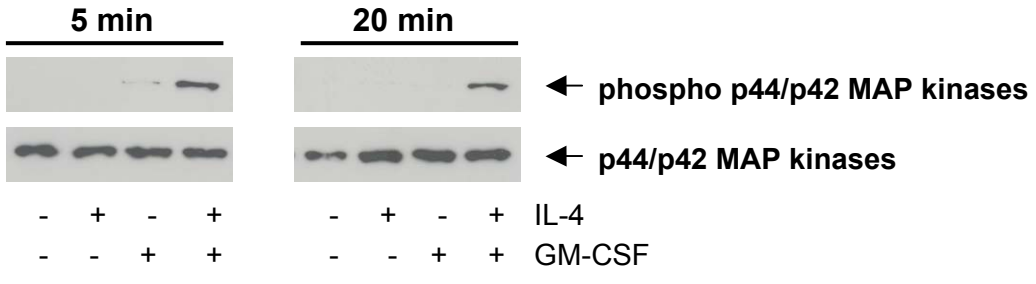

Figure 3.7.2.1: ***IL-4 + GM-CSF lead to phosphorylation of p44/p42 MAP kinases****. Total protein fraction of Monomac1 cells was isolated and the expression of phosphorylated and non-phosphorylated p44 and p42 MAP kinases was determined in the same samples using western blotting. At the right, positions of p44/p42 kinases are indicated.*

To examine the effects of VAF347 on the phosphorylation levels of p44/p42 MAP kinases, Monomac1 cells were stimulated with IL-4 + GM-CSF in the absence or presence of VAF347 for different time points (2.8.2). In a first series of experiments the presence of VAF347 seemed to increase and prolong the phosphorylation level of p44/p42 MAP kinases by IL-4 + GM-CSF. However, this effect was not reproducible (**Figure 3.7.2.2**).

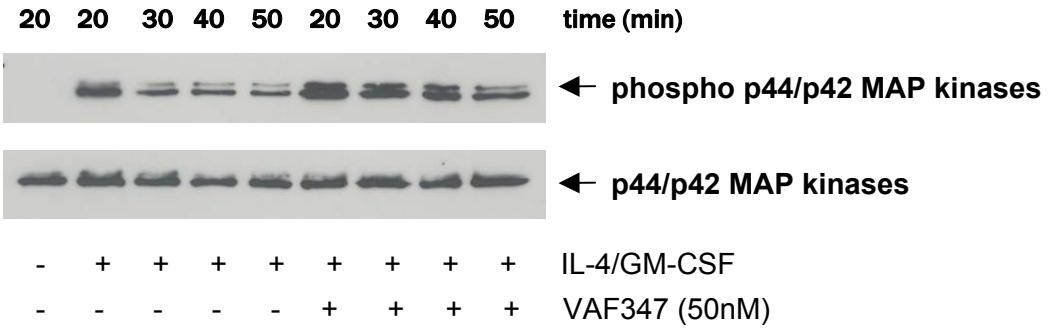

Figure 3.7.2.2: ***VAF347 does not reproducibly alter phosphorylation of p44/p42 MAP kinases****. Total protein fraction of Monomac1 cells was isolated and the expression of phosphorylated and non-phosphorylated p44 and p42 MAP kinases was determined in the same samples using western blotting. Only untreated control for 20 min is shown. At the right, positions of p44/p42 kinases are indicated.*

Earlier results showed that activation of the JAK/STAT pathway was involved in the signaling events that lead to IL-6 expression in Monomac1 cells (3.7.2). To test a possible link between the JAK/STAT pathway and the MAP kinase cascade MM1 cells (2.7.3) were stimulated with IL-4 + GM-CSF in the absence or presence of the JAK-3 inhibitor CP-690,550 and/or VAF347 for 20 min (2.8.2), before western blot for p44/p42 MAP kinases was performed.

In the presence of 20nM CP-690,550 stimulation of Monomac1 cells with IL-4 + GM-CSF lead to reduced phosphorylation of p44/p42 MAP kinases compared to cells that were induced with IL-4 + GM-CSF alone (**Figure 3.7.2.3**). VAF347 had no effect on the phosphorylation status of p44/p42 MAP kinases in cells treated with CP-690,550. VAF347 alone did not lead to phosphorylation of p44/p42 MAP kinases.

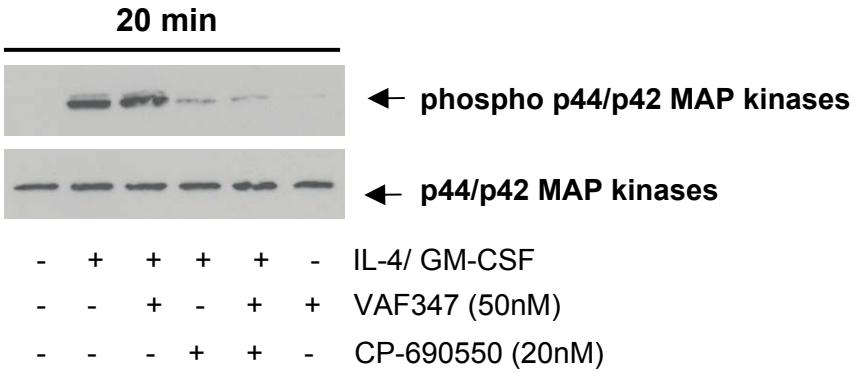

Figure 3.7.2.3: ***The JAK-3 inhibitor CP-690,550 inhibits the phosphorylation of p44/p42 MAP kinases****. Total protein fraction of Monomac1 cells was isolated and the expression of phosphorylated and non-phosphorylated p44 and p42 MAP kinases was determined in the same samples using western blotting. At the right, positions of p44/p42 kinases are indicated.*

These data demonstrated that activation of JAK-3 and maybe JAK2 was necessary for the phosphorylation of p44/p42 MAP kinases. However, these findings did not give information if activation of the MAP Kinase pathway was necessary for the induction of IL-6 expression in Monomac1 cells. One approach to examine a possible involvement of the p44/p42 MAP kinase cascade was to inhibit members of the MAP kinase family. PD98059 has been described to be a specific inhibitor of p44/p42 MAP kinases by inhibiting phosphorylation of these kinases (152). To test the biological activity of PD98059 in our experimental system, MM1 cells (2.7.3) were stimulated with IL-4+GM-CSF in the absence or presence of PD98059 for 20 min (2.8.2), before the phosphorylation levels of p44/p42 MAP Kinase were analyzed by western blotting (2.6.5).

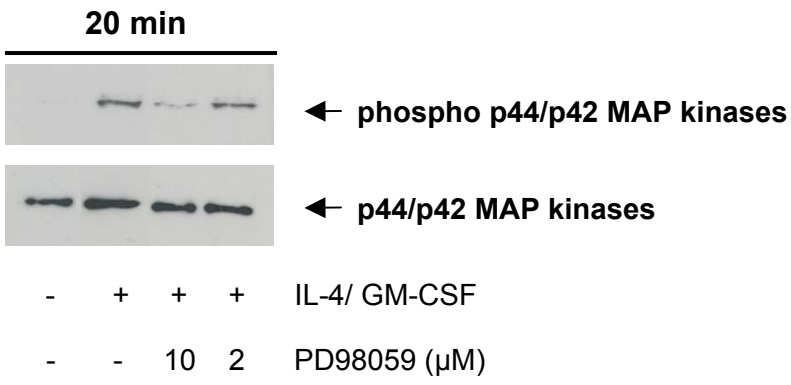

Figure 3.7.2.4: ***The MAP kinase inhibitor PD98059 inhibits the phosphorylation of p44/p42 MAP kinases****. Total protein fraction of Monomac1 cells was isolated and the expression of phosphorylated and non-phosphorylated p44 and p42 MAP kinases was determined in the same samples using western blotting. At the right, positions of p44/p42 kinases are indicated.*

At a concentration of 10µM PD98059 inhibited phosphorylation of p44/p42 MAP kinases in MM1 cells that had been induced with IL-4 + GM-CSF for 20 min (**Figure 3.7.2.4**).

To examine the effect of PD98059 on IL-6 expression Monomac1 cells were stimulated with IL-4 + GM-CSF in the absence or presence of PD98059 for 24 hours, before IL-6 expression was analyzed by quantitative RT-PCR (2.3). As shown in **Figure 3.7.2.5** PD98059 inhibited IL-4 + GM-CSF induced IL-6 mRNA expression in a concentration dependent-fashion in MM1 cells. These data suggested that activation of p44/p42 MAP kinases is involved in the signal events that lead to IL-6 expression in MM1 cells.

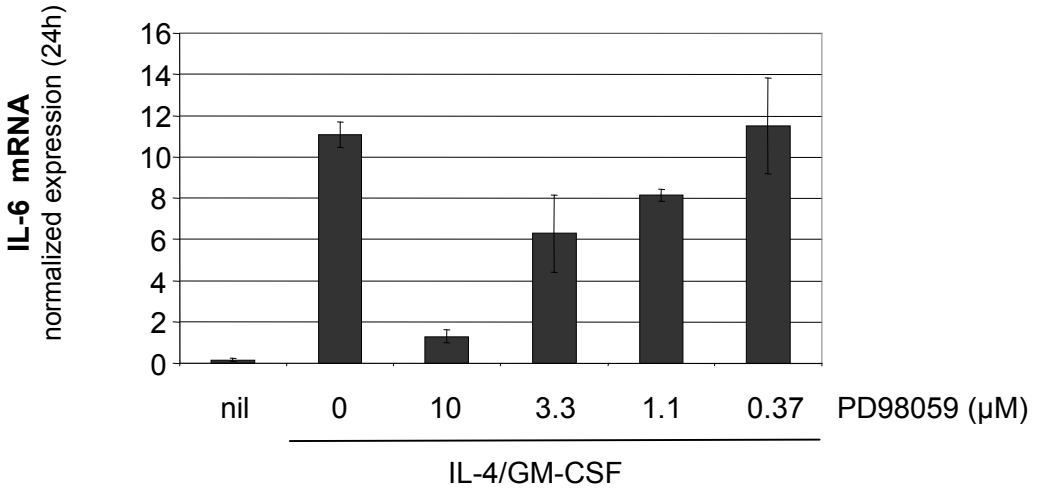

Figure 3.7.2.5: ***The MAP kinase inhibitor PD98059 inhibits IL-6 expression in Monomac1 cells****. IL-6 expression was measured 24h after stimulation by RT-PCR and normalized to eF-1α expression.*

3.7.3 Goe6979, a potent JAK-2 inhibitor, inhibits IL-6 expression in Monomac1

The protein kinase C (PKC) family of serine/threonine kinases has been shown to be a predominant downstream target of LPS signaling. The PKC family consists of at least 11 known isoforms that are divided into three subfamilies according to their substrate specifity: the conventional α, βI, βII and γ PKC which are dependent on calcium and diacylglycerol (DAG), the novel δ, ε, θ, and η PKC which are DAG dependent and calcium independent and finally the atypical ξ and λ/ι PKC which are DAG independent (153). PKC has been shown to be involved in the LPS induced production of TNF-α, IL-1β and IL-6 in monocytes and macrophages as well as the differentiation of immature cells into monocytes and macrophages (154,155).

To test a possible involvement of PKC proteins in the signaling events that lead to IL-6 synthesis, different PKC inhibitors were tested in their ability to block IL-6 expression in MM1. MM1 cells were stimulated with IL-4 + GM-CSF in the absence or presence of different PKC inhibitors (2.7.6) for 24h before IL-6 mRNA was measured as described above. As shown in **Figure 3.7.3.1** neither Calphostin C, BisindolylmalmeideI nor Ro-32-0432 inhibited IL-4 + GM-CSF induced IL-6 mRNA expression in MM1.

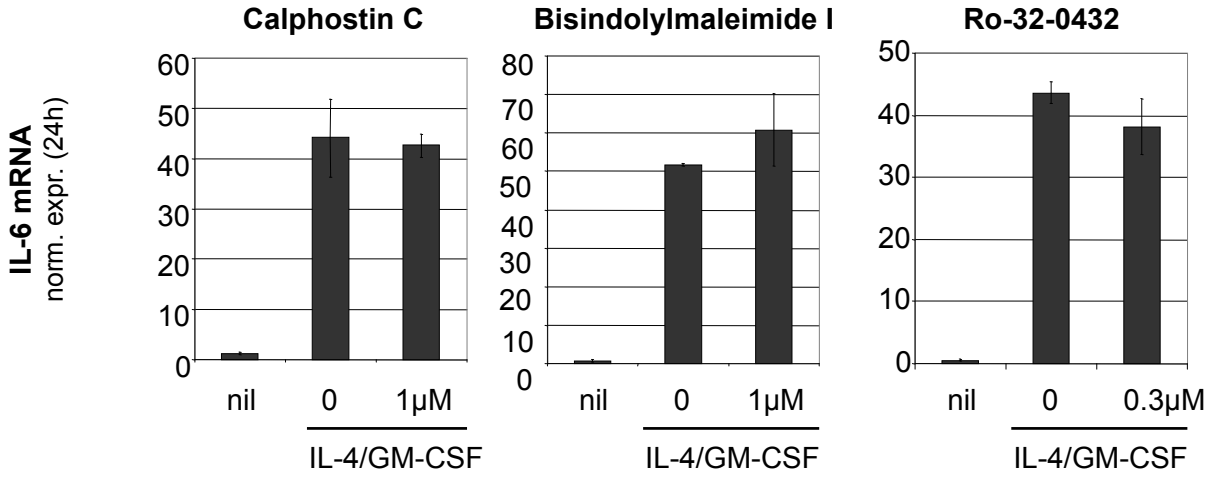

Figure 3.7.3.1: ***Different PKC inhibitors do not alter IL-4/GM-CSF induced IL-6 expression in Monomac1***. *IL-6 mRNA expression was measured by RT-PCR and normalized to eF-1α expression.*

In contrast, the PKC inhibitor Goe6976 inhibited the IL-6 response to IL-4 + GM-CSF in a dose-dependent fashion as shown in Figure **3.7.3.2**. In addition to block PKC this compound was shown to act as potent inhibitor of JAK2 in the nanomolar range (156).

Based on the negative data with the other PKC inhibitors and the known role of JAK2 in cytokine signaling it is plausible that the inhibitory effects of Goe6976 on IL-6 production was rather due to its anti-JAK2 activity rather than to its inhibitory effects on PKC. This concept would fit to the results obtained with the dual JAK3/JAK2 inhibitor CP-690,550 which also inhibited cytokine induced IL-6 expression.

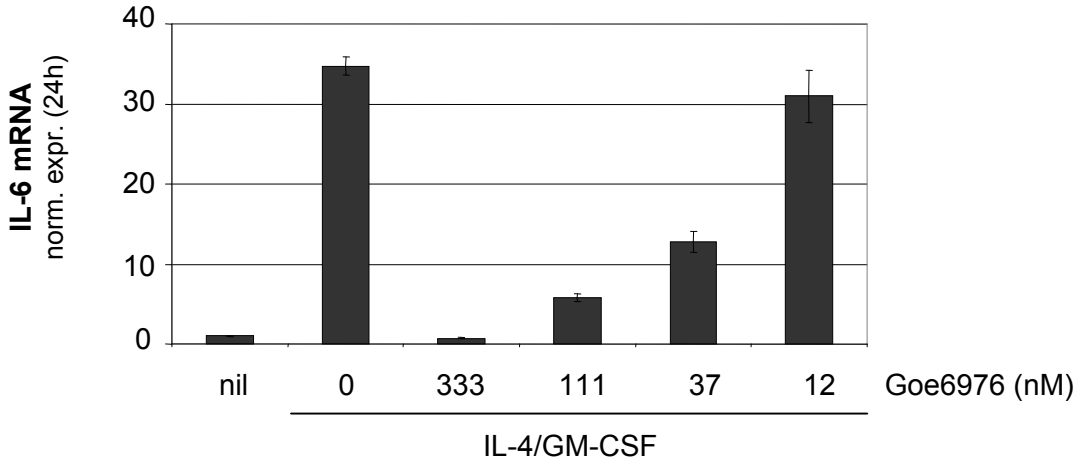

Figure 3.7.3.2: ***The PKC inhibitor Goe6976, which is also a potent JAK-2 inhibitor, ablates IL-4/GM-CSF induced IL-6 expression in Monomac1***. *IL-6 mRNA expression was measured by RT-PCR and normalized to eF-1α expression.*

These results demonstrated that induction of IL-6 expression in Monomac1 does not involve PKC, since various PKC inhibitors did not reduce the IL-6 response to IL-4 + GM-CSF stimulation.

3.7.4 NF-κB inhibitors do not alter IL-6 expression in Monomac1

NF-κB has been shown to be involved in the events that lead to induction of IL-6 expression in various cell types. To investigate if inhibition of NF-κB could abolish the induction of IL-6 synthesis in Monomac1, the two NF-κB inhibitors pyrrolidinedithiocarbamate and an "NF-κB activation inhibitor" (with a calculated IC_{50} of 11 nM in Jurkat cells) (2.7.6) were used.

MM1 cells were stimulated with IL-4 + GM-CSF in the presence or absence of these two NF-κB inhibitors for 24h before IL-6 expression was measured as described above. As shown in **Figure 3.7.4.1** neither pyrrolidinedithiocarbamate nor the "NF-κB activation inhibitor" could inhibit IL-4 + GM-CSF induced IL-6 expression in Monomac1.

These results suggested that NF-κB activation was not critically involved in the signaling events that lead to induction of IL-6 expression in MM1 cells.

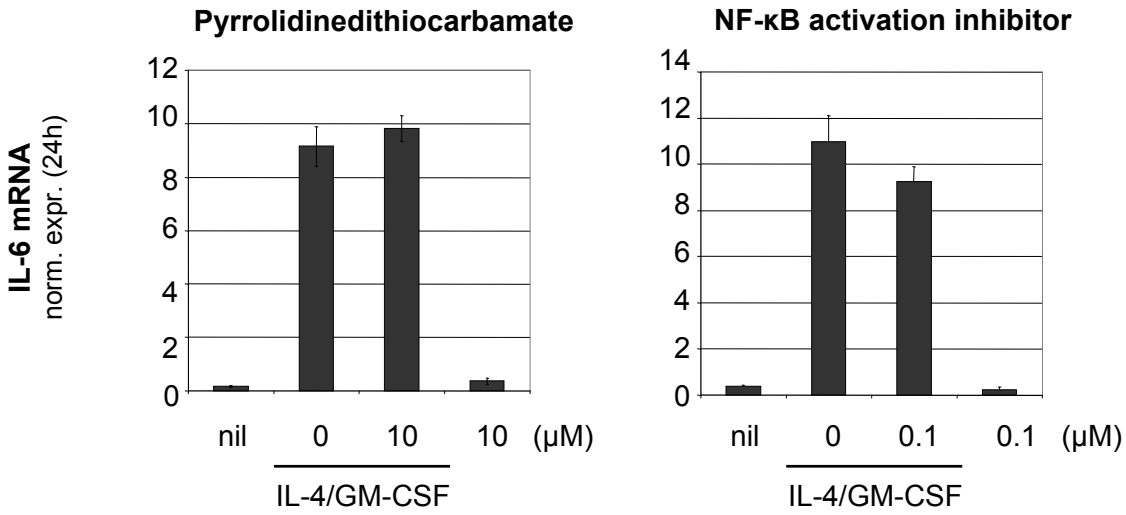

Figure 3.7.4.1: ***NF-κB inhibitors do not alter IL-4/GM-CSF induced IL-6 expression in Monomac1***. *IL-6 mRNA expression was measured by RT-PCR and normalized to eF-1α expression.*

3.8 IL-6 promoter studies

IL-6 expression can be induced by a variety of cell stimuli and different mechanisms may act individually to enhance IL-6 transcription, depending on the stimulus and cell type. So far, several regulatory elements in the IL-6 promoter have been described, including cis-regulatory elements for the transcription factors NF-IL6, NF-κB, CREB and AP-1.

So far, all available data indicated functional involvement of the AhR in the mode of action of VAF347. AhR has been shown to physically interact with other transcription factors, including NF-κB (157). Therefore, a possible explanation for the inhibitory activity of VAF347 on IL-6 mRNA may be that activation of AhR signaling interferes with IL-6 promoter activity as a consequence of AhR interaction with a transcription factor necessary for promoter activation.

3.8.1 VAF347 inhibits the induction of an IL-6 promoter reporter construct

To investigate the possibility that VAF347 activity interferes with IL-6 expression at the transcriptional level, an ~800bp IL-6 promoter fragment was cloned upstream of the reporter gene luciferase into the vector pGL3-basic (2.4.1). This construct, which was named 'pGL3b-IL-6 promoter', was transiently transfected into Monomac1 cells by electroporation using the Amaxa Nucleofector device™ (2.9). Briefly, $2x10^6$ Monomac1 cells were resuspended in nucleofection Solution-V containing 'pGL3b-IL-6 promoter' or empty vector, before cells were electroporated in the Amaxa Nucleofector device™. Cells were then stimulated with either PMA or IL-4+GM-CSF

in the presence or absence of VAF347 or VAG005 for 24 hours, before luciferase activity as a function of IL-6 promoter activity was measured in lysed cells (2.9.1).

As shown in **Figure 3.8.1.1** the presence of the IL-6 promoter resulted in higher constitutive expression of luciferase in untreated Monomac1 cells compared to vector transfected cells. The stimulation of pGL3b-IL-6 promoter transfectants with PMA increased reporter gene expression about 7-fold, while IL-4 + GM-CSF lead to 5-fold increase of reporter gene expression. Interestingly, the presence of VAF347 in both PMA or IL-4 + GM-CSF induced transfectants inhibited luciferase gene expression by either ~2.6–fold or 3-fold, respectively.

VAG005 is a closely related derivative of VAF347 which was found to be inactive on human B-cells to inhibit IgE production (67) and is only a weak ligand of AhR, with a binding potency of at least 100- fold less compared to VAF347. In contrast to VAF347, VAG005 did not inhibit luciferase gene induction in PMA or IL-4 + GM-CSF treated cells.

These data demonstrated that VAF347 signaling interferes with IL-6 expression at the transcriptional level, since VAF347 inhibits induction of an IL-6 promoter reporter construct. In contrast, VAG005, a much weaker ligand for AhR does not inhibit reporter gene expression. This is in line with earlier data of AhR being critically involved in suppression of the IL-6 response.

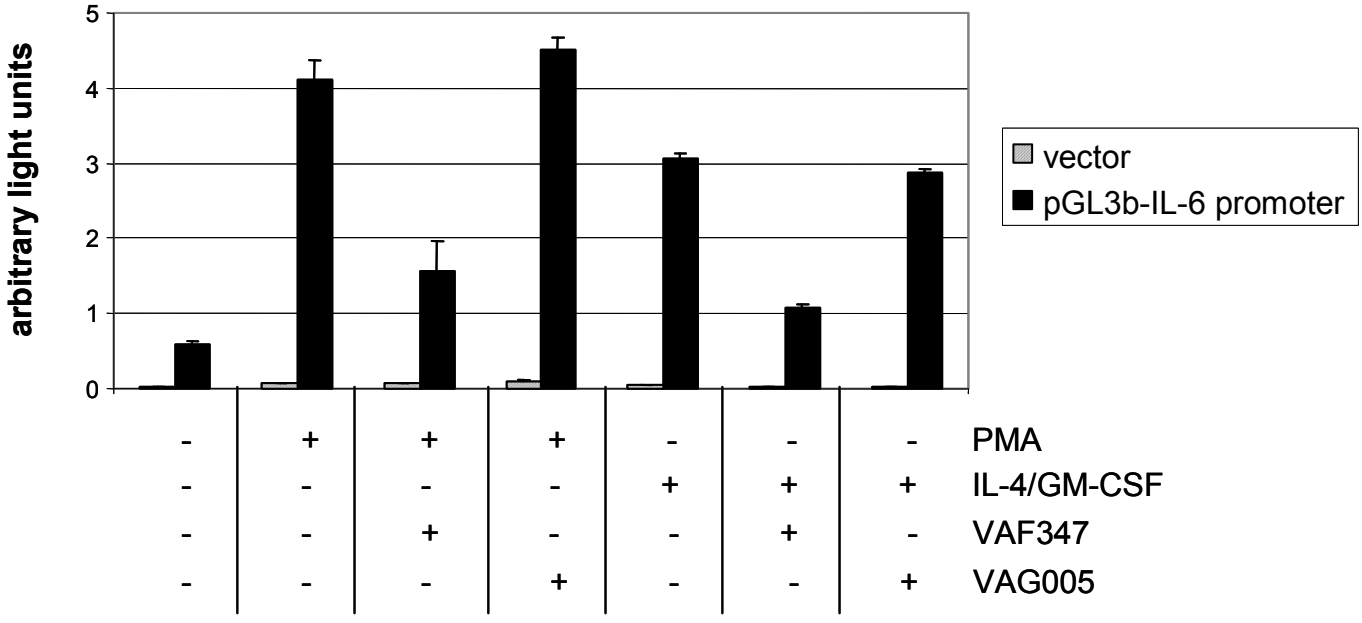

Figure 3.8.1.1: ***VAF347 inhibits reporter gene expression of a IL-6 promoter construct****. Transient transfection of Monomac1 cells with an IL-6 promoter construct. As negative control the empty vector (vector) was used. One representative experiment out of three is shown.*

3.8.2 VAF347 blocks the binding of NF-IL6 to the IL-6 promoter

A possible mechanism by which VAF347 could mediate inhibition of IL-6 expression at the transcriptional level is that VAF347 somehow alters the transcription factor composition binding to the IL-6 promoter DNA sequence. To determine whether transcription factors known to be important for the transcription of IL-6, bind to the IL-6 promoter chromatin immunoprecipitation (ChIP) assays were performed. The ChIP technique allows to examine whether a known transcription factor truly binds to a regulatory DNA sequence in living cells: live cells are treated with formaldehyde to generate protein-protein and protein-DNA cross-links between molecules in close proximity. Crosslinked nucleoprotein complexes containing the transcription factor of interest are then enriched by immunoprecipitation with anti-transcription factor specific antibodies. Reversal of the formaldehyde protein-DNA cross-links permits recovery and quantitative analysis of the co-immunoprecipitated DNA.

Briefly, Monomac1 cells were stimulated with IL-4 + GM-CSF in the presence or absence of VAF347 for 24 hours (2.11.1). Crosslinking of histones to DNA was achieved by the addition of formaldehyde to the cells at a final concentration of 0.7%, followed by lysis of the cells in SDS Lysis buffer (2.11.2). Random DNA fragmentation was done using the Diagenode Bioruptor™ machine. In 10 cycles of sonication, 30 sec each, the DNA was fragmented to a length of 100-400bp fragments (2.11.3). At this point aliquots of each sheared DNA sample were stored and labelled as Input to control the quality of the DNA.

Then, immunoprecipitation was performed by adding anti human NF-IL6 antibody or IgG control antibody to each ChIPsample (2.11.4). Following immunoprecipitation the DNA-histone complexes were eluted from the NF-IL6 antibody and Proteinase K digestion was performed (2.11.5). DNA was recovered by Phenol/Choroform extraction, followed by direct analysis of the DNA by PCR with primers amplifying the NF-IL6 binding region in the IL-6 promoter (2.11.6).

As shown in **Figure 3.8.2.1** a 130bp IL-6 promoter product was obtained in IL-4 + GM-CSF induced Monomac1 cells using the NF-IL6 antibody.

Interestingly, in the presence of VAF347 the IL-6 promoter product was not seen in Monomac1 cells that were induced with IL-4 + GM-CSF.

In control samples that were immunoprecipitated without anti-NF-IL6 or with control antibody (rabbit IgG), DNA-protein complexes did not generate the IL-6 promoter PCR product (**Figure 3.8.2.1**).

These studies demonstrated that IL-4 + GM-CSF induce the binding of NF-IL6 to the IL-6 promoter while in the presence of VAF347 NF-IL6 does not bind to the IL-6 promoter.

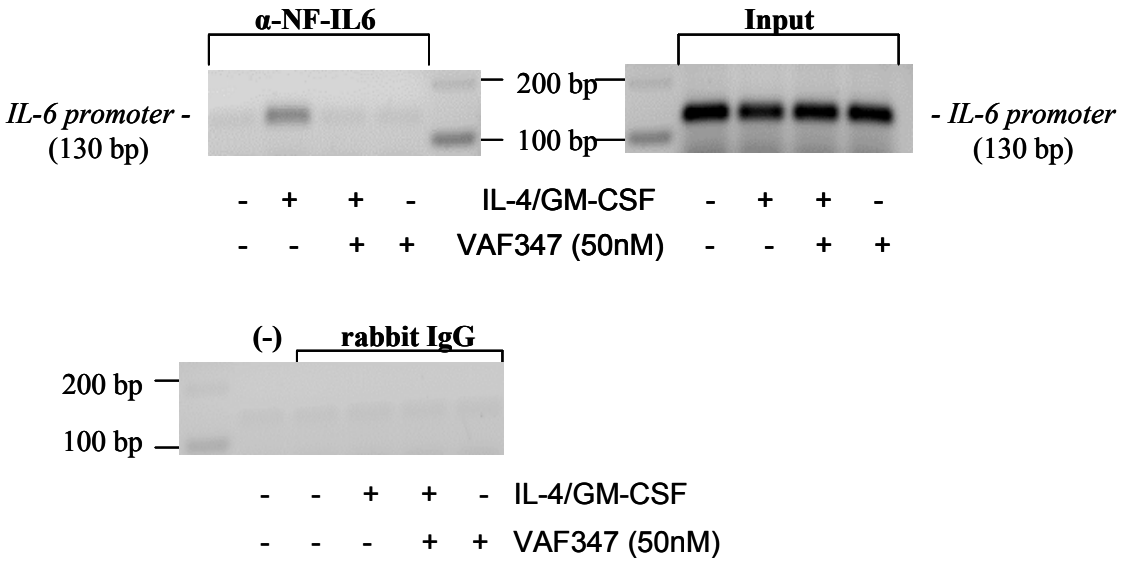

Figure 3.8.2.1: ***Binding of NF-IL6 to the IL-6 promoter in activated Monomac1 cells****. MM1 were stimulated with IL-4+GMCSF in the absence or presence of VAF347 for 24, before samples were subjected to ChIP analysis. DNA-protein complexes were immunoprecipitated without (-) or with anti-NF-IL6 (α-NF-IL6) or control antibodies (rabbit-IgG). The specific IL-6 promoter 130bp product is indicated. In addition the quality of the input DNA (Input) was controlled by PCR. One representative experiment out of two is shown.*

3.8.3 VAF347 does not inhibit the expression of IL-6 relevant transcription factors

A possible mechanism by which VAF347 could block the binding of NF-IL6 to the IL-6 promoter is that VAF347 alters the expression of NF-IL6 or other transcription factors necessary for the induction of IL-6 gene transcription. To examine the expression levels of NF-IL6, NF-κB p65 and c-Fos or c-Jun, MM1 cells were stimulated with IL-4 + GM-CSF in the presence or absence of VAF347 before mRNA expression was examined by RT-PCR (2.3).

As shown in **Figure 3.8.3.1** VAF347 did not inhibit the expression of NF-IL6, NF-κB p65, c-Fos or c-Jun in MM1 cells that were induced with IL-4 + CM-CSF.

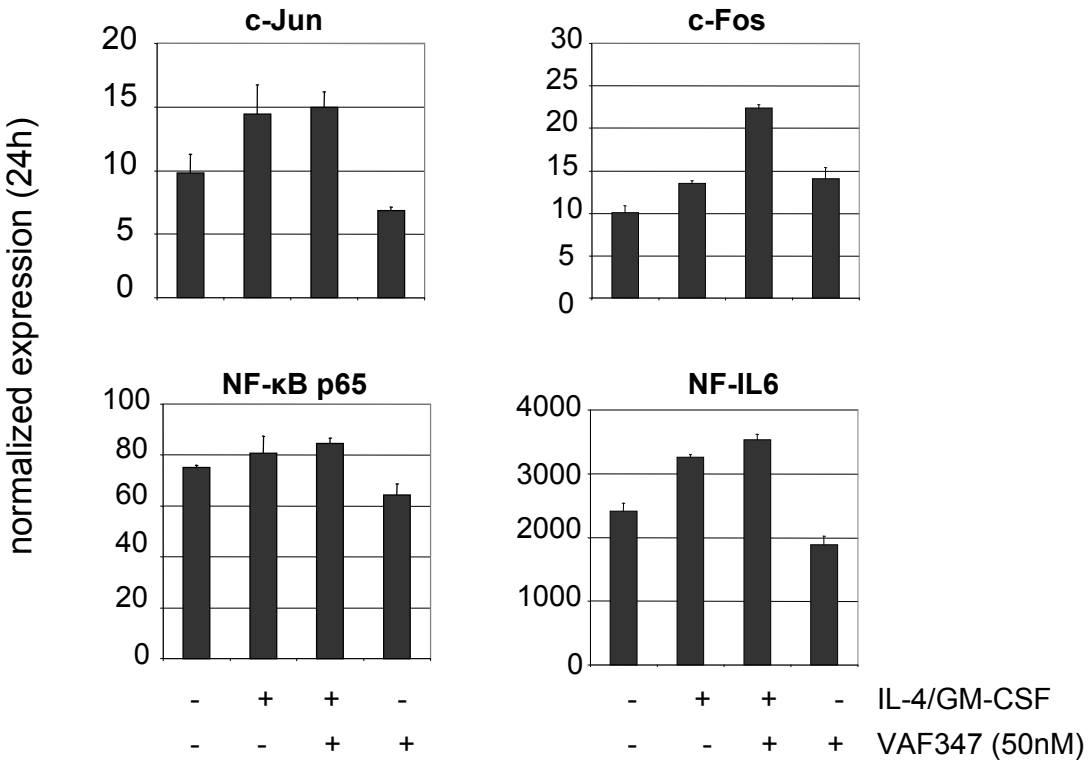

Figure 3.8.3.1: ***VAF347 does not inhibit the expression of transcription factors which are thought to be relevant in IL-6 transcription in Monomac1****. The top row shows RT-PCR for c-Jun and c-Fos mRNA in MM1 cells that were induced with IL-4/GM-CSF in the presence or absence of VAF347 for 24 hours. The bottom row shows mRNA expression levels of NF-κB p65 and NF-IL6. Expression was normalized to eF-1α expression.*

These results suggested that the inhibitory effect of VAF347 is not mediated via reduced expression of transcription factors which are thought to be relevant for the induction of IL-6 expression.

3.9 Interference of VAF347 with IL-6 relevant transcription factors

So far, all available data indicated that VAF347 interfered with IL-6 expression at the transcriptional level, since VAF347 inhibited the expression of an IL-6 promoter reporter construct and blocked the binding of NF-IL6 to the IL-6 promoter as seen in ChIP assays.

In order to substantiate the effects of VAF347 on NF-IL6 promoter interaction, the transcription factor was overexpressed in MM1 cells. The rationale for this approach was the possibility that VAF347 activated AhR exerted its regulatory effects by interaction with crucial transcription factors driving IL-6 expression (such as NF-IL6). In such a scenario, over-expression of a potential AhR partner protein to levels higher than endogenous AhR would still leave enough unliganded

factor available to perform its normal function. Consequently, one would expect a loss of VAF347 potency. To investigate if over-expression of either wild-type NF-κB p65, NF-IL6 or AP-1 could abolish the inhibitory effect of VAF347 in Monomac1 cells, each transcription factor was cloned into the retroviral expression vector pMX-pie.

As a first attempt, Monomac1 cells were retrovirally infected with the pMX-pie expression vector containing full-length c-Fos or c-Jun proteins, both components of the transcription factor AP-1. However, MM1 cells over-expressing c-Fos or c-Jun respectively were not viable and died shortly after infection, probably due to intolerance of MM1 cells to high amounts of c-Fos/c-Jun. Therefore, interference of VAF347 with AP-1 activity could not be examined.

3.9.1 Over-expression of NF-IL6 partially abolishes the inhibitory effect of VAF347

The full-length NF-IL6 sequence was amplified from cDNA of human MM1 cells and cloned into the recombinant retroviral expression vector pMX-pie, which contained an internal ribosome entry site (IRES)-GFP element (2.4.5). This construct was named pMX-pie-NF-IL6.

The human packaging cell line PhoenixA (2.7.4) was used to generate retroviral virus particles by transfecting PhoenixA cells with either the pMX-pie vector or pMX-pie-NF-IL6 (2.10.1). Retroviral infection of MM1 cells was done as described above.

Ectopic over-expression of full length NF-IL6 protein in Monomac1 cells was confirmed by western blotting (2.6.6). Since the NF-IL6 gene encodes several isoforms due to usage of alternative AUG translational initiation sites, NF-IL6 isoforms of 40 kDa, 35 kDa, 20 kDa and 8.5 kDa can be produced.

In whole cell lysates of MM1 infected with pMX-pie-NF-IL6 over-expression of NF-IL6 isoforms with a size of ~40 kDa and ~ 20 kDa was confirmed (**Figure 3.9.1.1.A**).

To analyze the effect of NF-IL6 over-expression on the IL-6 response, MM1 cells over-expressing wild-type NF-IL6 were stimulated with IL-4 + GM-CSF in the presence or absence of VAF347 for 24 hours, before IL-6 expression was measured by RT-PCR (2.3).

As shown in **Figure 3.9.1.1.B** over-expression of NF-IL6 resulted in constitutive higher expression levels of IL-6 mRNA in untreated NF-IL6 infectants compared to vector infected cells. Induction with IL-4 + GM-CSF lead to increased levels of IL-6 mRNA in cells over-expressing NF-IL6. Interestingly, the inhibitory effect of VAF347 on IL-6 expression was partially abolished in MM1 cells over-expressing NF-IL6.

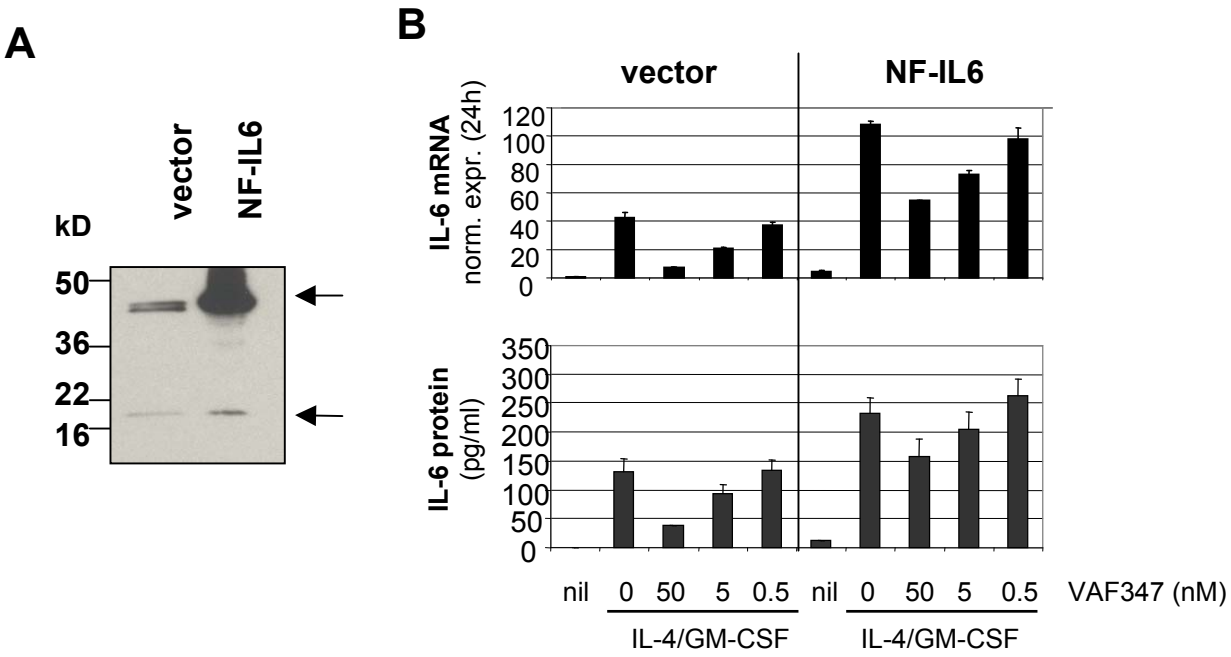

Figure 3.9.1.1: ***Ectopic over-expression of the transcription factor NF-IL6 partially abolishes the inhibitory effect of VAF347 on IL-4 + GM-CSF induced IL-6 expression****. A) Ectopic over-expression of NF-IL6 protein in Monomac1 cells infected with pMX-NF-IL6. A western blot analysis is shown. At the left, the positions of the molecular weight standards are indicated with the size given in kDa. At the right the positions of NF-IL6 isoforms are indicated.*

B) The top row shows RT-PCR for IL-6 mRNA in vector (vector) or pMX-NF-IL6 (NF-IL6) infected cells that were induced with IL-4+ GM-CSF in the presence or absence of VAF347 for 24 hours. IL-6 expression was normalized to eF-1α expression. In the bottom row IL-6 protein was measured in the supernatants of the same cells.

To confirm these data on the protein level, IL-6 protein was measured in the supernatants of the same samples by ELISA (2.5). Constitutive expression of very low amounts of IL-6 close to the detection limit of the ELISA was measurable in NF-IL6 infectants but not in control cells (**Figure 3.9.1.1.B**). Induction of NF-IL6 infectants with IL-4+GM-CSF lead to increased levels of IL-6 protein compared to vector infected cells, which was is accordance to the results seen at the mRNA level. The presence of VAF347 in IL-4+GM-CSF induced NF-IL6 infectants showed consistently less inhibition of IL-6 levels compared to vector infected cells. The reduced degree of inhibition was statistically significant but the inhibitory effect of VAF347 was not completely abrogated.

To test if the partial loss of VAF347 inhibitory activity was also seen with another induction stimulus of IL-6 expression, MM1 cells over-expressing wild-type NF-IL6 were stimulated with PMA in the presence or absence of VAF347 for 24 hours, before IL-6 mRNA expression was measured by quantitative RT-PCR (2.3).

As shown in **Figure 3.9.1.2** the inhibitory effect of VAF347 on PMA induced IL-6 expression was partially abolished in MM1 cells over-expressing NF-IL6, while in vector infected cells VAF347 inhibited IL-6 expression. Also at the protein level, the inhibitory activity of VAF347 was strongly abrogated in NF-IL6 infectants (**Figure 3.9.1.2**).

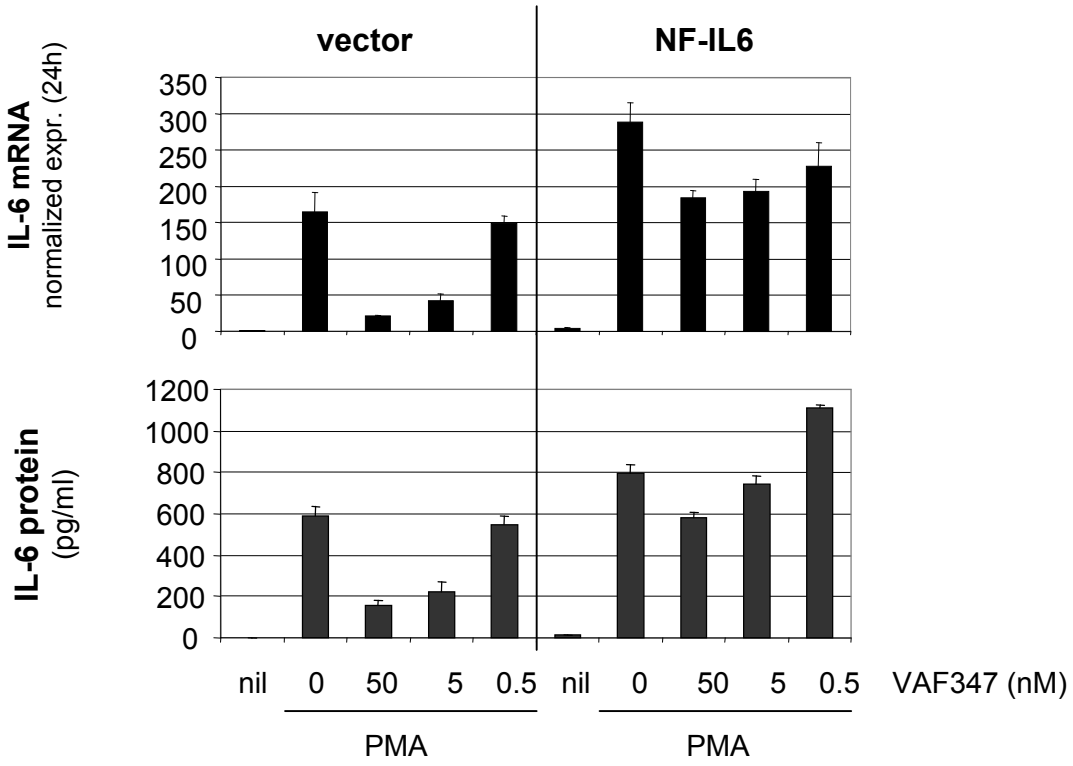

Figure 3.9.1.2: ***Over-expression of the transcription factor NF-IL6 partially abolishes the inhibitory effect of VAF347 on PMA induced IL-6 expression***. *The top row shows RT-PCR for IL-6 mRNA in vector (vector) or pMX-NF-IL6 (NF-IL6) infected cells that were induced with PMA in the presence or absence of VAF347 for 24 hours. IL-6 expression was normalized to eF-1α expression. In the bottom row IL-6 protein was measured in the supernatants of the same cells.*

Collectively, these data demonstrated that VAF347 mediates its inhibitory effect at least partially via interfering with NF-IL6, since VAF347 blocks the binding of NF-IL6 to the IL-6 promoter and over-expression of wild type NF-IL6 partially abolishes the inhibitory effect of VAF347.

3.9.2 Over-expression of NF-κB p65 does not alter the inhibitory effect of VAF347

The wild type protein NF-κB p65 was amplified from cDNA of human Monomac1 cells and cloned into the recombinant retroviral expression vector pMX-pie (2.4.6). The resulting construct was named pMX-pie- NF-κB p65.

Retroviral infection of Monomac1 cells with either vector or pMX-pie- NF-κB p65 was done as described above. Ectopic over-expression of full length NF-κB p65 protein was examined by western blotting (2.6.7). In whole cell lysates of MM1 cells infected with pMX-pie-NF-κB p65 over-expression of full-length NF-κB p65 protein was confirmed (**Figure 3.9.2.1.A**).

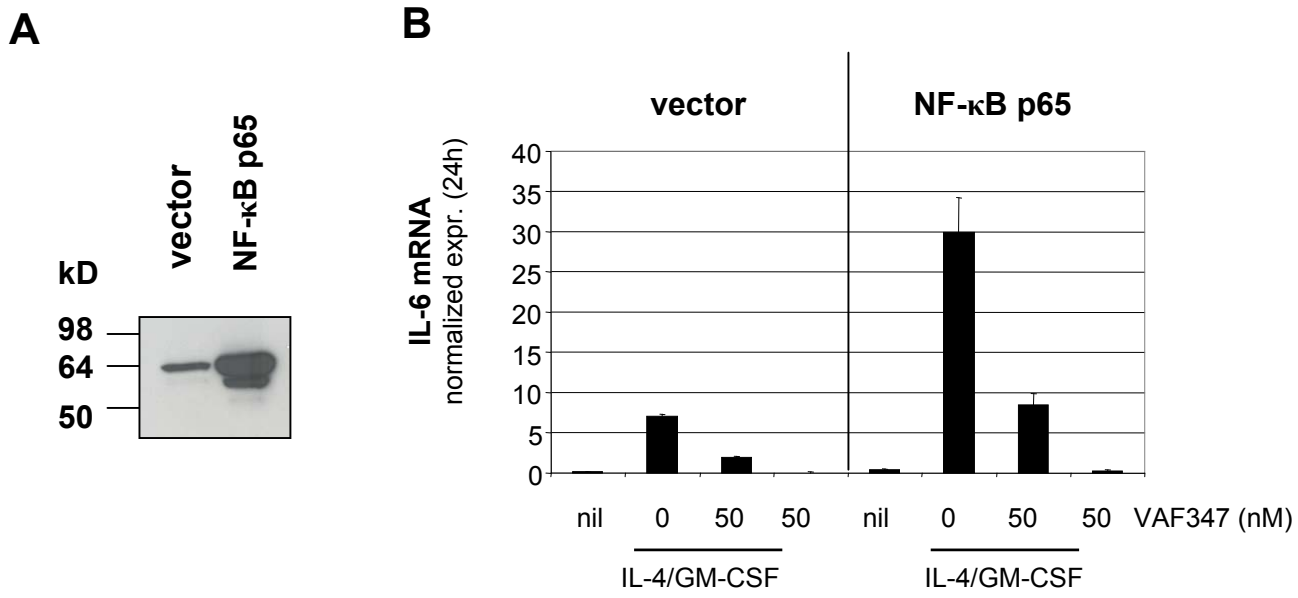

Figure 3.9.2.1: ***Ectopic over-expression of the transcription factor* NF-κB p65 *does not alter the inhibitory effect of VAF347 on IL-6 expression***. *A) Ectopic over-expression of NF-κB p65 protein in Monomac1 cells infected with pMX-NF-κB p65. A western blot analysis is shown. At the left, the positions of the molecular weight standards are indicated with the size given in kDa. At the right the position of NF-κB p65 is indicated.*

B) IL-6 mRNA was measured by RT-PCR in vector (vector) or pMX-NF-κB p65 (NF-κB p65) infected cells that were induced with IL-4+ GM-CSF in the presence or absence of VAF347 for 24 hours. IL-6 expression was normalized to eF-1α expression.

The biological effect of NF-κB p65 over-expression on the IL-6 response was investigated by stimulation of MM1 cells with IL-4 + GM-CSF in the presence or absence of VAF347 for 24 hours. IL-6 expression was measured by RT-PCR (2.3). As seen in **Figure 3.9.2.1.B** NF-κB p65 infectants showed higher induction of IL-6 mRNA after IL-4 + GM-CSF stimulation than vector infected cells

consistent with the activating role of NF-κB p65 in IL-6 gene regulation (17,21). However, VAF347 was not altered in is ability to inhibit IL-6 expression in MM1 cells over-expressing NF-κB p65.

These results suggested that VAF347 mediates its inhibitory effect on IL-6 mRNA production independently of NF-κB p65, since over-expression of NF-κB p65 could not abrogate the inhibitory effect of VAF347.

3.9.3 Silencing of the PU.1 gene abolishes the inhibitory effect of VAF347

A previous study has demonstrated that NF-IL6 vigorously activates IL-1β gene expression in human HeLa cells via a protein-protein tether with the transcription factor Purine-rich box 1 (PU.1) (158). Transient transfection assays in PU.1 deficient HeLa cells showed that NF-IL6 strongly synergized with PU.1 on the IL-1β core promoter. Furthermore, Glutathione *S*-transferase (GST) pull-down protein-interaction assays demonstrated a physical interaction between the basic leucine zipper region of NF-IL6 and the winged helix-turn-helix (wHTH) DNA binding domain of PU.1.

PU.1, also known as Spi-1, belongs to the family of ETS transcription factors which regulate the expression of a variety of genes that participate in diverse cellular activities including mitosis, apoptosis as well as the regulation of the immune system (159). PU.1 is expressed in mature macrophages, granulocytes and B cells as well as the immature precursors of these cell types (160) and is required for the development of myeloid and lymphoid cells.

To analyze a possible involvement of the PU.1 gene in the mechanism that drives IL-6 expression in MM1 cells, the PU.1 gene was silenced by using the microRNA adapted short hairpin RNA (shRNAmir) interference technique (as described above).

The human packaging cell line PhoenixGP (2.7.5), was used to generate lentiviral virus particles by transfecting PhoenixGP cells with either the GIPZ-sh-Control vector (sh-control) or a GIPZ-sh-PU.1 construct, which both contained an internal ribosome entry site (IRES)-GFP element (2.10.2). This allowed for the selection of MM1 cells successfully infected with the sh-PU.1 construct based on GFP positivity.

To test the functional activity of the GIPZ-sh-PU.1 construct, PU.1 protein expression in MM1 cells was analyzed by western blot (2.6.8). In whole cell lysates of Monomac1 cells infected with a sh-control construct wild type PU.1 protein with a size of approximately 40 kDa was detectable (**Figure 3.9.3.1.A**). In contrast, PU.1 protein expression was strongly reduced in MM1 cells infected with the GIPZ-sh-PU.1 construct.

To analyze the biological consequences of PU.1 gene silencing, MM1 cells infected with either sh-control or sh-PU.1 were stimulated with IL-4 + GM-CSF in the presence or absence of VAF347 for 24 hours, before expression of the IL-6 gene was measured by RT-PCR (2.3).

As seen in **Figure 3.9.3.1.B** IL-4 + GM-CSF still induced IL-6 expression in MM1 sh-PU.1 infectants, although the maximal IL-6 response in these cells was strongly reduced compared to sh-control infected cells. Interestingly, VAF347 was no longer able to inhibit the IL-4 + GM-CSF induced IL-6 response in MM1 cells infected with sh-PU.1, whereas in sh-control infected cells VAF347 still inhibited IL-6 expression.

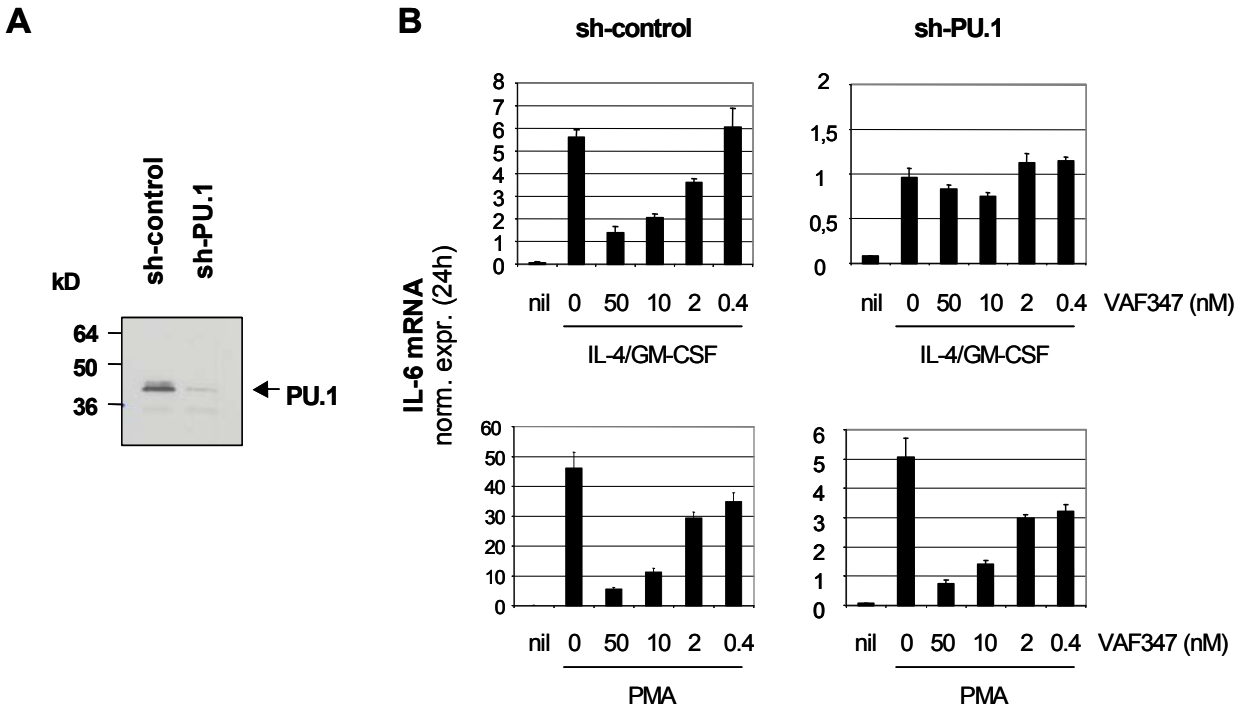

Figure 3.9.3.1: ***Silencing of the PU.1 gene partially abolishes VAF347 activity.*** *A) Reduced expression of PU.1 protein in Monomac1 cells infected with sh-PU.1. A western blot analysis is shown. At the left, the positions of the molecular weight standards are indicated with the size given in kDa. At the right the position of PU.1 is indicated.*

B) IL-6 mRNA was measured by RT-PCR in sh-control (vector) or sh-PU.1 infected cells that were induced with IL-4+ GM-CSF (top row) or PMA (bottom row) in the presence or absence of VAF347 for 24 hours. IL-6 expression was normalized to eF-1α expression.

To test if the loss of the inhibitory effect of VAF347 on IL-4 + GM-CSF induced IL-6 expression in sh-PU.1 infectants was also observed after PMA stimulation, MM1 sh-PU.1 infected cells were stimulated with PMA in the presence or absence of VAF347 for 24 hours, before IL-6 mRNA levels

were measured by RT-PCR. As shown in **Figure 3.9.3.1.B** PMA induced IL-6 expression in sh-PU.1 infectants, though the total level of IL-6 in response to PMA was strongly reduced in sh-PU.1 infectants compared to sh-control infected cells. Interestingly, VAF347 inhibited PMA induced IL-6 expression in both MM1 sh-PU.1 and sh-control infectants to the same extent.

Since the IL-6 levels in response to IL-4 + GM-CSF or PMA were strongly reduced in MM1 sh-PU.1 infectants compared to sh-control cells, it was unclear whether this effect was due to overall reduced gene expression in MM1 cells infected with the sh-PU.1 construct. Therefore, the expression of CYP1A1 was determined by RT-PCR (2.3) in the same samples as shown in figure 3.9.3.1. As shown in **Figure 3.9.3.2** VAF347 induced CYP1A1 gene expression in both sh-control or sh-PU.1 infectants at comparable levels.

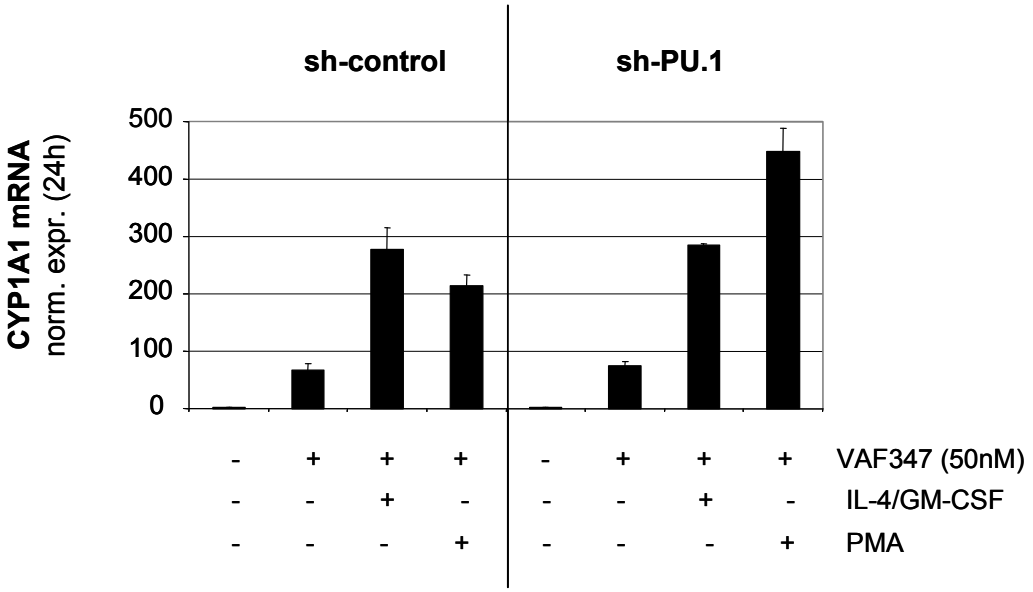

Figure 3.9.3.2: ***Silencing of the PU.1 gene does not abolish VAF347 activity on CYP1A1 expression.*** *CYP1A1 mRNA was measured by RT-PCR in sh-control (vector) sh-PU.1 infected cells that were induced with IL-4+ GM-CSF in the presence or absence of VAF347 for 24 hours. CYP1A1 expression was normalized to eF-1α expression.*

These additional data suggested that the reduced IL-6 expression levels in MM1 sh-PU.1 infectants resulted from a specific effect of PU.1 gene silencing and were not due to a general inhibitory effect on gene expression. Therefore, PU.1 might positively contribute to the induction of IL-6 mRNA synthesis in MM1 cells.

The inhibitory effect of VAF347 on IL-6 gene transcription was only abolished in IL-4 + GM-CSF but not in PMA induced MM1 sh-PU.1 infectants, suggesting different roles of PU.1 in IL-6 gene induction depending on the stimuli.

To examine the effect of VAF347 on the expression level of the PU.1 gene, wild type MM1 cells were stimulated with IL-4 + CM-CSF in the presence or absence of VAF347 for 24 hours before PU.1 mRNA expression was examined by RT-PCR (2.3).
As shown in **Figure 3.9.3.3** VAF347 did not alter the expression levels of PU.1 in MM1 cells suggesting that the inhibitory effect of VAF347 is not mediated via altered expression of the transcription factor PU.1.

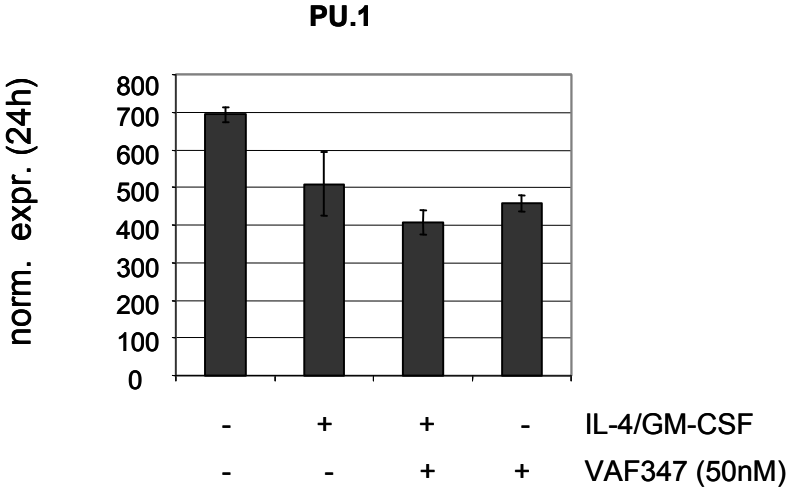

Figure 3.9.3.3: ***VAF347 does not alter the mRNA expression level of the transcription factor PU.1.*** *PU.1 mRNA was measured by RT-PCR in MM1 cells that were induced with IL-4+ GM-CSF in the presence or absence of VAF347 for 24 hours. PU.1 expression was normalized to eF-1α expression.*

4. DISCUSSION

The aim of this study was the identification of the molecular target(s) of the novel immunomodulator VAF347 and its molecular mechanism of action in the human monocytic cell line Monomac1. First, we showed that IL-4 and GM-CSF in combination as well as PMA induced IL-6 mRNA and protein expression in MM1 cells. VAF347 inhibited both IL-4/GM-CSF and PMA induced IL-6 expression in a dose-dependent fashion, with an IC_{50} of approximately 5nM. In contrast to IL-6, the CYP1A1 gene was strongly induced by VAF347 in MM1. Since the CYP1A1 gene is known to be induced by activation of AhR, a possible involvement of AhR in the mode of action of VAF347 was proposed.

This hypothesis was verified at several levels: First, we showed that the prototypical AhR ligand TCDD as well as the AhR agonist omeprazole, a proton pump inhibitor, displayed similar activity profiles in MM1 compared to VAF347. Second, over-expression of a trans-dominant negative AhR (AhR515) was sufficient to abolish the inhibitory effect of VAF347 or TCDD on IL-6 expression. Third, silencing of endogenous AhR gene expression abrogated VAF347 activity. Collectively, these data identified the AhR as a critical molecular target involved in the mode of action of VAF347.

Independent experiments in our laboratory confirmed the AhR as the essential functional target of VAF347: the compound competitively displaced ~50% of [^{3}H]TCDD bound to AhR at a concentration of 10nM VAF347 Most importantly, the lack of AhR protein in homozygous AhR deficient mice led to unresponsiveness of VAG539 (a VAF347 analog) treatment in a model of pulmonary inflammation (67).

Similar to VAF347, other AhR agonists have been shown to inhibit IL-6 expression. In a mouse bone marrow stromal cell line TCDD and 7,12-dimethylbenz[a]anthracene (DMBA) both selectively abrogated LPS induced IL-6 synthesis, possibly due to reduced binding of NF-κB to its recognition site in the IL-6 promoter in the presence of DMBA (161). Another study showed that the AhR agonist β-naphthoflavone disturbed cAMP-induced astrocyte differentiation of C6 rat glioma cells by inhibiting the production of IL-6, an important autocrine differentiation factor for these cells (162).

With the identification of AhR as the critical molecular target for VAF347, the question was raised about the molecular mode of action by which AhR activation interfered with IL-6 expression in MM1 cells.

To investigate if *de novo* protein synthesis is necessary for the inhibitory effect of VAF347, we tested the effects of the translation inhibitor cycloheximide on IL-6 expression. Interestingly, cycloheximide on its own induced expression of IL-6 and high levels of the CYP1A1 gene. Cycloheximide as well as other translation inhibitors such as anisomycin and puromycin have been shown to induce CYP1A1 expression (163). This effect is possibly mediated by a cycloheximide-sensitive factor that stabilizes AhR and prevents AhR degradation (164). Therefore, the question whether *de novo* protein synthesis is necessary for the inhibitory effect of VAF347 could not be answered and remains to be elucidated.

Since very little was known about the intracellular events that trigger IL-6 expression in MM1 cells, we examined the role of different common cytokine signaling pathways known to contribute to the induction of cytokine synthesis. Stimulation of MM1 with IL-4 and GM-CSF lead to phosphorylation of STAT5 and STAT6 proteins. Inhibition of JAK2 and JAK3, both known to be involved in GM-CSF or IL-4 signaling respectively, abolished IL-6 expression in response to IL-4 + GM-CSF, demonstrating a functional involvement of the JAK/STAT pathway in the signal cascade that leads to induction of IL-6 synthesis in MM1.

STAT5 has already been described to induce IL-6 expression in murine leukemic M1 cells (165). In these cells activation of STAT5 lead to enhanced binding of NF-κB p65 to the promoter region of IL-6 possibly via transactivation of NF-κB p65 by STAT5. To our knowledge no functional STAT responsive elements have been described in the IL-6 promoter. So far we can only speculate that activated STAT contributes to the signals that trigger IL-6 expression, for example via transactivation of other transcription factors relevant for IL-6 transcription. Pre-treatment of IL-4 and GM-CSF stimulated MM1 cells with VAF347 did not change the level of STAT protein phosphorylation indicating that AhR activation did not interfere with receptor proximal signaling events of the JAK/STAT pathway.

Furthermore, we showed that IL-4 and GM-CSF in combination lead to phosphorylation of p44/p42 (ERK1 and ERK2) MAP kinases. Inhibition of p44/p42 MAP kinases with the MAPK inhibitor PD98059 abrogated IL-6 synthesis, demonstrating an involvement of p44/p42 MAP kinases in the signaling pathway that leads to IL-6 expression in MM1. Inhibition of JAK3 activity with CP-690,550 also inhibited phosphorylation of p44/p42 MAPK by IL-4/GM-CSF. These results demonstrated that ERK1/2 phosphorylation represented a critical step in the IL-4 and GM-CSF signaling chain for IL-6 expression in MM1 cells. In addition, ERK1/2 phosphorylation appeared to be dependent on JAK3 activation indicating that p44/p42 MAPK activation occurred downstream of JAK phosphorylation.

The p44/p42 MAP kinases have already been shown to be involved in IL-6 expression in human monocytes: in one study IL-6 expression induced by okadaic acid was abolished in the presence of the MAPK inhibitor PD98059, possibly due to reduced transcriptional activity of NF-κB (166). Another study showed that in human monocyte derived DCs LPS/lysophosphatidic acid induced IL-6 expression was dependent on activation of p44/p42 MAP kinases, since inhibition of p44/p42 MAP kinases with PD98059 abolished the IL-6 response in these cells (167).

VAF347 did not block IL-4+GM-CSF triggered ERK1/2 activation suggesting that activated AhR may block IL-6 expression at a stage downstream of p44/p42 activation.

To identify additional signaling molecules involved in IL-6 regulation, low molecular weight inhibitors of protein kinase C, JNKs or p38 MAP kinase family members were tested for their inhibitory effects on IL-6 secretion in IL-4+GM-CSF stimulated MM1 cells. None of these compounds had any effects on the IL-6 response indicating that these signaling molecules were dispensable for IL-6 expression. The negative results with the p38 MAPK inhibitor is in contrast to previous studies: in LPS maturated murine dendritic cells induction of IL-6 expression by engagement of CD40 was dependent on the activation of p38 MAPK (168). Another study in human osteoblasts demonstrated that induction of IL-6 expression by IL-1β was also dependent on p38 MAPK (169). It is possible that the involvement of p38 is dependent on the cell type and/or the stimulus used. In fact, the regulation of IL-6 gene expression is quite complex. For example, the human cervix carcinoma HeLa cell line produced high levels of IL-6 in response to TNF-α and IL-1β while the human colon adenocarcinoma HTM-29 line completely failed to produce IL-6 although NF-κB p65 and NF-IL6, which are thought to be the main transcription factors involved in IL-6 gene activation, were activated in both cell lines (170). In human B-cells, engagement of CD40 induced IL-6 expression. By using wild-type or mutant IL-6 promoter reporter constructs it was shown that the NF-κB, the NF-IL6 as well as the AP-1 regulatory DNA elements were necessary for the activation of the IL-6 promoter by CD40 (171).

In addition to the transcription factors NF-κB and NF-IL6, also AP1 was reported to regulate IL-6 transcription in various systems (19,20). To determine if VAF347 was acting at the level of IL-6 transcription we performed transient transfections with an IL-6 promoter reporter construct. VAF347 could inhibit both PMA and IL-4 + GM-CSF induced IL-6 promoter activity. In contrast, VAG005, which is only a weak ligand of AhR, did not interfere with IL-6 promoter activity. These results demonstrated that VAF347 interfered with IL-6 expression at the transcriptional level.

One attractive point of VAF347 intervention was NF-κB. A previous study demonstrated that in a mouse bone marrow stromal cell line the AhR agonist DMBA abrogated LPS induced IL-6 synthesis possibly due to reduced binding of NF-κB to its recognition site in the IL-6 promoter in the presence of DMBA (161). In addition, NF-κB p65 has been shown to physically interact with

AhR (157). Immunoprecipitation experiments intended to examine a possible interaction of AhR and NF-κB were performed in cytokine stimulated MM1 cells. However, preliminary data were unsuccessful to demonstrate direct interactions between these transcription factors (data not shown). Chromatin immunoprecipitation (ChIP) assays were also performed with a NF-κB p65 antibody, but no PCR product was observed indicating binding of the transcription factor to its recognition sequence on the IL-6 promoter in response to IL-4+GM-CSF (data not shown). It is possible that these negative data were due to the poor quality of the antibody used. In addition, two different NF-κB inhibitors did not influence IL-6 synthesis in MM1 suggesting no major role of NF-κB in IL-6 gene regulation. On the other hand, ectopic over-expression of NF-κB p65 resulted in significantly increased production of IL-6. Overall, the role of NF-κB proteins in IL-6 gene activation in MM1 cells remains to be more closely investigated. If NF-κB plays a major regulating role we tend to suggest that it is not involved in the mode of action of VAF347 since in NF-κB p65 overexpressing MM1 cells the compound was as potent to inhibit IL-6 expression as in wild type cells (in contrast to NF-IL6 overproducing MM1 cells, see below).

Another attractive target appeared to be NF-IL6 due to its functional link with ERK1/2 MAPK activation: stimulation of human chondrocytes with IL-1β has been shown to induce transcription of matrix metalloproteinase-1 (MMP-1) (172). Expression of MMP-1 required phosphorylation of NF-IL6 by p44/p42 MAP kinases, since inhibition of MAP kinases with PD98059 abrogated both NF-IL6 phosphorylation as well as MMP-1 expression.

Chromatin immunoprecipitation (ChIP) assays demonstrated that IL-4 + GM-CSF induced the binding of NF-IL6 to the IL-6 promoter in MM1 cells. In the presence of VAF347 binding of NF-IL6 to the IL-6 promoter was completely absent. These data strongly indicated that VAF347 blocked IL-6 expression by preventing the interaction of the critical transcription factor NF-IL-6 with its recognition sequence at the IL-6 promoter. The involvement of NF-IL6 in the mode of action of VAF347 was further substantiated in MM1 cells overexpressing NF-IL6. In these cells, the inhibitory effects of VAF347 to block IL-6 secretion was greatly (but not completely) diminished.

The ability of VAF347 to block the binding of NF-IL6 to the IL-6 promoter was not due to reduced transcription of the NF-IL6 gene, since the expression levels of NF-IL6, NF-κB p65, c-Fos and c-Jun after cytokine stimulation or exposure to VAF347 remained constant in MM1 cells. In contrast, activation of the p44/p42 MAP Kinases by IFN-γ has been shown to activate the transcription of NF-IL6 in a murine macrophage cell line and required activation of STAT1 (173).

The mechanism by which VAF347 interferes with binding of NF-IL6 is unknown. A possible explanation is that AhR not only interacts with DNA but with other signaling molecules involved in induction of IL-6 transcription

Ectopic over-expression of wild-type NF-IL6 protein partially abolished the inhibitory effect of VAF347 on IL-6 expression in both IL-4 + GM-CSF or PMA induced MM1 cells. Over-expression of wild-type NF-κB p65 did not alter the inhibitory activity of VAF347 on IL-6 expression. Taken together, these results suggested that NF-IL6 was at least partially involved in the events that inhibit IL-6 expression by VAF347.

Since a previous study has demonstrated that NF-IL6 vigorously activated IL-1β gene expression in human HeLa cells via a protein-protein tether with the transcription factor PU.1 (158), we examined a possible involvement of PU.1 in the signaling events that lead to induction of IL-6 in MM1 by silencing of PU.1 gene expression. MM1 cells lacking the PU.1 protein showed a reduced maximal IL-6 response in comparison to control cells, while the expression of the CYP1A1 gene was not reduced. Due to the specific reduced IL-6 response in MM1 cells lacking PU.1 protein, we suggest that PU.1 positively contributes to the induction of the IL-6 promoter. One explanation could be that PU.1 enhances transactivation of NF-IL6 in a similar way described for the human IL-1β promoter (158). However, in contrast to the IL-1β promoter, no functional PU.1 binding sites have been identified in the IL-6 promoter to our knowledge.

Multiple studies have demonstrated that different cellular concentrations of PU.1 direct distinct cell fates, with high concentrations of PU.1 required for macrophage development and lower concentrations for B-cell and granulocyte fate adoption (174). Primary human monocytes were shown to express only low levels of PU.1, while stimulation of these cells with IL-4 and GM-CSF, thus inducing DC differentiation, lead to strong up-regulation of PU.1 (175). In MM1 cells PU.1 expression was not altered by IL-4 and GM-CSF or VAF347 respectively.

Interestingly, the inhibitory effect of VAF347 on IL-6 expression in response to IL-4 + GM-CSF was abolished in MM1 cells lacking the PU.1 protein. Therefore, PU.1 might possibly be involved in the mechanism by which VAF347 interferes with IL-4 + GM-CSF induced IL-6 synthesis. In contrast, IL-6 mRNA synthesis in response to PMA was still inhibited by VAF347. These results suggest that PMA induced IL-6 expression does not include PU.1 as essential factor.

Several possibilities exist to explain the molecular events by which VAF347 blocks IL-6 expression via activation of AhR. In principle, AhR could act as transcription factor by binding to cis-acting elements in regulatory regions or, alternatively, could interact with other factors important for IL-6 production and disturb their functions. The former possibility calls for the presence of a negatively acting AhR binding site in the IL-6 promoter. Up to now several genes have been described to be negatively regulated by AhR due to the presence of such a negatively cis-acting XRE element, including the cathepsin D, c-Fos and pS2 gene (176-178). However, examination of the IL-6 promoter has not revealed the presence of any bona fide XRE motifs (data not shown) making this possibility less likely. For the second possibility, several scenarios can be envisioned.

First, activated AhR may inhibit nuclear translocation of NF-IL6. Second, activated AhR or VAF347 itself may inhibit phosphorylation of NF-IL6. Phosphorylation of NF-IL6 has been shown to increase its transcriptional activity (14). Another possibility could be that AhR disturbs the interaction of transcription factors relevant for induction of IL-6 transcription, for instance by inhibiting a possible protein-protein tether between NF-IL6 and PU.1, an interaction which was already described for the IL-1β promoter (158).

A summary of the signaling events thought to be involved in the mechanism that drives IL-6 expression in MM1 is shown in **Figure 4.1**: Binding of IL-4 and GM-CSF to their receptors lead to activation of JAK2 and JAK3 which phosphorylate STAT5 and STAT6.

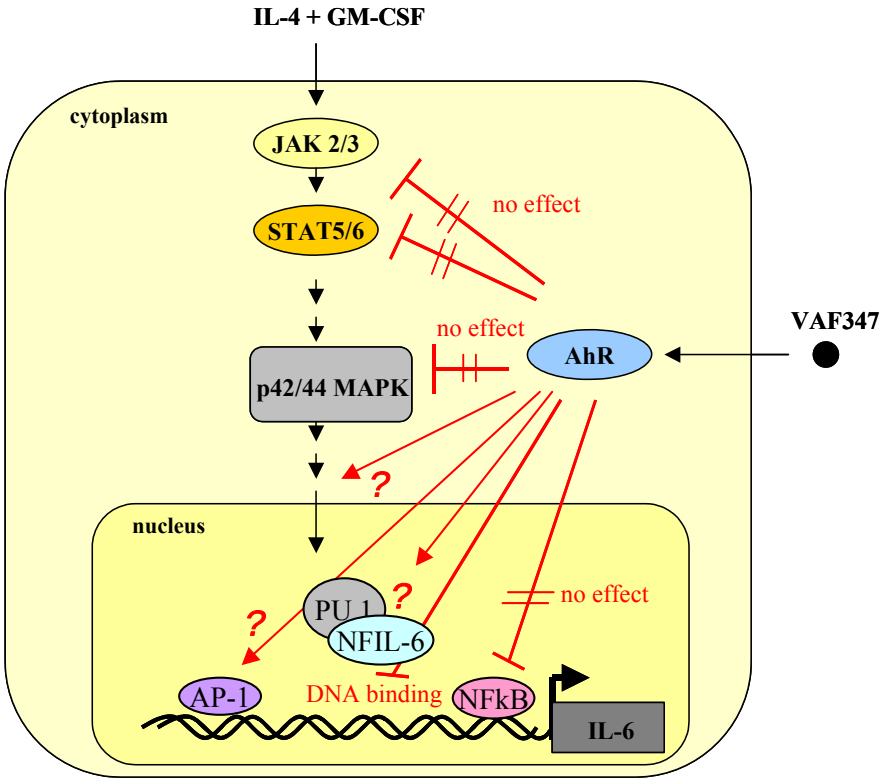

Figure 4.1: ***Signaling events in Monomac1 cells leading to IL-6 production.*** *Stimulation of MM1 with IL-4 + GM-CSF leads to activation of JAK2/3 resulting in phosphorylation of STAT5/6. STAT activation is necessary for subsequent phosphorylation of p42/44 MAP kinases. VAF347 activates AhR and leads to reduced binding of NF-IL6 to the IL-6 promoter via an unexplained mechanism(s). One attractive possibility may be that activated AhR interferes with PU.1/NF-IL6 heterodimerization or NF-IL6 phosphorylation or nuclear translocation resulting in abrogated binding to the IL-6 promoter. Alternatively, activated AhR may interfere with the function of AP-1 to co-activate IL-6 gene transcription.*

Consequently, p42 and p44 MAP kinases (ERK1/2) are rapidly activated upon cytokine stimulation. The molecular link(s) between activation of STATs and MAP kinase activation remain to be determined. Activated ERK1/2 may activate directly or indirectly transcription factors important for IL-6 gene activation, such as NF-κB, NF-IL6 or AP1. Support for an indirect function of MAP kinases comes from a study in COS cells demonstrating that ERK1/2 phosphorylated $p90^{RSK1}$ which in turn led to activation of NF-κB (179). Since VAF347 had no inhibitory effects on STAT or MAP kinase activation, the compound appears to act downstream of MAP kinase activation by interfering with DNA binding of NF-IL6.

In summary, we have identified the AhR as the functional molecular target for VAF347. Activation of AhR by this compound is essential for mediating the inhibitory effect on IL-6 expression in Monomac1 cells. Further data allowed for the identification of NF-IL6 and PU.1 as functionally relevant factors which mediate the inhibitory effects of VAF347. Future studies will be designed to understand the link between activated AhR and these proteins. Overall, these results highlight the AhR as a novel target for the therapeutic manipulation of the immune response.

5. REFERENCES

1. Yoshizaki K., Nakagawa T., Fukunaga K., Tseng L.T., Yamamura Y., and T. Kishimoto. 1984. Isolation and characterization of B cell differentiation factor (BCDF) secreted from a human B lymphoblastoid cell line. J. Immunol. 132:2948-54.

2. Hirano T., Yasukawa K., Harada H., Taga T., Watanabe Y., Matsuda T., Kashiwamura S., Nakajima K., Koyama K., Iwamatsu A., et al. 1986. Complementary DNA for a novel human interleukin (BSF-2) that induces B lymphocytes to produce immunoglobulin. Nature 324:73-6.

3. Haegeman G., Content J., Volckaert G., Derynck R., Tavernier J., and W. Fiers. 1986. Structural analysis of the sequence coding for an inducible 26-kDa protein in human fibroblasts. Eur. J. Biochem. 159:625-32.

4. Zilberstein A., Ruggieri R., Korn J.H., and M. Revel. 1986. Structure and expression of cDNA and genes for human interferon-beta-2, a distinct species inducible by growth-stimulatory cytokines. EMBO J. 5:2529-37.

5. Van Damme J., Cayphas S., Van Snick J., Conings R., Put W., Lenaerts J.P., Simpson R.J., and A. Billiau. 1987. Purification and characterization of human fibroblast-derived hybridoma growth factor identical to T-cell-derived B-cell stimulatory factor-2 (interleukin-6). Eur. J. Biochem. 168:543-50.

6. Van Damme J., Opdenakker G., Simpson R.J., Rubira M.R., Cayphas S., Vink A., Billiau A., and J. Van Snick. 1987. Identification of the human 26-kD protein, interferon beta 2 (IFN-beta 2), as a B cell hybridoma/plasmacytoma growth factor induced by interleukin 1 and tumor necrosis factor. J. Exp. Med. 165:914-9.

7. Gauldie J., Richards C., Harnish D., Lansdorp P., and H. Baumann. 1987. Interferon beta 2/B-cell stimulatory factor type 2 shares identity with monocyte-derived hepatocyte-stimulating factor and regulates the major acute phase protein response in liver cells. Proc. Natl. Acad. Sci. USA. 84:7251-5.

8. Sehgal P.B., Zilberstein A., Ruggieri R.M., May L.T., Ferguson-Smith A., Slate D.L., Revel M., and F.H. Ruddle. 1986. Human chromosome 7 carries the beta 2 interferon gene. Proc. Natl. Acad. Sci. USA. 83:5219-22.

9. Jambou R.C., Snouwaert J.N., Bishop G.A., Stebbins J.R., Frelinger J.A., and D.M. Fowlkes. 1988. High-level expression of a bioengineered, cysteine-free hepatocyte-stimulating factor (interleukin 6)-like protein. Proc. Natl. Acad. Sci. USA. 85:9426-30.

10. Tanabe O., Akira S., Kamiya T., Wong G.G., Hirano T., and T. Kishimoto. 1988. Genomic structure of the murine IL-6 gene. High degree conservation of potential regulatory sequences between mouse and human. J. Immunol. 141:3875-81.

11. Ray A., Tatter S.B., May L.T., and P.B. Sehgal. 1988. Activation of the human "beta 2-interferon/hepatocyte-stimulating factor/interleukin 6" promoter by cytokines, viruses, and second messenger agonists. Proc. Natl. Acad. Sci. USA. 85:6701-5.

12. Gilmore T.D. 2006. Introduction to NF-kappaB: players, pathways, perspectives. Oncogene 25:6680-4.

13. Akira S., Isshiki H., Nakajima T., Kinoshita S., Nishio Y., Natsuka S., and T. Kishimoto. 1992. Regulation of expression of the interleukin 6 gene: structure and function of the transcription factor NF-IL6. Ciba. Found. Symp.167:47-62.

14. Trautwein C., Caelles C., van der Geer P., Hunter T., Karin M., and M. Chojkier. 1993. Transactivation by NF-IL6/LAP is enhanced by phosphorylation of its activation domain. Nature 364:544-7.

15. Angel P., and M. Karin. 1991. The role of Jun, Fos and the AP-1 complex in cell-proliferation and transformation. Biochim. Biophys. Acta. 1072:129-57.

16. Ryseck R.P., and R. Bravo. 1991. c-JUN, JUN B, and JUN D differ in their binding affinities to AP-1 and CRE consensus sequences: effect of FOS proteins. Oncogene 6:533-42.

17. Dendorfer U., Oettgen P., and T.A. Libermann. 1994. Multiple regulatory elements in the interleukin-6 gene mediate induction by prostaglandins, cyclic AMP, and lipopolysaccharide. Mol Cell. Biol. 14:4443-54.

18. Grassl C., Luckow B., Schlöndorff D., and U. Dendorfer. 1999. Transcriptional regulation of the interleukin-6 gene in mesangial cells. J. Am. Soc. Nephrol. 10:1466-77.

19. Eickelberg O., Pansky A., Mussmann R., Bihl M., Tamm M., Hildebrand P., Perruchoud A.P., and M. Roth. 1999. Transforming growth factor-beta1 induces interleukin-6 expression via activating protein-1 consisting of JunD homodimers in primary human lung fibroblasts. J. Biol. Chem. 274:12933-8.

20. Smart D.E., Vincent K.J., Arthur M.J., Eickelberg O., Castellazzi M., Mann J., and D.A. Mann. 2001. JunD regulates transcription of the tissue inhibitor of metalloproteinases-1 and interleukin-6 genes in activated hepatic stellate cells. J. Biol. Chem. 276:24414-21.

21. Xiao W., Hodge D.R., Wang L., Yang X., Zhang X., and W.L. Farrar. 2004. Co-operative functions between nuclear factors NFkappaB and CCAT/enhancer-binding protein-beta (C/EBP-beta) regulate the IL-6 promoter in autocrine human prostate cancer cells. Prostate 61:354-70.

22. Hirano T., Taga T., Matsuda T., Hibi M., Suematsu S., Tang B., Murakami M., and T. Kishimoto. 1990. Interleukin 6 and its receptor in the immune response and hematopoiesis. Int. J. Cell Cloning. 8 Suppl. 1:155-66.

23. Yamasaki K., Taga T., Hirata Y., Yawata H., Kawanishi Y., Seed B., Taniguchi T., Hirano T., and T. Kishimoto. 1988. Cloning and expression of the human interleukin-6 (BSF-2/IFN beta 2) receptor. Science 241:825-8.

24. Taga T., Hibi M., Hirata Y., Yamasaki K., Yasukawa K., Matsuda T., Hirano T., and T. Kishimoto. 1989. Interleukin-6 triggers the association of its receptor with a possible signal transducer, gp130. Cell 58:573-81.

25. Hibi M., Murakami M., Saito M., Hirano T., Taga T., and T. Kishimoto. 1990. Molecular cloning and expression of an IL-6 signal transducer, gp130. Cell 63:1149-57.

26. Scheller J., Ohnesorge N., and S. Rose-John. 2006. Interleukin-6 trans-signalling in chronic inflammation and cancer. Scand J. Immunol. 63:321-9.

27. Schmitz J., Weissenbach M., Haan S., Heinrich P.C., and F. Schaper. 2000. SOCS3 exerts its inhibitory function on interleukin-6 signal transduction through the SHP2 recruitment site of gp130. J. Biol. Chem. 275:12848-56.

28. Chung C.D., Liao J., Liu B., Rao X., Jay P., Berta P., and K. Shuai. 1997. Specific inhibition of Stat3 signal transduction by PIAS3. Science 278:1803-5.

29. Muraguchi A., Hirano T., Tang B., Matsuda T., Horii Y., Nakajima K., and T. Kishimoto. 1988. The essential role of B cell stimulatory factor 2 (BSF-2/IL-6) for the terminal differentiation of B cells. J. Exp. Med. 167:332-44.

30. Garman R.D., Jacobs K.A., Clark S.C., and D.H Raulet. 1987. B-cell-stimulatory factor 2 (beta 2 interferon) functions as a second signal for interleukin 2 production by mature murine T cells. Proc. Natl. Acad. Sci. USA. 84:7629-33.

31. Noma T., Mizuta T., Rosén A., Hirano T., Kishimoto T., and T. Honjo. 1987. Enhancement of the interleukin 2 receptor expression on T cells by multiple B-lymphotropic lymphokines. Immunol. Lett. 15:249-53.

32. Takai Y., Wong G.G., Clark S.C., Burakoff S.J., and S.H. Herrmann. 1988. B cell stimulatory factor-2 is involved in the differentiation of cytotoxic T lymphocytes. J. Immunol. 140:508-12.

33. Sachs L., Lotem J., and Y. Shabo. 1989. The molecular regulators of macrophage and granulocyte development. Role of MGI-2/IL-6. Ann. NY. Acad. Sci. 557:417-35.

34. Sehgal P.B., Helfgott D.C., Santhanam U., Tatter S.B., Clarick R.H., Ghrayeb J., and L.T. May. 1988. Regulation of the acute phase and immune responses in viral disease. Enhanced expression of the beta 2-interferon/hepatocyte-stimulating factor/interleukin 6 gene in virus-infected human fibroblasts. J. Exp. Med. 167:1951-6.

35. Heinrich P.C., Castell J.V., and T. Andus. 1990. Interleukin-6 and the acute phase response. Biochem. J. 265:621-36.

36. Andus T., Geiger T., Hirano T., Northoff H., Ganter U., Bauer J., Kishimoto T., and P.C. Heinrich. 1987. Recombinant human B cell stimulatory factor 2 (BSF-2/IFN-beta 2) regulates beta-fibrinogen and albumin mRNA levels in Fao-9 cells. FEBS Lett. 221:18-22.

37. Ikebuchi K., Wong G.G., Clark S.C., Ihle J.N., Hirai Y., and M. Ogawa. 1987. Interleukin 6 enhancement of interleukin 3-dependent proliferation of multipotential hemopoietic progenitors. Proc. Natl. Acad. Sci. USA. 84:9035-9.

38. Tamura T., Udagawa N., Takahashi N., Miyaura C., Tanaka S., Yamada Y., Koishihara Y., Ohsugi Y., Kumaki K., Taga T., et al. 1993. Soluble interleukin-6 receptor triggers osteoclast formation by interleukin 6. Proc. Natl. Acad. Sci. USA. 90:11924-8.

39. Ishibashi T., Kimura H., Uchida T., Kariyone S., Friese P., and S.A. Burstein. 1989. Human interleukin 6 is a direct promoter of maturation of megakaryocytes in vitro. Proc. Natl. Acad. Sci. USA. 86:5953-7.

40. Satoh T., Nakamura S., Taga T., Matsuda T., Hirano T., Kishimoto T., and Y. Kaziro. 1988. Induction of neuronal differentiation in PC12 cells by B-cell stimulatory factor 2/interleukin 6. Mol. Cell. Biol. 8:3546-9.

41. Hama T., Miyamoto M., Tsukui H., Nishio C., and H. Hatanaka. 1989. Interleukin-6 as a neurotrophic factor for promoting the survival of cultured basal forebrain cholinergic neurons from postnatal rats. Neurosci. Lett. 104:340-4.

42. Guerne P.A., Zuraw B.L., Vaughan J.H., Carson D.A., and M. Lotz. 1989. Synovium as a source of interleukin 6 in vitro. Contribution to local and systemic manifestations of arthritis. J. Clin. Invest. 83:585-92.

43. Hirano T., Matsuda T., Turner M., Miyasaka N., Buchan G., Tang B., Sato K., Shimizu M., Maini R., Feldmann M., et al. 1988. Excessive production of interleukin 6/B cell stimulatory factor-2 in rheumatoid arthritis. Eur. J. Immunol. 18:1797-801.

44. Houssiau F.A., Devogelaer J.P., Van Damme J., de Deuxchaisnes C.N., and J. Van Snick. 1988. Interleukin-6 in synovial fluid and serum of patients with rheumatoid arthritis and other inflammatory arthritides. Arthritis Rheum. 31:784-8.

45. Madhok R., Crilly A., Watson J., and H.A. Capell. 1993. Serum interleukin 6 levels in rheumatoid arthritis: correlations with clinical and laboratory indices of disease activity. Ann. Rheum. Dis. 52:232-4.

46. Sack U., Kinne R.W., Marx T., Heppt P., Bender S., and F. Emmrich. 1993. Interleukin-6 in synovial fluid is closely associated with chronic synovitis in rheumatoid arthritis. Rheumatol. Int. 13:45-51.

47. Pawlik A., Wrzesniewska J., Florczak M., Gawronska-Szklarz B., and M. Herczynska. 2005. IL-6 promoter polymorphism in patients with rheumatoid arthritis. Scand. J. Rheumatol. 34:109-13.

48. Sato K., Tsuchiya M., Saldanha J., Koishihara Y., Ohsugi Y., Kishimoto T., and M.M. Bendig. 1994. Humanization of a mouse anti-human interleukin-6 receptor antibody comparing two methods for selecting human framework regions. Mol. Immunol. 31:371-81.

49. Sato K., Tsuchiya M., Saldanha J., Koishihara Y., Ohsugi Y., Kishimoto T., and M.M. Bendig. 1993. Reshaping a human antibody to inhibit the interleukin 6-dependent tumor cell growth. Cancer Res. 53:851-6.

50. Nishimoto N., Yoshizaki K., Miyasaka N., Yamamoto K., Kawai S., Takeuchi T., Hashimoto J., Azuma J., and T. Kishimoto. 2004. Treatment of rheumatoid arthritis with humanized anti-interleukin-6 receptor antibody: a multicenter, double-blind, placebo-controlled trial. Arthritis Rheum. 50:1761-9.

51. Maini R.N., Taylor P.C., Szechinski J., Pavelka K., Bröll J., Balint G., Emery P., Raemen F., Petersen J., Smolen J., Thomson D., and T. Kishimoto. 2006. Double-blind randomized controlled clinical trial of the interleukin-6 receptor antagonist, tocilizumab, in European patients with rheumatoid arthritis who had an incomplete response to methotrexate. Arthritis Rheum. 54:2817-29.

52. Nishimoto N., Sasai M., Shima Y., Nakagawa M., Matsumoto T., Shirai T., Kishimoto T., and K. Yoshizaki. 2000. Improvement in Castleman's disease by humanized anti-interleukin-6 receptor antibody therapy. Blood 95:56-61.

53. Nishimoto N., Kanakura Y., Aozasa K., Johkoh T., Nakamura M., Nakano S., Nakano N., Ikeda Y., Sasaki T., Nishioka K., Hara M., Taguchi H., Kimura Y., Kato Y., Asaoku H., Kumagai S.,

Kodama F., Nakahara H., Hagihara K., Yoshizaki K., and T. Kishimoto. 2005. Humanized anti-interleukin-6 receptor antibody treatment of multicentric Castleman disease. Blood 106:2627-32.

54. Yokota S., Miyamae T., Imagawa T., Iwata N., Katakura S., Mori M., Woo P., Nishimoto N., Yoshizaki K., and T. Kishimoto. 2005. Therapeutic efficacy of humanized recombinant anti-interleukin-6 receptor antibody in children with systemic-onset juvenile idiopathic arthritis. Arthritis Rheum. 52:818-25.

55. Ito H., Takazoe M., Fukuda Y., Hibi T., Kusugami K., Andoh A., Matsumoto T., Yamamura T., Azuma J., Nishimoto N., Yoshizaki K., Shimoyama T., and T. Kishimoto. 2004. A pilot randomized trial of a human anti-interleukin-6 receptor monoclonal antibody in active Crohn's disease. Gastroenterology 126:989-96.

56. Shortman K., and Y.J. Liu. 2002. Mouse and human dendritic cell subtypes. Nat. Rev. Immunol. 2:151–61.

57. Rincon M., Anguita J., Nakamura T., Fikrig E., and R.A. Flavell. 1997. Interleukin (IL)-6 directs the differentiation of IL-4-producing CD4+ T cells. J. Exp. Med. 185:461–9.

58. Dodge I.L., Carr M.W., Cernadas M., and M.B. Brenner. 2003. IL-6 production by pulmonary dendritic cells impedes Th1 immune responses. J. Immunol. 170:4457–64.

59. Wan S., Xia C., and L. Morel. 2006. IL-6 produced by dendritic cells from lupus-prone mice inhibits CD4+CD25+ T cell regulatory functions. J. Immunol. 178:271-9.

60. Hubert P., Jacobs N., Caberg J.H., Boniver J., and P. Delvenne. 2007. The cross-talk between dendritic and regulatory T cells: good or evil? J. Leukoc. Biol. 82:781-94.

61. Sakaguchi S., Ono M., Setoguchi R., Yagi H., Hori S., Fehervari Z., Shimizu J., Takahashi T., and T. Nomura. 2006. Foxp3+ CD25+ CD4+ natural regulatory T cells in dominant self-tolerance and autoimmune disease. Immunol. Rev. 212:8-27.

62. Geha R.S., Jabara H.H., and S.R. Brodeur. 2003. The regulation of immunoglobulin E class-switch recombination. Nat. Rev. Immunol. 3:721-32.

63. Ettmayer P., Mayer P., Kalthoff F., Neruda W., Harrer N., Hartmann G., Epstein M.M., Brinkmann V., Heusser C., and M. Woisetschläger. 2006. A novel low molecular weight inhibitor of dendritic cells and B cells blocks allergic inflammation. Am. J. Respir. Crit. Care. Med. 173:599-606.

64. Yanagihara Y., Kiniwa M., Ikizawa K., Shida T., Matsuura N., and A. Koda. 1993. Suppression of IgE production by IPD-1151T (suplatast tosilate), a new dimethylsulfonium agent. 2. Regulation of human IgE response. Jpn. J. Pharmacol. 61:31–39.

65. Zhao G.D., Yokoyama A., Kohno N., Sakai K., Hamada H., and K. Hiwada. 1999. Effect of suplatast tosilate (IPD-1151T) on a mouse model of asthma: inhibition of eosinophilic inflammation and bronchial hyperresponsiveness. Int. Arch. Allergy. Immunol. 121:116–122.

66. Hauben E., Gregori S., Draghici E., Migliavacca B., Olivieri S., Woisetschlager M., and M.G. Roncarolo. 2008. Activation of the aryl hydrocarbon receptor promotes allograft specific tolerance through direct- and DC-mediated effects on regulatory T cells. Blood 112:1214-22.

67. Lawrence B.P., Denison M.S., Novak H., Vorderstrasse B.A, Harrer N., Neruda W., Reichel C., and M. Woisetschläger. 2008. Activation of the aryl hydrocarbon receptor is essential for mediating the anti-inflammatory effects of a novel low molecular weight compound. Blood 112:1158-65.

68. Yamamoto J., Ihara K., Nakayama H., Hikino S., Satoh K., Kubo N., Iida T., Fujii Y., and T. Hara. 2004. Characteristic expression of aryl hydrocarbon receptor repressor gene in human tissues: organ-specific distribution and variable induction patterns in mononuclear cells. Life. Sci. 74:1039-49.

69. Vrzal R., Ulrichová J., and Z. Dvorák. 2004. Aromatic hydrocarbon receptor status in the metabolism of xenobiotics under normal and pathophysiological conditions. Biomed. Pap. Med. Fac. Univ. Palacky. Olomouc. Czech. Repub. 148:3-10.

70. Nambu J.R., Lewis J.O., Wharton K.A. Jr., and S.T. Crews. 1991. The Drosophila single-minded gene encodes a helix-loop-helix protein that acts as a master regulator of CNS midline development. Cell 67:1157-67.

71. Zhulin I.B., Taylor B.L., and R. Dixon. 1997. PAS domain S-boxes in Archaea, Bacteria and sensors for oxygen and redox. Trends. Biochem. Sci. 22:331-3.

72. Powell-Coffman J.A., Bradfield C.A., and W.B. Wood. 1998. Caenorhabditis elegans orthologs of the aryl hydrocarbon receptor and its heterodimerization partner the aryl hydrocarbon receptor nuclear translocator. Proc. Natl. Acad. Sci. USA. 95:2844-9.

73. Reyes H., Reisz-Porszasz S., and O. Hankinson. 1992. Identification of the Ah receptor nuclear translocator protein (Arnt) as a component of the DNA binding form of the Ah receptor. Science 256:1193-5.

74. Coumailleau P., Poellinger L., Gustafsson J.A., and M.L. Whitelaw. 1995. Definition of a minimal domain of the dioxin receptor that is associated with Hsp90 and maintains wild type ligand binding affinity and specificity. J. Biol. Chem. 270:25291-300.

75. Ikuta T., Eguchi H., Tachibana T., Yoneda Y., and K. Kawajiri. 1998. Nuclear localization and export signals of the human aryl hydrocarbon receptor. J. Biol. Chem. 273:2895-904.

76. Kobayashi A., Sogawa K., and Y. Fujii-Kuriyama. 1996. Cooperative interaction between AhR. Arnt and Sp1 for the drug-inducible expression of CYP1A1 gene. J. Biol. Chem. 271:12310-6.

77. Kobayashi A., Numayama-Tsuruta K., Sogawa K., and Y. Fujii-Kuriyama. 1997. CBP/p300 functions as a possible transcriptional coactivator of Ah receptor nuclear translocator (Arnt). J. Biochem. 122:703-10.

78. Kumar M.B., Tarpey R.W., and G.H. Perdew. 1999. Differential recruitment of coactivator RIP140 by Ah and estrogen receptors. Absence of a role for LXXLL motifs. J. Biol. Chem. 274:22155-64.

79. Kumar M.B., and G.H. Perdew. 1999. Nuclear receptor coactivator SRC-1 interacts with the Q-rich subdomain of the AhR and modulates its transactivation potential. Gene. Expr. 8:273-86.

80. Gasiewicz T.A., Kende A.S., Rucci G., Whitney B., and J.J. Willey. 1996. Analysis of structural requirements for Ah receptor antagonist activity: ellipticines, flavones, and related compounds. Biochem. Pharmacol. 52:1787-803.

81. Denison M.S., Pandini A., Nagy S.R., Baldwin E.P., and L. Bonati. 2002. Ligand binding and activation of the Ah receptor. Chem. Biol. Interact. 141:3-24.

82. Diaz D., Fabre I., Daujat M., Saint Aubert B., Bories P., Michel H., and P. Maurel. 1990. Omeprazole is an aryl hydrocarbon-like inducer of human hepatic cytochrome P450. Gastroenterology 99:737-47.

83. Quattrochi L.C., and R.H. Tukey. 1993. Nuclear uptake of the Ah (dioxin) receptor in response to omeprazole: transcriptional activation of the human CYP1A1 gene. Mol. Pharmacol. 43:504-8.

84. Adachi J., Mori Y., Matsui S., Takigami H., Fujino J., Kitagawa H., Miller C.A. 3rd, Kato T., Saeki K., and T. Matsuda. 2001. Indirubin and indigo are potent aryl hydrocarbon receptor ligands present in human urine. J. Biol. Chem. 276:31475-8.

85. Peter Guengerich F., Martin M.V., McCormick W.A., Nguyen L.P., Glover E., and C.A. Bradfield. 2004. Aryl hydrocarbon receptor response to indigoids in vitro and in vivo. Arch. Biochem. Biophys. 423:309-16.

86. Sinal C.J., and J.R. Bend. 1997. Aryl hydrocarbon receptor-dependent induction of cyp1a1 by bilirubin in mouse hepatoma hepa 1c1c7 cells. Mol. Pharmacol. 52:590-9.

87. Mufti N.A., and M.L. Shuler. 1996. Possible role of arachidonic acid in stress-induced cytochrome P450IA1 activity. Biotechnol. Prog. 12:847-54.

88. Kroetz D.L., and D.C. Zeldin. 2002. Cytochrome P450 pathways of arachidonic acid metabolism. Curr. Opin. Lipidol. 13:273-83.

89. Heath-Pagliuso S., Rogers W.J., Tullis K., Seidel S.D., Cenijn P.H., Brouwer A., and M.S. Denison. 1998. Activation of the Ah receptor by tryptophan and tryptophan metabolites. Biochemistry 37:11508-15.

90. Nguyen L.P., and C.A. Bradfield. 2008. The search for endogenous activators of the aryl hydrocarbon receptor. Chem. Res. Toxicol. 21:102-16.

91. Denis M., Cuthill S., Wikström A.C., Poellinger L., and J.A. Gustafsson. 1988. Association of the dioxin receptor with the Mr 90,000 heat shock protein: a structural kinship with the glucocorticoid receptor. Biochem. Biophys. Res. Commun. 155:801-7.

92. Perdew G.H. 1988. Association of the Ah receptor with the 90-kDa heat shock protein. J. Biol. Chem. 263:13802-5.

93. Perdew G.H., and C.A. Bradfield.1996. Mapping the 90 kDa heat shock protein binding region of the Ah receptor. Biochem. Mol. Biol. Int. 39:589-93.

94. Carver L.A., and C.A. Bradfield. 1997. Ligand-dependent interaction of the aryl hydrocarbon receptor with a novel immunophilin homolog in vivo. J. Biol. Chem. 272:11452-6.

95. Ma Q., and J.P. Whitlock Jr. 1997. A novel cytoplasmic protein that interacts with the Ah receptor, contains tetratricopeptide repeat motifs, and augments the transcriptional response to 2,3,7,8-tetrachlorodibenzo-p-dioxin. J. Biol. Chem. 272:8878-84.

96. Meyer B.K., Pray-Grant M.G., Vanden Heuvel J.P., and G.H. Perdew. 1998. Hepatitis B virus X-associated protein 2 is a subunit of the unliganded aryl hydrocarbon receptor core complex and exhibits transcriptional enhancer activity. Mol. Cell. Biol. 18:978-88.

97. Kazlauskas A., Poellinger L., and I. Pongratz. 1999. Evidence that the co-chaperone p23 regulates ligand responsiveness of the dioxin (Aryl hydrocarbon) receptor. J. Biol. Chem. 274:13519-24.

98. Ikuta T., Tachibana T., Watanabe J., Yoshida M., Yoneda Y., and K. Kawajiri. 2000. Nucleocytoplasmic shuttling of the aryl hydrocarbon receptor. J. Biochem. 127:503-9.

99. Petrulis J.R., Hord N.G., and G.H. Perdew. 2000. Subcellular localization of the aryl hydrocarbon receptor is modulated by the immunophilin homolog hepatitis B virus X-associated protein 2. J. Biol. Chem. 275:37448-53.

100. Pollenz R.S., and E.R. Barbour. 2000. Analysis of the complex relationship between nuclear export and aryl hydrocarbon receptor-mediated gene regulation. Mol. Cell. Biol. 20:6095-104.

101. Denison M.S., Fisher J.M., and J.P. Whitlock Jr. 1988. The DNA recognition site for the dioxin-Ah receptor complex. Nucleotide sequence and functional analysis. J. Biol. Chem. 263:17221-4.

102. Mimura J., Ema M., Sogawa K., and Y. Fujii-Kuriyama. 1999. Identification of a novel mechanism of regulation of Ah (dioxin) receptor function. Genes Dev. 13:20-5.

103. Roberts B.J., and M.L. Whitelaw. 1999. Degradation of the basic helix-loop-helix/Per-ARNT-Sim homology domain dioxin receptor via the ubiquitin/proteasome pathway. J. Biol. Chem. 274:36351-6.

104. Davarinos N.A., and R.S. Pollenz. 1999. Aryl hydrocarbon receptor imported into the nucleus following ligand binding is rapidly degraded via the cytosplasmic proteasome following nuclear export. J. Biol. Chem. 274:28708-15.

105. Ma Q., and K.T. Baldwin. 2000. 2,3,7,8-tetrachlorodibenzo-p-dioxin-induced degradation of aryl hydrocarbon receptor (AhR) by the ubiquitin-proteasome pathway. Role of the transcription activaton and DNA binding of AhR. J. Biol. Chem. 275:8432-8.

106. Conney A.H. 1982. Induction of microsomal enzymes by foreign chemicals and carcinogenesis by polycyclic aromatic hydrocarbons: G. H. A. Clowes Memorial Lecture. Cancer Res. 42:4875-917.

107. Hasler J.A. 1999. Pharmacogenetics of cytochromes P450. Mol. Aspects Med. 20:12-137.

108. Shimada T., and Y. Fujii-Kuriyama. 2004. Metabolic activation of polycyclic aromatic hydrocarbons to carcinogens by cytochromes P450 1A1 and 1B1. Cancer Sci. 95:1-6.

109. Ko H.P., Okino S.T., Ma Q., and J.P. Whitlock Jr. 1996. Dioxin-induced CYP1A1 transcription in vivo: the aromatic hydrocarbon receptor mediates transactivation, enhancer-promoter communication, and changes in chromatin structure. Mol. Cell. Biol. 16:430-6.

110. Fernandez-Salguero P.M., Hilbert D.M., Rudikoff S., Ward J.M., and F.J. Gonzalez. 1996. Aryl-hydrocarbon receptor-deficient mice are resistant to 2,3,7,8-tetrachlorodibenzo-p-dioxin-induced toxicity. Toxicol. Appl. Pharmacol. 140:173-9.

111. Shimizu Y., Nakatsuru Y., Ichinose M., Takahashi Y., Kume H., Mimura J., Fujii-Kuriyama Y., and T. Ishikawa. 2000. Benzo[a]pyrene carcinogenicity is lost in mice lacking the aryl hydrocarbon receptor. Proc. Natl. Acad. Sci. USA. 97:779-82.

112. Fernandez-Salguero P.M., Ward J.M., Sundberg J.P., and F.J. Gonzalez. 1997. Lesions of aryl-hydrocarbon receptor-deficient mice. Vet. Pathol. 34:605-14.

113. Lund A.K., Goens M.B., Nuñez B.A., and M.K. Walker. 2006. Characterizing the role of endothelin-1 in the progression of cardiac hypertrophy in aryl hydrocarbon receptor (AhR) null mice. Toxicol. Appl. Pharmacol. 212:127-35.

114. Fernandez-Salguero P., Pineau T., Hilbert D.M., McPhail T., Lee S.S., Kimura S., Nebert D.W., Rudikoff S., Ward J.M., and F.J. Gonzalez. 1995. Immune system impairment and hepatic fibrosis in mice lacking the dioxin-binding Ah receptor. Science 268:722-6.

115. Schmidt J.V., Su G.H., Reddy J.K., Simon M.C., and C.A. Bradfield. 1996. Characterization of a murine Ahr null allele: involvement of the Ah receptor in hepatic growth and development. Proc. Natl. Acad. Sci. USA. 93:6731-6.

116. Abbott B.D., Schmid J.E., Pitt J.A., Buckalew A.R., Wood C.R., Held G.A., and J.J. Diliberto. 1999. Adverse reproductive outcomes in the transgenic Ah receptor-deficient mouse. Toxicol. Appl. Pharmacol. 155:62-70.

117. Abbott B.D., Birnbaum L.S., and G.H. Perdew. 1995. Developmental expression of two members of a new class of transcription factors: I. Expression of aryl hydrocarbon receptor in the C57BL/6N mouse embryo. Dev. Dyn. 204:133-43.

118. Hahn M.E. 2002. Aryl hydrocarbon receptors: diversity and evolution. Chem. Biol. Interact. 141:131-60.

119. Schmidt J.V., Su G.H., Reddy J.K., Simon M.C., and C.A. Bradfield. 1996. Characterization of a murine Ahr null allele: involvement of the Ah receptor in hepatic growth and development. Proc. Natl. Acad. Sci. USA. 93:6731-6.

120. Mimura J., Yamashita K., Nakamura K., Morita M., Takagi T.N., Nakao K., Ema M., Sogawa K., Yasuda M., Katsuki M., and Y. Fujii-Kuriyama. 1997. Loss of teratogenic response to 2,3,7,8-tetrachlorodibenzo-p-dioxin (TCDD) in mice lacking the Ah (dioxin) receptor. Genes Cells 2:645-54.

121. Kim D.W., Gazourian L., Quadri S.A., Romieu-Mourez R., Sherr D.H., and G.E. Sonenshein. 2000. The RelA NF-kappaB subunit and the aryl hydrocarbon receptor (AhR) cooperate to transactivate the c-myc promoter in mammary cells. Oncogene 19:5498-506.

122. Moennikes O., Loeppen S., Buchmann A., Andersson P., Ittrich C., Poellinger L., and M. Schwarz. 2004. A constitutively active dioxin/aryl hydrocarbon receptor promotes hepatocarcinogenesis in mice. Cancer Res. 64:4707-10.

123. Andersson P., McGuire J., Rubio C., Gradin K., Whitelaw M.L., Pettersson S., Hanberg A., and L. Poellinger. 2002. A constitutively active dioxin/aryl hydrocarbon receptor induces stomach tumors. Proc. Natl. Acad. Sci. USA. 99:9990-5.

124. Puga A., Barnes S.J., Dalton T.P., Chang C., Knudsen E.S., and M.A. Maier. 2000. Aromatic hydrocarbon receptor interaction with the retinoblastoma protein potentiates repression of E2F-dependent transcription and cell cycle arrest. J. Biol. Chem. 275:2943-50.

125. Kerkvliet N. I. 2002. Recent advances in understanding the mechanisms of TCDD immunotoxicity. Int. Immunopharmacol. 2:277–291.

126. Tonn T., Esser C., Schneider E.M., Steinmann-Steiner-Haldenstatt W., and E. Gleichmann. 1996. Persistence of decreased T-helper cell function in industrial workers 20 years after exposure to 2,3,7,8-tetrachlorodibenzo-p-dioxin. Environ. Health Perspect. 104:422–426.

127. Weisglas-Kuperus N., Patandin S., Berbers G.A., Sas T.C., Mulder P.G., Sauer P.J., and H. Hooijkaas. 2000. Immunologic effects of background exposure to polychlorinated biphenyls and dioxins in Dutch preschool children. Environ. Health Perspect. 108:1203–1207.

128. Funatake C.J., Marshall N.B., Steppan L.B., Mourich D.V., and N.I. Kerkvliet. 2005. Cutting edge: activation of the aryl hydrocarbon receptor by 2,3,7,8-tetrachlorodibenzo-p-dioxin generates a population of CD4+ CD25+ cells with characteristics of regulatory T cells. J. Immunol. 175:4184-8.

129. Fontenot J.D., Gavin M.A., and A.Y. Rudensky. 2003. Foxp3 programs the development and function of CD4+CD25+ regulatory T cells. Nature Immunol. 4:330–336.

130. Hori S., Nomura T., and S. Sakaguchi. 2003. Control of regulatory T cell development by the transcription factor Foxp3. Science 299:1057–1061.

131. Ivanov I.I., McKenzie B.S., Zhou L., Tadokoro C.E., Lepelley A., Lafaille J.J., Cua D.J., and D.R. Littman. 2006. The orphan nuclear receptor RORgammat directs the differentiation program of proinflammatory IL-17+ T helper cells. Cell 126:1121-33.

132. Bettelli E., Oukka M., and V.K. Kuchroo. 2007. T(H)-17 cells in the circle of immunity and autoimmunity. Nat. Immunol. 8:345-50.

133. Veldhoen M., Hocking R.J., Atkins C.J., Locksley R.M., and B. Stockinger. 2007. TGFbeta in the context of an inflammatory cytokine milieu supports de novo differentiation of IL-17-producing T cells. Immunity 24:179-89.

134. Korn T., Bettelli E., Gao W., Awasthi A., Jäger A., Strom T.B., Oukka M., and V.K. Kuchroo. 2007. IL-21 initiates an alternative pathway to induce proinflammatory T(H)17 cells. Nature 448:484-7.

135. Quintana F.J., Basso A.S., Iglesias A.H., Korn T., Farez M.F., Bettelli E., Caccamo M., Oukka M., and H.L. Weiner. 2008. Control of T(reg) and T(H)17 cell differentiation by the aryl hydrocarbon receptor. Nature 453:65-71.

136. Veldhoen M., Hirota K., Westendorf A.M., Buer J., Dumoutier L., Renauld J.C., and B. Stockinger. 2008. The aryl hydrocarbon receptor links TH17-cell-mediated autoimmunity to environmental toxins. Nature 453:106-9.

137. Kobayashi S., Okamoto H., Iwamoto T., Toyama Y., Tomatsu T., Yamanaka H., and S. Momohara. 2008. A role for the aryl hydrocarbon receptor and the dioxin TCDD in rheumatoid arthritis. Rheumatology (Oxford). 47:1317-22.

138. Kikuchi H., Kato H., Mizuno M., Hossain A., Ikawa S., Miyazaki J., and M. Watanabe. 1996. Differences in inducibility of CYP1A1-mRNA by benzimidazole compounds between human and mouse cells: evidences of a human-specific signal transduction pathway for CYP1A1 induction. Arch. Biochem. Biophys. 334:235-40.

139. Shih H., Pickwell G.V., Guenette D.K., Bilir B., and L.C. Quattrochi. 1999. Species differences in hepatocyte induction of CYP1A1 and CYP1A2 by omeprazole. Hum. Exp. Toxicol. 18:95-105.

140. Mann J., Oakley F., Johnson P.W., and D.A. Mann. 2002. CD40 induces interleukin-6 gene transcription in dendritic cells: regulation by TRAF2, AP-1, NF-kappa B, AND CBF1. J. Biol. Chem. 277:17125-38.

141. Costanzo C., Piacentini G., Vicentini L., Armenante F., Mazzi P., Savio C., Faggioli L., Boner A., and M. Palmieri. 1999. Cell-specific differences in the regulation of IL-6 expression by PMA. Biochem. Biophys. Res. Commun. 260:577-81.

142. Ko H.P., Okino S.T., Ma Q., and J.P. Whitlock Jr. 1997. Transactivation domains facilitate promoter occupancy for the dioxin-inducible CYP1A1 gene in vivo. Mol. Cell. Biol. 17:3497-507.

143. Bartel D.P. 2004. MicroRNAs: genomics, biogenesis, mechanism, and function. Cell 116:281-97.

144. Kisseleva T., Bhattacharya S., Braunstein J., and C.W. Schindler. 2002. Signaling through the JAK/STAT pathway, recent advances and future challenges. Gene 285:1-24.

145. Hebenstreit D., Wirnsberger G., Horejs-Hoeck J., and A. Duschl. 2006. Signaling mechanisms, interaction partners, and target genes of STAT6. Cytokine Growth Factor Rev. 17:173-88.

146. Quelle F.W., Sato N., Witthuhn B.A., Inhorn R.C., Eder M., Miyajima A., Griffin J.D., and J.N. Ihle. 1994. JAK2 associates with the beta c chain of the receptor for granulocyte-macrophage

colony-stimulating factor, and its activation requires the membrane-proximal region. Mol. Cell. Biol. 14:4335-41.

147. Mui A. L., Wakao H., O'Farrell A.M., Harada N., and A. Miyajima. 1995. Interleukin-3, granulocyte-macrophage colony stimulating factor and interleukin- 5 transduce signals through two STAT5 homologs. EMBO J. 14:1166-75.

148. Changelian P.S., Flanagan M.E., Ball D.J., Kent C.R., Magnuson K.S., Martin W.H., Rizzuti B.J., Sawyer P.S., Perry B.D., Brissette W.H., McCurdy S.P., Kudlacz E.M., Conklyn M.J., Elliott E.A., Koslov E.R., Fisher M.B., Strelevitz T.J., Yoon K., Whipple D.A., Sun J., Munchhof M.J., Doty J.L., Casavant J.M., Blumenkopf T.A., Hines M., Brown M.F., Lillie B.M., Subramanyam C., Shang-Poa C., Milici A.J., Beckius G.E., Moyer J.D., Su C., Woodworth T.G., Gaweco A.S., Beals C.R., Littman B.H., Fisher D.A., Smith J.F., Zagouras P., Magna H.A., Saltarelli M.J., Johnson K.S., Nelms L.F., Des Etages S.G., Hayes L.S., Kawabata T.T., Finco-Kent D., Baker D.L., Larson M., Si M.S., Paniagua R., Higgins J., Holm B., Reitz B., Zhou Y.J., Morris R.E., O'Shea J.J., and D.C. Borie. 2003. Prevention of organ allograft rejection by a specific Janus kinase 3 inhibitor. Science 302:875-8.

149. Geijsen N., Koenderman L., and P.J. Coffer. 2001. Specificity in cytokine signal transduction: lessons learned from the IL-3/IL-5/GM-CSF receptor family. Cytokine Growth Factor Rev. 12:19-25.

150. Suzuki H., Katayama N., Ikuta Y., Mukai K., Fujieda A., Mitani H., Araki H., Miyashita H., Hoshino N., Nishikawa H., Nishii K., Minami N., and H. Shiku. 2004. Activities of granulocyte-macrophage colony-stimulating factor and interleukin-3 on monocytes. Am. J. Hematol. 75:179-89.

151. Weston C.R., and R.J. Davis. 2007. The JNK signal transduction pathway. Curr. Opin. Cell. Biol. 19:142-9.

152. Dudley D.T., Pang L., Decker S.J., Bridges A.J., and A.R. Saltiel. 1995. A synthetic inhibitor of the mitogen-activated protein kinase cascade. Proc. Natl. Acad. Sci. USA. 92:7686-9.

153. Breitkreutz D., Braiman-Wiksman L., Daum N., Denning M.F., and T. Tennenbaum. 2007. Protein kinase C family: on the crossroads of cell signaling in skin and tumor epithelium. J. Cancer Res. Clin. Oncol. 133:793-808.

154. Kontny E., Ziółkowska M., Ryzewska A., and W. Maśliński. 1999. Protein kinase c-dependent pathway is critical for the production of pro-inflammatory cytokines (TNF-alpha, IL-1beta, IL-6). Cytokine 11:839-48.

155. Kontny E., Kurowska M., Szczepańska K., and W. Maśliński. 2000. Rottlerin, a PKC isozyme-selective inhibitor, affects signaling events and cytokine production in human monocytes. J. Leukoc. Biol. 67:249-58.

156. Grandage V.L., Everington T., Linch D.C., and A. Khwaja. 2006. Gö6976 is a potent inhibitor of the JAK 2 and FLT3 tyrosine kinases with significant activity in primary acute myeloid leukaemia cells. Br. J. Haematol. 135:303-16.

157. Tian Y., Ke S., Denison M.S., Rabson A.B., and M.A. Gallo. 1999. Ah receptor and NF-kappaB interactions, a potential mechanism for dioxin toxicity. J. Biol. Chem. 274:510-5.

158. Yang Z., Wara-Aswapati N., Chen C., Tsukada J., and P.E. Auron. 2000. NF-IL6 (C/EBPbeta) vigorously activates il1b gene expression via a Spi-1 (PU.1) protein-protein tether. J. Biol. Chem. 275:21272-7.

159. Gallant S., and G. Gilkeson. 2006. ETS transcription factors and regulation of immunity. Arch. Immunol. Ther. Exp. (Warsz). 54:149-63.

160. Hromas R., Orazi A., Neiman R.S., Maki R., Van Beveran C., Moore J., and M. Klemsz. 1993. Hematopoietic lineage- and stage-restricted expression of the ETS oncogene family member PU.1. Blood 82:2998-3004.

161. Jensen B.A., Leeman R.J., Schlezinger J.J., and D.H. Sherr. 2003. Aryl hydrocarbon receptor (AhR) agonists suppress interleukin-6 expression by bone marrow stromal cells: an immunotoxicology study. Environ. Health. 2:16.

162. Takanaga H., Yoshitake T., Yatabe E., Hara S., and M. Kunimoto. 2004. Beta-naphthoflavone disturbs astrocytic differentiation of C6 glioma cells by inhibiting autocrine interleukin-6. J. Neurochem. 90:750-7.

163. Joiakim A., Mathieu P.A., Elliott A.A., and J.J. Reiners Jr. 2004. Superinduction of CYP1A1 in MCF10A cultures by cycloheximide, anisomycin, and puromycin: a process independent of effects on protein translation and unrelated to suppression of aryl hydrocarbon receptor proteolysis by the proteasome. Mol. Pharmacol. 66:936-47.

164. Ma Q., and K.T. Baldwin. 2002. A cycloheximide-sensitive factor regulates TCDD-induced degradation of the aryl hydrocarbon receptor. Chemosphere 46:1491-500.

165. Kawashima T., Murata K., Akira S., Tonozuka Y., Minoshima Y., Feng S., Kumagai H., Tsuruga H., Ikeda Y., Asano S., Nosaka T., and T. Kitamura. 2001. STAT5 induces macrophage differentiation of M1 leukemia cells through activation of IL-6 production mediated by NF-kappaB p65. J. Immunol. 167:3652-60.

166. Tuyt L.M., Dokter W.H., Birkenkamp K., Koopmans S.B., Lummen C., Kruijer W., and E. Vellenga. 1999. Extracellular-regulated kinase 1/2, Jun N-terminal kinase, and c-Jun are involved in NF-kappa B-dependent IL-6 expression in human monocytes. J. Immunol. 162:4893-902.

167. Oz-Arslan D., Rüscher W., Myrtek D., Ziemer M., Jin Y., Damaj B.B., Sorichter S., Idzko M., Norgauer J., and A.A. Maghazachi. 2006. IL-6 and IL-8 release is mediated via multiple signaling pathways after stimulating dendritic cells with lysophospholipids. J. Leukoc. Biol. 80:287-97.

168. Yanagawa Y., and K. Onoé. 2006. Distinct regulation of CD40-mediated interleukin-6 and interleukin-12 productions via mitogen-activated protein kinase and nuclear factor kappaB-inducing kinase in mature dendritic cells. Immunology 117:526-35.

169. Patil C., Zhu X., Rossa C. Jr., Kim Y.J., and K.L. Kirkwood. 2004. p38 MAPK regulates IL-1beta induced IL-6 expression through mRNA stability in osteoblasts. Immunol. Invest. 33:213-33.

170. Legrand-Poels S., Schoonbroodt S., and J. Piette. 2000. Regulation of interleukin-6 gene expression by pro-inflammatory cytokines in a colon cancer cell line. Biochem. J. 349 Pt.3:765-73.

171. Baccam M., Woo S.Y., Vinson C., and G.A. Bishop. 2003. CD40-mediated transcriptional regulation of the IL-6 gene in B lymphocytes: involvement of NF-kappa B, AP-1, and C/EBP. J. Immunol. 170:3099-108.

172. Raymond L., Eck S., Mollmark J., Hays E., Tomek I., Kantor S., Elliott S., and M. Vincenti. 2006. Interleukin-1 beta induction of matrix metalloproteinase-1 transcription in chondrocytes requires ERK-dependent activation of CCAAT enhancer-binding protein-beta. J. Cell. Physiol. 207:683-8.

173. Hu J., Roy S.K., Shapiro P.S., Rodig S.R., Reddy S.P., Platanias L.C., Schreiber R.D., and D.V. Kalvakolanu. 2001. ERK1 and ERK2 activate CCAAAT/enhancer-binding protein-beta-dependent gene transcription in response to interferon-gamma. J. Biol. Chem. 276:287-97.

174. Dahl R., and M.C. Simon. 2003. The importance of PU.1 concentration in hematopoietic lineage commitment and maturation. Blood Cells. Mol. Dis. 31:229-33.

175. Bakri Y., Sarrazin S., Mayer U.P., Tillmanns S., Nerlov C., Boned A., and M.H. Sieweke. 2005. Balance of MafB and PU.1 specifies alternative macrophage or dendritic cell fate. Blood 105:2707-16.

176. Krishnan V., Porter W., Santostefano M., Wang X., and S. Safe. 1995. Molecular mechanism of inhibition of estrogen-induced cathepsin D gene expression by 2,3,7,8-tetrachloro-dibenzo-pdioxin (TCDD) in MCF-7 cells. Mol. Cell. Biol. 15:6710-6719.

177. Duan R., Porter W., Samudio I., Vyhlidal C., Kladde M., and S. Safe. 1999. Transcriptional activation of c-fos protooncogene by 17β-estradiol: mechanism of aryl hydrocarbon receptor-mediated inhibition. Mol. Endocrinol. 13:1511-1521.

178. Gillesby B., Santostefano M., Porter W., Wu Z.F., Safe S., and T. Zacharewski. 1997. Identification of a motif within the 5'-regulatory region on pS2 which is responsible for Ap1 binding and TCDD-mediated suppression. Biochemistry 36:6080-6089.

179. Ghoda L., Lin X., and W.C. Greene. 1997. The 90-kDa ribosomal S6 kinase (pp90rsk) phosphorylates the N-terminal regulatory domain of IkappaBalpha and stimulates its degradation in vitro. J. Biol. Chem. 272:21281-8.

CURRICULUM VITAE

Name:	Hermann Novak
Date of birth:	1981, June 22nd
Place of birth:	Hallein, Austria

Education:

1988 - 1991	Primary school Maxglan, Salzburg
1991 - 1999	High School (Privatgymnasium) Herz-Jesu-Missionare, Salzburg
06/1999	Final examination (Matura)
1999 - 2002	University of Salzburg, Biology/Genetics
2002 - 2005	University of Vienna, Biology/Genetics
10/2003 - 10/2004	Diploma work Novartis Institutes for Biomedical Research (NIBR), Vienna Univ.-Doz. Dr. Maximilian Woisetschläger **Title:** *Interleukin-4 induces CCL23 expression by primary human blood monocytes in a STAT6 dependent fashion*
03/2005 - 04/2008	Ph.D. thesis Novartis Institutes for Biomedical Research (NIBR), Vienna Univ.-Doz. Dr. Maximilian Woisetschläger **Title:** *VAF347, a novel low molecular weight immunomodulator, inhibits Interleukin-6 production in the human monocytic cell line Monomac1 via activation of the aryl hydrocarbon receptor*
10/2007 - present	University of Vienna, Ph.D. studies, Genetics - Microbiology

Publications:

Novak H., Müller A., Harrer N., Günther C., Carballido J.M., and M. Woisetschläger. 2007. CCL23 expression is induced by IL-4 in a STAT6-dependent fashion. J. Immunol. 178:4335-41.

Lawrence B.P., Denison M.S., Novak H., Vorderstrasse B.A., Harrer N., Neruda W., Reichel C., and M. Woisetschläger. 2008. Activation of the aryl hydrocarbon receptor is essential for mediating the anti-inflammatory effects of a novel low molecular weight compound. Blood 112:1158-65.

LEBENSLAUF

Name:	Hermann Novak
Geburtsdatum:	22. Juni 1981
Geburtsort:	Hallein, Österreich

Ausbildung:

1988 - 1991	Volkschule Maxglan, Salzburg
1991 - 1999	Privatgymnasium der Herz-Jesu-Missionare, Salzburg
06/1999	Maturaabschluss mit Auszeichnung
1999 - 2002	Studium der Biologie mit Studienzweig Genetik, Universität Salzburg
2002 - 2005	Studium des Studienzweigs Genetik an der Universität Wien
10/2003 - 10/2004	Diplomarbeit Novartis Institutes for Biomedical Research (NIBR), Wien Univ.-Doz. Dr. Maximilian Woisetschläger **Titel:** *Interleukin-4 induces CCL23 expression by primary human blood monocytes in a STAT6 dependent fashion*
03/2005 - 04/2008	Doktorarbeit Novartis Institutes for Biomedical Research (NIBR), Wien Univ.-Doz. Dr. Maximilian Woisetschläger **Titel:** *VAF347, a novel low molecular weight immunomodulator, inhibits Interleukin-6 production in the human monocytic cell line Monomac1 via activation of the aryl hydrocarbon receptor*
10/2007 - heute	Doktoratsstudium Genetik – Mikrobiologie, Universität Wien

Publikationen:

Novak H., Müller A., Harrer N., Günther C., Carballido J.M., and M. Woisetschläger. 2007. CCL23 expression is induced by IL-4 in a STAT6-dependent fashion. J. Immunol. 178:4335-41.

Lawrence B.P., Denison M.S., Novak H., Vorderstrasse B.A., Harrer N., Neruda W., Reichel C., and M. Woisetschläger. 2008. Activation of the aryl hydrocarbon receptor is essential for mediating the anti-inflammatory effects of a novel low molecular weight compound. Blood 112:1158-65.